

Georgia State University
ScholarWorks @ Georgia State University

Biology Dissertations

Department of Biology

7-17-2009

Biofiltration of Acrylonitrile by Rhodococcus Rhodochrous DAP 96622 on a Trickle Bed Bioreactor

Jie Zhang

Follow this and additional works at: https://scholarworks.gsu.edu/biology_diss

 Part of the [Biology Commons](#)

Recommended Citation

Zhang, Jie, "Biofiltration of Acrylonitrile by Rhodococcus Rhodochrous DAP 96622 on a Trickle Bed Bioreactor." Dissertation, Georgia State University, 2009.
https://scholarworks.gsu.edu/biology_diss/64

This Dissertation is brought to you for free and open access by the Department of Biology at ScholarWorks @ Georgia State University. It has been accepted for inclusion in Biology Dissertations by an authorized administrator of ScholarWorks @ Georgia State University. For more information, please contact scholarworks@gsu.edu.

**BIOFILTRATION OF ACRYLONITRILE BY *RHODOCOCCLUS RHODOCHROUS* DAP
96622 ON A TRICKLING BED BIOREACTOR**

JIE ZHANG

NOTICE TO BORROWERS

In presenting this thesis as partial fulfillment of the requirements for an advanced degree from Georgia State University, I agree that the library of the university will make it available for inspection and circulation in accordance with its regulations governing materials of this type. I agree that permission to quote from, to copy from, or to publish from this thesis may be granted by the author, by the professor under whose direction it was written, or by the Dean of the College of Arts and Sciences. Such quoting, copying or publishing must be solely for scholarly purpose and must not involve potential financial gain. It is understood that any copying from or publication of this thesis that involves potential financial gain will not be allowed without written permission of the author.

All dissertations and theses deposited in the Georgia State University Library may be used only in accordance with the stipulation prescribed by the author in the preceding statement.

The author of this dissertation is

Jie Zhang
Atlanta, Georgia 30303

The director of this thesis is

Dr. Georgia Pierce
Department of Biology
College of Arts and Science

**BIOFILTRATION OF ACRYLONITRILE BY *RHODOCOCCLUS RHODOCHROUS* DAP
96622 ON A TRICKLING BED BIOREACTOR**

by

JIE ZHANG

Under the Direction of George E. Pierce

ABSTRACT:

Acrylonitrile (AN) is a major volatile waste generated in the production of acrylamide and often associated with aromatic contaminants (toluene and styrene) in plant effluents. We examined *Rhodococcus rhodochrous* DAP 96622 to determine if it could be adapted to efficient biodegradation of acrylonitrile (AN) in a bioreactor. A model bioreactor with granular activated carbon (GAC) as a substratum for *Rhodococcus* with AN as sole carbon or in combination with toluene was established. The kinetics of AN biodegradation by immobilized and planktonic cells were evaluated and compared. Inlet load and empty retention time were varied to test the removal efficiency in fed-batch and single-pass mode reactor. In addition, the three dimensional structure and characteristics of the biofilm were followed using confocal scanning laser microscopy (CSLM) and relative software. Immobilized cells in the bioreactor, at starting concentrations of AN up to 1150 mg l^{-1} in the presence of Tol, had at least 13 fold higher AN degradation rates than that seen of planktonic cells. A near steady state of AN degradation was maintained at 75-85% for AN and 80%-90% for Tol within the parameter of EBRT=8 min and AN and Tol inlet loads between $50\text{-}200 \text{ mg l}^{-1} \text{ h}^{-1}$ and $200\text{-}500 \text{ mg l}^{-1} \text{ h}^{-1}$, respectively.

However, when the inlet load of AN was increased to more than $200\text{mg l}^{-1} \text{ h}^{-1}$ and $500 \text{ mg l}^{-1} \text{ h}^{-1}$ for Tol, a reduction in efficiency of AN degradation was observed. Biofilms with discrete microcolonies interspersed with voids and channels were observed. Precise measurement of biofilm characteristics agreed with the assumption that the biomass and thickness of the biofilm increased along the carbon column depth. With a porous attachment material like GAC, substrate diffusion is most likely not a limiting factor for AN degradation. *Rhodococcus rhodochrous* DAP 96622 in a non-sterile activated charcoal column showed efficient degradation of AN in the presence of Tol. The *Rhodococcus* bioreactor may provide a potential practical waste gas and water treatment system.

INDEX WORDS: *Rhodococcus*, Acrylonitrile, Wastewater treatment, Trickling bed bioreactor

BIOFILTRATION OF ACRYLONITRILE BY *RHODOCOCCLUS RHODOCHROUS* DAP
96622 ON A TRICKLING BED BIOREACTOR

by

JIE ZHANG

A Dissertation Submitted in Partial Fulfillment of the Requirements for the Degree of
Doctor of Philosophy
in the College of Arts and Sciences
Georgia State University

2008

Copyright by
Jie Zhang
2008

BIOFILTRATION OF ACRYLONITRILE BY *RHODOCOCCLUS RHODOCHROUS* DAP
96622 ON A TRICKLING BED BIOREACTOR

by

JIE ZHANG

Major Professor: George E. Pierce
Committee: Sidney A. Crow
Eric S. Gilbert

Electronic Version Approved:

Office of Graduate Studies
College of Arts and Sciences
Georgia State University
August 2008

ACKNOWLEDGEMENTS

First I would like to acknowledge my advisor, Dr. George E. Pierce for the help and direction in my gradate studies and the completion of this dissertation. I am very grateful for the inspiration and encouragement you gave to me over the last few years. I also wish to give my gratitude to the doctoral committee and would like to thank Dr. Sidney A. Crow and Dr. Eric S. Gilbert for their advices and continual support. Very special thanks to Dr. Robert Simmons, for all the excellent microscopic works you did for me, and Dr. Gene K. Drago, for the bioreactor set-up and maintenance. I deeply appreciate the help from my labmates and colleagues, Sangeeta Ganguly, Trudy Tucker, Jennifer Hooker, Rollin Dennard, Emad Hussein, Samandra Demons and Anthony Jones. Thank you all for the patience, compatibility and understanding. Finally, and most importantly, I would like to thank my parents, who have always supported, encouraged and believed in me, thank you for letting me go half-way across the world, believing in me all these years no matter what I have chosen to do, and putting up the years without me.

TABLE OF CONTENTS

ACKNOWLEDGEMENTS.....	iv
LIST OF TABLES.....	viii
LIST OF FIGURES.....	x
LIST OF ABBREVIATIONS	xii
CHAPTER	
1. INTRODUCTION.....	1
Nature of VOCs and AN.....	1
Release and transformation of AN.....	4
Health and environmental effects.....	4
Methods developed for VOC treatment.....	5
Biotrickling filter design, application and optimization.....	7
Microorganisms which can metabolize nitriles.....	11
<i>Rhodococcus</i>	12
Nitrile Hydratase (NHase).....	14
Major strategies for biotreatment system of AN.....	15
Biofilm on carbon surface.....	16
Mathematical model.....	17
Objectives.....	18
2. MATERIALS AND METHODS.....	21
Microorganisms	21

Preparation of Media	21
Kinetic studies of free cells in flasks and immobilized cells in the bioreactor.....	22
Bioreactor setup and operation.....	23
1) Design and setup of trickling carbon bed biofilter.....	23
2) Reactor start-up and operation.....	26
A) Initial inoculation of trickling bed.....	26
B) Biofiltration study ---batch-mode reactor.....	27
C) Biofiltration study---Single-pass mode reactor	28
a) AN-toluene mixture (flow rate 1:8 from syringe pump) ...	28
a1 Effect of inlet AN and Tol concentration (C_{in}, ppm) on the removal efficiency and elimination capacity.....	28
a2 Effect of volumetric liquid flow rate (Q, ml/min) on the removal efficiency and elimination capacity.....	28
a3 Effect of inlet load ($IL=C_{in}/EBRT$) on the removal efficiency and elimination capacity.....	28
a4 Effect of environment factors on the removal efficiency.....	28
b) AN as single feed.....	29
Calculation.....	30
Biofilm cell activity.....	30
Adsorption and bioavailability test.....	31
Electron Microscopy	32
1) Scanning electron microscopy (SEM).....	32
2) Confocal laser scanning microscopy (CLSM).....	32
Analytical Methods.....	33
1) Organics	33
2) pH	34
3) Biomass	34
4) Ammonia assay	34

3. RESULTS	36
Morphology and physiological characterization.....	36
Growth curve and effect of different substrates/substrate Concentrations.....	36
Kinetics studies of free cells in flasks and immobilized cell in The bioreactor.....	42
Fed-batch mode reactor	45
1) Start-up of fed-batch mode.....	45
2) Effects of different AN and toluene flow rates on batch-mode reactor performance.....	52
Single-pass mode reactor	56
1) AN-Tol combined feed.....	56
A) Reactor start-up.....	56
B) Reactor performance at steady-state ----effects of inlet load on removal efficiency.....	59
C) Reactor performance at steady-state ----effects of EBRT on removal efficiency.....	62
2) AN as single feed	67
Adsorption and bioavailability test.....	70
1) Adsorption test in flasks with GAC and different concentrations of AN.....	70
2) Adsorption test in the reactor----batch-open switch mode....	78
3) Biofilm activity.....	82
4. DISCUSSION.....	85
5. REFERENCES.....	97
6. APPENDICE.....	104

LIST OF TABLES

Table 1. Composition of two major waste effluents.....	3
Table 2. Trickling bed parameters.....	25
Table 3. Experimental setup and initial operating parameters of the biotrickling filter.....	25
Table 4. The feeding schedule of nutrients and chemical inducers for preparation of a trickling bed inoculum culture.....	27
Table 5. Characteristics of <i>Rhodococcus rhodochrous</i> DAP 96622.....	38
Table 6. Average and maximum growth rate for different situations.....	39
Table 7. Concentration of carbon, C/N ratio, average and maximum cell growth rate for different AN concentrations in flasks.....	43
Table 8. Counts (log counts/ml) of microbial populations in the recycle liquid on different media at the start-up of feed-batch mode bioreactor	49
Table 9. AN and Tol removal efficiency with different flow rates of AN and toluene in fed-batch-mode bioreactor.....	52
Table 10. Bioavailability of AN 22 days after adsorption to GAC	75
Table 11 Degradation of AN in GAC reactor during open mode operation, % of AN degraded is based on NH₃ release in column effluent	80
Table 12. Biofilm cell activity of different sections of the column, expressed as the oxygen consumption rate referred to the homogenate volume.....	83
Table 13. Total biomass, average/maximum thickness, roughness, substratum coverage and surface to volume ratio of biofilms on GAC taken from upper, middle and lower part of the reactor. Values are means from two image stacks. The standard deviation is calculated as the square root of the mean of the variances of each of the two groups.....	84

LIST OF FIGURES

Figure 1. AN manufacturing processes	3
Figure 2. Biotransformation pathways of nitriles.....	13
Figure 3. Schematic representation of the experimental set-up.....	24
Figure 4. Ammonia assay: standard curve.....	35
Figure 5. Growth of <i>Rhodococcus</i> sp. 33278 on 500 ppm AN.....	39
Figure 6a. Growth of <i>Rhodococcus</i> sp. 33278 on different concentrations of AN in flasks (with 1000ppm toluene, urea, cobalt, cocktail and amidase inducer solution)	40
Figure 6b. AN concentration vs. maximum growth rate.....	41
Figure 7. Effect of substrate concentration on degradation rate and specific growth rate for free cells grown on AN in flasks.....	43
Figure 8. Effect of substrate concentration on growth rate and degradation rate of immobilized cells grown on AN in the feed-batch mode carbon-bed bioreactor (toluene is present).....	44
Figure 9 Cell density profile, and kinetics of AN and Tol degradation in batch-mode reactor.	46
Figure 10. Viable cell counts vs. time on Stanier's agar with AN and toluene at the start-up of feed-batch mode bioreactor	48
Figure 11. Scanning electronic microscopic image of the biofilm: A) 5000x magnification and B) 15,000x magnification.....	51
Figure 12. Cell density profile with different flow rates of AN and toluene in fed-batch-mode bioreactor	53
Figure 13. AN removal efficiency with different flow rates of AN and toluene in fed-batch-mode bioreactor	54

Figure 14. Tol removal efficiency with different flow rates of AN and toluene in feed-batch mode bioreactor.....	55
Figure 15a. Start-up performance of the biofilter: AN inlet and outlet concentration vs. time.....	57
Figure 15b. Start-up performance of the biofilter: AN inlet load and removal efficiency vs. time.....	57
Figure 16. AN and Tol removal efficiencies during the start-up period.....	58
Figure 17. Effect of inlet load of AN and EBRT on removal efficiency (flow rate AN 0.1µl/min toluene 0.8µl/min).....	60
Figure 18. Effect of inlet load of Tol and EBRT on removal efficiency (flow rate AN 0.1ul/min toluene 0.8ul/min).....	61
Figure 19. Effects of EBRT on AN removal efficiency at different AN and Tol flow rates.....	63
Figure 20. AN and Tol elimination capacity vs. inlet load at EBRT=8min.....	65
Figure 21. AN and Tol elimination capacity vs. inlet load at EBRT=4min.....	66
Figure 22. AN removal efficiency and elimination capacity vs. AN inlet concentration at EBRT=8min.....	68
Figure 23. AN removal efficiency and elimination capacity vs. AN inlet concentration at EBRT=4min.....	69
Figure 24. Bioavailability of adsorbed AN for biofilm development	72
Figure 25. Degradation of AN in flasks with GAC.....	73
Figure 26. pH evolution in the medium.....	74
Figure 27. CLSM image of biofilm attached to GAC particle in flasks with <i>Rhodococcus</i> sp. and 1080ppm AN after 30 days.....	76
Figure 28. Optical sectioning of the AN-degrading biofilm taken from flasks with GAC, visualizing the special distribution of <i>R. rhodococcus</i>. Optical thin sections at different depths of the biofilm are shown. 0um indicates the surface of the biofilm, whereas 20, 40, 60,80,100 and 120µm indicate the	

distance from the surface. Optical sections were sampled with 1.0 increment.....	77
Figure 29. Adsorption and degradation test in batch-open switch mode reactor.....	80
Figure 30. CLSM image of biofilm attached to GAC particles, taken from upper (A), middle (B) and lower (C) part of the reactor. Magnification, 400x. Red line: axis X; Green line: axis Y; Blue line: axis Z.	81
Figure 31. Biofilm cell activity expresses as the oxygen consumption rate (upper section)	83
Figure 32. AN inlet concentration VS. $(C_{in} - C_{out}) / \ln (C_{in} / C_{out})$ when AN was single feed at EBRT=8min	91

LIST OF ABBREVIATIONS

VOC.....	Volatile organic compounds
AN.....	Acrylonitrile
AMD.....	Acrylamide
NHase.....	Nitrile hydratase
Tol.....	Toluene
GAC.....	Granule activated carbon
DO.....	Dissolved oxygen
NSB.....	Net stripper bottoms
WWCB.....	Waste water column bottoms
EBRT.....	Empty bed retention time
IL.....	Inlet load
RE.....	Removal efficiency
EC.....	Elimination capacity

Nomenclature

C_{in} : inlet concentration (g m^{-3})
 C_{out} : outlet concentration (g m^{-3})
 V : volume of the biofilter bed
 Q : liquid flow rate

INTRODUCTION

Nature of VOCs and AN

Volatile organic compounds (VOCs) are a group of chemicals that evaporate (or volatilize) when they are exposed to air. These chemicals are used in the manufacture of, or are present in, many products used daily in both homes and businesses. One class of VOCs, volatile nitrile compounds, are widespread in the environment. They are organo-cyanides ($R-CN$) occurring naturally in plants and are widely used by the chemical industry as feedstock, solvents, extractants, pesticides, and other uses (U.S. EPA 1994a). Nitriles are toxic to human for they can inactivate the respiration system by binding tightly to cytochrome-c-oxidase (Wilson 1983).

Acrylonitrile (AN) is a color-less, liquid, synthetic chemical which is commercially important, and one of the nitrile compounds manufactured on the largest scale (ATSDR 1999). The chemical AN (the monomer, small molecules bonded to each other to form a polymer) is the raw material and chemical intermediate used in the production of acrylic fibers, plastics, polymers and synthetic rubber (U.S. EPA 1994a). It is also involved in the reactions to form compounds used as solvents, polymeric materials, dyes, pharmaceuticals and insecticides. The production of AN generates significant amount of by-products which can pollute the environment. In 1994, the estimated total capacity of AN production in the United States was 1.4 million tons (English) and 4.3 million tons wastewater containing AN was generated. In 1996 approximately in the world, 80 plants in 22 countries produced 4.3 million tons of AN (Weissermel and Arpe 1997). World annual production of AN in 2001 was 3.9 million tons, and in 2005 5.9 million tons, with just under half of that coming from the United States. Most industrial acrylonitrile (over 90%) is produced through the catalytic ammoxidation of propylene (the Sohio process). In this process, propylene, oxygen, and ammonia are catalytically

converted directly to AN in a fluidized-bed reactor at temperatures between 400 C and 500 C and at gauge pressures between 0.3 and 2 bar (Gates, 1979; Languardt, 1979). The by-products formed during the ammoxidation reaction are hydrogen cyanide and acetonitrile, which are separated during the distillation process. The wastewater from the Sohio process contains a complex mixture of organic nitriles, amides and acids including acetonitrile (AC), propionitrile(PN), succinonitrile (SN), fumaronitrile (FN), 3-cyanopyridine and AN, together with AMD, maleimide, acrolein, acrylic acid and acetic acid (Wyatt and Knowles, 1995a).

Figure 1 outlined the basic manufacturing process of AN (Wyatt and Knowles 1995b). They also gave the composition of two major waste effluents produced, the wastewater column bottom (WWCB) and the stripper column bottom (SCB) (Table 1, Wyatt and Knowles 1995b). WWCB and SCB was obtained from an AN manufacturing plant (Monsanto Company, Texas City, TX). Pierce (1999) also provided typical compositions present in Fortier waste, which is generated by Cytec Industries Inc. Fortier Manufacturing Plant. The plant was first constructed to produce acrylonitrile, ammonia, sulfuric acid and many other petrochemical products. The level of operation of the manufacturing plant may cause the waste composition and concentration to change. In a typical AN production facility, the absorber (see Figure 1) is the major source of VOC's, generating on average AN emissions of 2.00 kg/hr (Wilkinsin 1976).

In 1992, environmental releases of the chemical, as reported to the Toxic Release Inventory by certain types of US industries, totaled about 5.5 million pounds, 1.6 million pounds went to the atmosphere, 3.9 million pounds to underground injection sites and 9500 pounds to land and surface water (U.S. EPA 1994a).

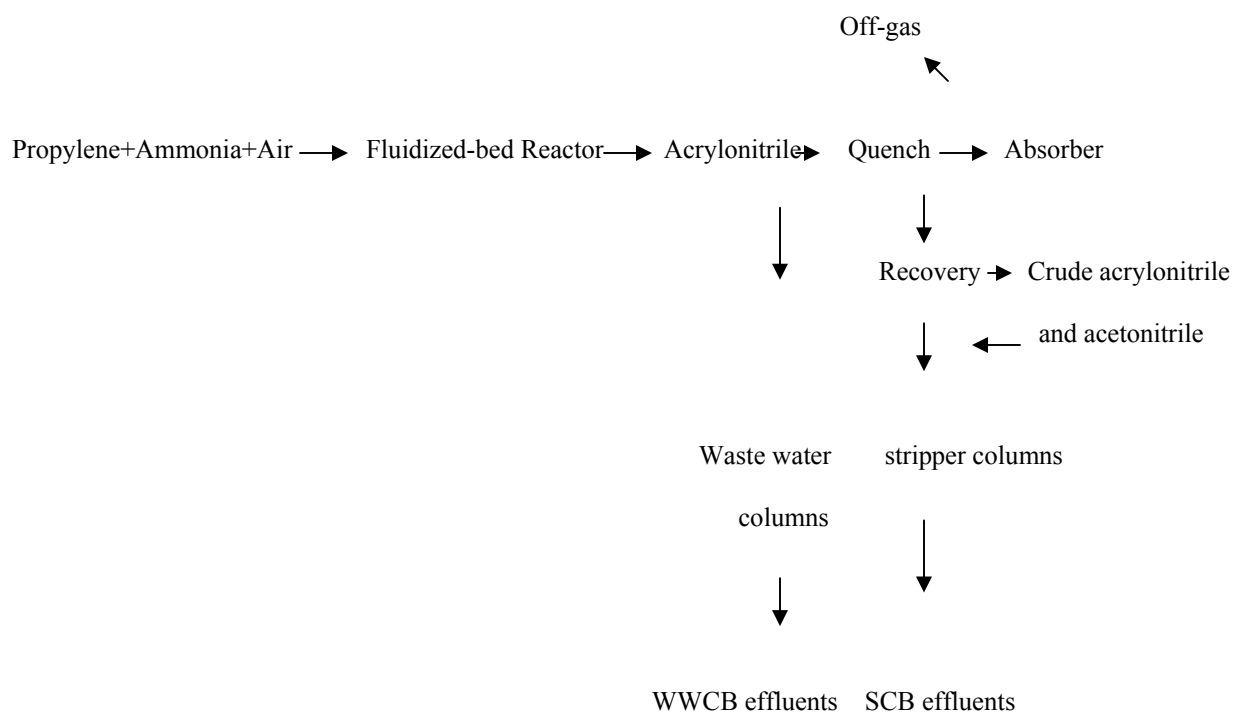


Figure 1. AN manufacturing processes (Wyatt and Knowles 1995b).

Table 1. Composition of two major waste effluents. (Wyatt and Knowles 1995a¹; Pierce 1999²)

Name	Monsanto Waste ¹		Fortier Waste ²	
	Stream 1 average mg/l	Stream 2 average mg/l	NSB(ppm)	WWCB(ppm)
Acetyldehyde	28	5	NR	NR
Acrolein	52	36	10-100	50-1200
Acetic acid	1310	2323	NR	NR
Acrylic acid	1827	786	NR	NR
Acrylamide (AMD)	821	49	10-130	1100-1500
Acrylonitrile(AN)	NR	NR	5-180	10-1250
Cyanopyridine	620	65	NR	NR
Fumaronitrile (FN)	794	66	<=100	20-1500
Maleimide	1818	91	NR	NR
Succinonitrile (SN)	231	2380	300-40,000	50-5000

WWSB=waste water column bottom NSB=net stripper bottom

NR= Not Reported

Release and transformation of AN

If released to air, AN can degrade by reaction with atomic oxygen and hydroxyl radicals, resulting in the formation of formaldehyde mainly but also other compounds, such as formic acid, formyl cyanide, carbon monoxide and hydrogen cyanide (Environment Canada, 2000).

The main removal pathways for AN in water are evaporation and slow biodegradation.

Photolysis and hydrolysis are generally not significant processes. Due to its high Henry's Law constant and low adsorption to soil the most likely fate of AN in soil is evaporation or may leach into the groundwater while adsorption is not significant. The potential for bioconcentration of AN in aquatic organisms is low (U.S. EPA, 1994a).

Health and environmental effects

Probable routes of human exposure to AN are inhalation and dermal contact. AN is a central nervous system and a respiratory irritant. It is metabolized to cyanide (<http://www.scorecard.org/chemical-profiles/html/acrylonitrile.html>). Exposure to AN can result in difficulty breathing, nausea, nose and throat irritation. The symptoms of acute toxicity for AN may resemble those of cyanide and ingestion and inhalation can be fatal. The association with cancer to chronic long-term exposure to AN in human has been either negative or inconclusive (U.S. EPA 1994a).

AN is also a probable human carcinogen and mutagen (Xu et al 2003, De Meester et al 1978, Collins et al 1989). The U.S. EPA has calculated a cancer inhalation unit risk estimate of 6.8×10^{-5} (microgram per cubic meter)⁻¹. It estimates that if an individual were to breathe air containing AN at 0.01 µg/m³ over an entire lifetime, that person would theoretically have no more than a 1 in 1 million increased chance of developing cancer as a direct result of breathing air containing this chemical (U.S. EPA 1994a). The International Agency for Research on

Cancer (IARC) has classified AN as a Group 2A: (Probable human carcinogen), based on sufficient evidence in animals and limited evidence in humans (IARC 1987). Acute exposure to wastewater of AN, if not appropriately treated, is moderately toxic to most aquatic species (U.S.EPA 2003). The EPA recommends that levels in lakes and streams should be limited to 0.058 parts of AN per billion parts of water (0.058 ppb) to prevent possible health effects (ATSDR 1999). The Clean Air Act Amendments of 1990 also list AN as a hazardous air pollutant (U.S. EPA 1990). Given these concerns, AN manufacturing industries are required to reduce primarily the organic load from their discharges (U.S EPA 1985).

A major waste generated in AN production and a metabolite in AN degradation, acrylamide (AMD), also has been observed to have toxic effects after dermal and oral exposure. AMD is irritating to the skin and respiratory tract in humans (IARC 1985). Although inadequate evidence is available from human studies, several laboratory animal studies have shown that AMD causes a variety of tumors in rats and mice. AMD is not likely to be acutely toxic to aquatic or terrestrial animals at levels found in the environment. Long-term exposure to terrestrial animals may increase tumor incidence or adversely affect reproductive abilities (U.S.EPA 1994b). EPA now (effective July 30, 1994) requires a treatment technique for AMD.

Methods developed for VOC treatment

Several methods have been developed for VOCs treatment, including activated carbon adsorption, UV radiation, incineration, catalytic thermal oxidation, ozonation, and chlorination. There also are a few techniques used to treat AN waste water, such as deep well injection and wet air oxidation. Deep well injection is a liquid waste disposal technology. It consists of concentric pipes, which extend several thousand feet down from the surface level, and the waste is injected through the injection tubing without treatment. In the U.S., the use Deep Well

Injection can only occur into a formation where geologic analysis supports a “10,000 year-no-migration” claim. Waste injected underground may have potential to contaminate water resources. In addition, there are many possible routes for vertical migration of hazardous waste to the surface. Wet air oxidation uses elevated temperature and pressure to oxidize dissolved or finely divided organics in a waste water stream. The aqueous solution is heated to about 300 F and pressurized to 130 or more atmospheres in the presence of compressed air. The process is very energy-consuming and does not always achieve complete oxidation of the organic constituents. It is also not legal in US because it results in stripping of many VOCs (especially HCN). In conclusion, both of the two techniques are not only costly, but also generate secondary air or water pollution, which is considered ineffective and unacceptable.

Fortunately, many chemicals used in industry are natural, thereby biodegradable. As an alternative to treat wastewater, and to save on costs of traditional chemical treatment processes, biodegradation has been investigated in detail over the past twenty years. Biological waste air and water treatment has been recognized as a cost-effective and environmentally friendly technique, and is becoming popular among industries which require stringent environmental regulations. Two air pollution control bioreactors, biofilter and biotrickling filter, have become methods of choice for treating malodorous gases and vapor-phase organic contaminants in an air stream. Both of them are biological scrubbers in which gas-phase pollutants are passed through a packed bed which is usually made of an inert material, which provides surface for natural immobilization of pollutant-degrading organisms and gas-liquid contact. The difference between biofilter and biotrickling filter is that if there is a moving water phase. For biotrickling filters, the contaminated air flows through the packed bed (upward or downward) while the liquid is trickled down from the top of the reactor to supply the nutrient

and provide moisture. Biotrickling filters could have been more superior to biofilters for treating pollutant in high elimination rates and in accurate control of environment conditions. Generally, if the trickling liquid is recycled, co-current flow which can minimize stripping is preferred over counter-current flow (upflow air stream) (Deshusses and Cox 1998).

Biotrickling filter design, application and optimization

When wastewater is applied intermittently or continuously over a medium, microorganisms become attached to the medium and form a biological layer or fixed film. In the biofilm, a complex ecosystem formed by mixed bacteria and fungi mediate the process of biodegradation. The harmful chemicals are then converted into benign end products if the organisms have the appropriate biocatalytic potential. Environmental conditions such as temperature, pH, oxygen and mineral nutrient availability, as well as mass transfer of substrates, can influence the kinetics of pollutant elimination in the biofilter.

Optimization of process parameters leads to more efficient clean-up of the contaminant and economical biofilter operation. Design and optimization of the biofilter is based on a number of variables that characterize the hydrodynamics of a biotrickling filter. Some of the most important variables and parameters include: type and concentration of the air contaminant, strains of degrader microorganisms, air and liquid flow rate, the type and size of packing used as a biofilm support, support media characteristics, biofilter dimensions, amount of the biomass present, bed void fraction, pressure drop, liquid hold-up, liquid distribution and maintenance (moisture control and clogging prevention). Several of these also have a strong impact on mass transfer coefficients and on the physical characteristics of the biofilm itself.

Once a biofilter is built up and begins running, dynamic changes can characterize and affect biofilter performance. In chemical industries, the waste air compositions are varied due to

weekly rotation in production. A number of studies have been conducted toward biofiltration under varying loading conditions, such as variable air flow rate and contaminant concentration, or transient state between batch and continuous mode, or periodically shut down of the reactor (Kim et al. 2004, Cox and Deshusses 1998, Moe and Irvine 2000, Martin and Loehr 1996).

However, the effect of dynamic changes of the contaminants or community composition degradative activity has not been well understood. In a trickling bed reactor, the liquid flow mediates substrate and oxygen transport from the gas/water to the biofilm. Liquid flow affects the wetting of the bed and the distribution of the pollutant. It has been found that there is a strong relationship between liquid flow and the elimination capacity (Diks and Ottengraf 1991). However, it is not certain whether the non-wetted parts of a biofilm (biofilm without a liquid film flowing over it) in a trickling filter exert biological activity on the removal process. Also, biological treatment remains limited, especially when the target compounds are toxic volatile and present at high concentrations.

In microbial ecosystems, microorganisms are able to respond dynamically to environmental changes, particularly when the changes are stressful. However, if one is able to control the variability of the substances and conditions at a great level, the constraints on the ability of a bioreactor to control VOCs could also be great. Empty bed retention time (EBRT) is a very important factor in biofilter operation, especially when a biofilter is treating different types of chemicals by rotation. Retention time indicates how long a contaminant is in contact with the filtering material when it passes through the biofilter. Biofilter performance is influenced by the length of the retention time. Aromatic compounds usually require longer EBRTs to be utilized than the aliphatic compounds (Kim et al. 2004 and 2005). A number of studies have indicated that the increase of gas flow rate (the decrease of the EBRT) resulted in a decrease of removal

efficiency and elimination capacity in biofilters, which may be due to the decrease of contact time between the pollutants and microbial population (Kiared et al. 1997, Sorial et al. 1997, Jorio et al 2000, Namkoong et al. 2004).

Several applications of laboratory-scale biotrickling filter have been developed to remove pollutants in contaminated air. Oh and Bartha (1994) immobilized the microbial consortium from a sewage sludge on perlite and successfully eliminated nitrobenzene vapors in a lab-scale biotrickling filter. Subsequently, Zhou et al. (1998) reported a novel trickling fibrous-bed biofilter for treating waste gas containing benzene as a sole carbon source. Over 90% removal efficiency was achieved with inlet concentrations of 0.37-0.95 g m⁻³ and a superficial air flow rate of ~1.44 m³ m⁻² h⁻¹ or at an EBRT of ~10 min. A mathematical model was developed to simulate the biofiltration. The apparent first order parameter, K_1 , in the model is linearly related to the inlet benzene concentration. Calderia et al. (1999) isolated a bacterial consortium from the rhizosphere of the reed *Phragmites communis* and attached the consortium to granular activated carbon (GAC) reactor to degrade 4-Chlorophenol (4-CP). 4-CP adsorbed to GAC during the open mode (single-pass system, no recirculation) became available to the consortium after the system was returned to closed mode (recycle system). They also revealed a heterogeneous biofilm structure using confocal laser scanning microscope (CLSM). This indicated that the structure organization of GAC and the biofilm community established on the GAC, may be important to its function. Sa and Boanvenura (2001) used a trickling bed biofilm reactor packed with a siliceous granular material (PORAVER particles, from Dennert PORAVER GmbH, Germany) to evaluate phenol removal efficiency by *Pseudomonas putida*. They obtained biokinetic constants by developing the overall reactor kinetics following a pseudo first-order model. Cox and Deshusses (2002) investigated the use of biotrickling filters for the co-treatment

of high loadings of H_2S and toluene. A population developed which had a limited tolerance to low pH in the neutral-pH biotrickling filter while showed a broader pH range for removal of H_2S and toluene in the acidic biotrickling filter. Kornaros and Lyberatos (2006) assessed the effectiveness of a biotrickling filter for the treatment of waste water from a dye manufacturing company. A stable chemical oxygen demand (COD) removal efficiency of 60-70% was achieved in continuously operated filter. The microorganisms were able to remove COD levels up to 36000mg/l under optimized conditions. This proved the promising role of biofilter in removing a significant portion of the organic content in manufacturing wastewater.

Biotreatment of AN plant effluent by powdered activated carbon-activated sludge (PAC-AS) was conducted by Ramakrishna et al. They observed advantageous effects on COD reduction and specific respiration rate. However, the adsorption of some biodegradable components inhibited in situ biodegradation of PAC (1989). Wyatt and Knowles (1995a, 1995b) analyzed AN waste water and isolated microorganisms capable of utilizing major components. The defined mixed population was used to biodegrade a synthetic mixture of the major components of AN waste effluents. In addition, the mixed culture was adapted to degrade more recalcitrant compounds, maleimide, acrolein and fumaronitrile. Mixed culture of nitrile-hydrolyzing bacteria grown on batch and continuous culture on waste containing AN, fumaronitrile and succinonitrile etc. demonstrated a 75% reduction in COD and 99% removal of detectable toxic components. This appears that specialized consortium of microorganisms to degrade toxic industrial wastes could be an alternative to classical adaptation procedure of activated sludge. Pierce (2000) discovered that induced pure cultures of two *Rhodococcus* strains, DAP 96622 and DAP 96253, are able to detoxify a mixture of nitriles or a mixture of nitriles and amides which are typically present in high concentration(s) in nitrile production

waste streams. The author also described the effects of reaction conditions on detoxification and demonstrated that the detoxification reactions can proceed under a variety of different conditions. The induced *Rhodococcus rhodochros* strain DAP 96622 is able to detoxify nitrile compounds found in both diluted and the full strength WWCB, on the order of minutes to hours.

Some studies presented removal or bioconversion of liquid-phase nitriles using packed-bed filling with glass beads. Immobilization of nitrile converting bacteria is a means of increasing catalyst longevity in chemical syntheses or for use in bioremediations. A thermophilic *Bacillus* spp. capable of transforming nitriles was used as a free cell suspension and immobilized in alginate beads to study the transformation of acetonitrile and AN. It was found that alginate beads provided little additional thermal or chemical stability and the initial rate was limited by mass transfer and possibly by the oxygen supply to the cells (Graham et al. 2000). Manolov et al. (2004) tested a 20 liter packed-bed reactor filled with foamed glass beads for treatment of acetonitrile. At a feed rate of 0.77g acetonitrile l⁻¹ reactor day⁻¹, 99% of the acetonitrile was removed, which confirm the potential of packed-bed reactor for the treatment of a concentrated mixture of volatile pollutants. However, it is still not reported that liquid or gas-phase acrylonitrile can be used as sole carbon and energy source by immobilized cells and get eliminated through a biofilter.

Microorganisms which can metabolize nitriles

Several microorganisms [e.g. *Acinetobacter* (Yamamoto et al 1990), *Corynebacterium* (Martinkova et al. 1992), *Pseudomonas* (Nawaz et al. 1990), *Nocardia* (Harper 1985), *Rhodococcus* (Watanable 1987a, Wyatt and Knowles 1995a and b)] are known to metabolize nitriles, using them as sole carbon and/or nitrogen source. Many nitrile compounds are synthesized by plants, fungi, bacteria, algae, insects and sponges; it is not surprising, that there

are several biochemical pathways for nitrile degradation. One of the most interesting pathways is nitrile hydrolysis. There are two major metabolic pathways, a single-step conversion of nitriles to corresponding acids and ammonia catalyzed by nitrilases, and a two-step process of the formation from nitriles to amides catalyzed by nitrile hydratase (NHase), then to acid and ammonia by amidase (AMDase) (Figure 2. Harper 1977; Nagasawa and Yamada 1990). Two types of enzymes act via distinctly different mechanisms. It has been assumed that the pathway for nitrile hydrolysis is mainly dependent on the substrate structure and the product of a given reaction can be predetermined to a certain extent - *i.e.* aromatic, unsaturated and heteroaromatic nitriles are hydrolyzed *via* nitrilases, whereas aliphatic nitriles are transformed through two steps.

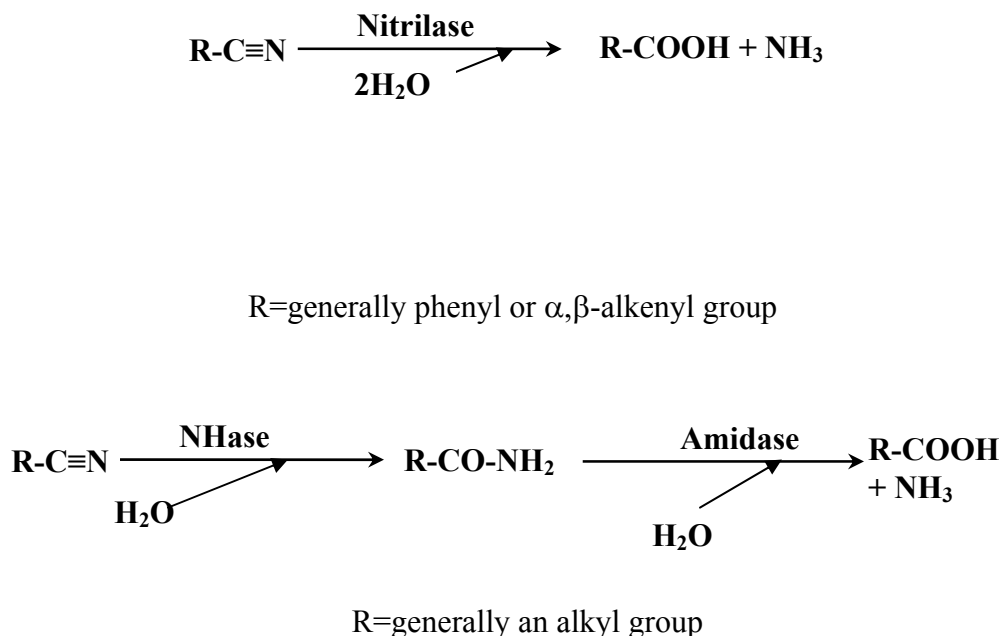


Figure 2. Biotransformation pathways of nitriles. (Harper 1977; Nagasawa and Yamada 1990)

Rhodococcus

Rhodococcus strains represent the most commonly isolated microorganisms which exhibit high NHase activity. *Rhodococci* are gram-positive, aerobic, and nonmotile nocardioform actinomycetes. They have a variety of growth patterns, starting with the coccus or short-rod stage, and then form filaments with side projection, show elementary branching, or produce extensively branched hyphae. They are partially acid-fast with an oxidative type of metabolism and grow well in standard laboratory media (Goodfellow 1989). Some species of *Rhodococcus* are also known pathogens for humans, animal and plants (Edwards and Simpson 1988, Elliott et al 1986, Murai et al 1980).

The genus *Rhodococcus* consists of microorganisms that exhibit broad metabolic diversity, particularly to hydrophobic compounds such as hydrocarbons, chlorinated phenolics, steroids, lignin, coal and petroleum. Various *Rhodococcus* strains are employed in operational bioprocessing systems for industrial and environmental applications, such as production of acrylic acid and acrylamide, steroid conversions and bioremediation of chlorinated hydrocarbons and phenolics (Finnerty 1992).

As early as 1970s, it was found that six nitrile compounds and two amide derivatives were degraded by *Nocardia rhodochrous* LL100-21. AN and AMD supported growth but only as a source of nitrogen. The enzyme system for hydrolysis of acetonitrile was shown to be intracellular and inducible. It involved two enzymatic steps for breaking down acetonitrile with acetamide as intermediate and acetic acid and ammonia as the final product (Digeronimo and Antonine 1976). Microbial metabolism of aromatic nitriles was reported in 1977. An organism utilizing benzonitrile as sole carbon and nitrogen source was isolated and identified as a

Nocardia sp. of *rhodochrous* group and the nitrilase enzyme which catalyzed the degradation was purified (Harper 1977). *Rhodococcus* strain N774 which was isolated by early screens had high acrylamide synthesizing activity and was able to use other mono- and di-nitriles (Watanabe et al. 1987). In a subsequent screen, *Rhodococcus rhodochrous* J1 was isolated, which was capable of one of the most productive syntheses ever observed in microorganisms (Nagasawa et al. 1988). In 1990s, mechanisms of biotransformation of nitriles were more characterized and well established (Kobayshi et al. 1992, Nagasawa and Yamada 1990).

NHase

NHase is a key enzyme in the two-step enzymatic pathway for conversion of nitriles to acids, which catalyzes the hydrolysis of nitriles to corresponding amides. It could be used as a potential nitrile-degrading enzyme for biotransformation and waste treatment. Organisms expressing NHases are capable of utilizing aliphatic nitriles as the sole source of nitrogen. A number of microorganisms with NHase activity have been isolated and the enzymes have been purified and characterized (Okada et al. 1997, Yamada and Kobayashi 1996, Alfani et al. 2001, Yamaki et al. 1997, Bauer et al. 1994, Asano et al. 1982, Ganguly 2005).

NHase is a metalloenzyme which consists of α and β subunits containing either nonheme iron or cobalt atoms. Ferric NHase (e.g. the NHase from *Rhodococcus* R 312 and *Pseudomonas chlororaphis* B23) is photo-activated due to the iron complex in the β -subunit. The conformational change of the subunit induced by the light irradiation cause the release of endogeneous NO molecule, which recovers the original NHase activity (Endo et al. 1999; Popescu et al. 2001). Cobalt NHase (e.g. the NHase from *R. rhodococcus* J1) has a tryptophan residue instead of tyrosine in ferric enzyme. *R. rhodochrous* has been reported to produce a high-molecular-weight NHase and a low-molecular-weight NHase, which were selectively induced by

the reaction products (amides) and by urea, respectively. The high-molecular-weight NHase catalyzes the transformation of aliphatic nitriles and is used for the industrial production of acrylamide from acrylonitrile. The light-molecular-weight NHase works on aromatic nitriles and is used for the production of nicotinamide from 3-cyanopyridine (Kobayashi and Shimizu 1998). *Rhodococcus* have been induced to produce elevated levels of NHase to about 40-50% of total cell protein, by adding cobalt and urea as enzyme cofactor to medium containing one nitrile compound. It is also found that NHase activity of *Rhodococcus* increase and can be stabilized in the presence of nitriles and amides (Pierce 1999&2000). For the dissertation study, a biofilm mainly consisting of *Rhodococcus* strain 96622 was established in a bioreactor for filtration of AN-contaminated water and gas.

Major strategies for biotreatment system of AN

Generally, biotreatment systems for VOCs have developed along two major strategies: the use of specialized microbial cultures of microorganisms with unique metabolic capabilities and the adaptation of reactor systems to biodegrade the waste gas/water. For the microbial culture, enzyme system of the Gram-positive bacteria *Rhodococcus rhodochrous* DAP 96253 and 96622 have been found able to form the basis of a biocatalyst for detoxification of liquid AN. Nitrile hydratase that catalyzes the transformation of AN in *Rhodococcus* has been chemically stabilized and prolonged the active period by nitriles, amides, cyanide, and calcium alginate (Ganguly 2005). Biofiltration system is open and when a specific strain is inoculated, it has to compete with others from the outside environment in complex biological ecosystem. *R. rhodochrous* is the bacterial strain which was picked up for biofiltration and a selective pressure should be given to maintain its predominant development. The activity of NHase is induced by nitrile and if nitrile is not present, NHase will not be produced at significantly elevated levels.

Since NHase is a specific enzyme produced by *Rhodococcus* in this situation and other organisms would feed on acrylamide and acrylic acid generated from AN, nitrile can be used as the selective pressure. For the reaction system, the biological attachment media which can support long-term, consistent treatment of AN, was brought to focus. Conventional biofilters are generally made of a variety of natural attachment media, such as soil, compost, bark and activated sludge, but they have low porosity and high compactness. Mass transfer and humidity control are also difficult. They are limited to the elimination of VOCs also because the environmental conditions are not easily controlled and toxic metabolites cannot be purged out of the system. As an alternative, granular activated carbon (GAC) is a good bacterial immobilization matrix as it is very adsorptive and has a high volume-surface ratio, due to the large number of internal pores and rough surface texture. Bioreactor containing a packed bed of GAC can overcome those disadvantages because the loose package and relatively large space between granular carbons allow liquid to trickle down and gas to flow upward or downward freely through the packed bed. The high surface area also provides good contact for cell growth and reactions to take place for the task of the biological removal of VOCs.

Biofilm on carbon surface

Another advantage for biofilm reactors in treating toxic effluent is that attached microorganisms are more resistant towards toxic effects (Parkin and Speece 1983). Many complicated and independent processes take place simultaneously inside the biofilm as a result of pollutant elimination. In a trickling filter, bacteria are usually dominant in pollutant degradation. Fungi may also play an important role. Estevez et al. (2005) inoculated two biofilters fed toluent-polluted air with two fungal isolates and a third one with a defined consortium of fungi and bacteria. For the fungal reactors, the strains remained single dominant

populations throughout the experiment while in the bacterial-fungal reactor; the bacteria were gradually overgrown by the fungi with near complete mineralization of toluene. Weber and Hartmans (1996) also found that under limited conditions the biotrickling filter containing predominantly fungi showed a much higher toluene removal capacity. The competition between bacteria and fungi and the use of fungi in air biotrickling-filter, remains relatively unexplored.

Little has been known about the characterization and architecture of constructed biofilm in biotrickling filter. In aerobic fixed-film or compost bioreactors for toluene, it was observed that a large fraction of the biomass may be inactive and does not degrade toluene (Arcangeli and Arvin 1992; Juteau et al. 1999). Some authors reported significant biomass decay in early growth phase (12 days) of the biofilm in a toluene-degrading biotrickling filter (Pedersen 1997). It has also been indicated that active biofilm layer, into which substrate and oxygen can diffuse does not usually exceed 100-200 μm (Kennes and Veige 2001), and the thickest biofilm on average as usually found closest to the outlet of the biofilters. To understand pollutant mass transfer in biotrickling filter, some techniques have been applied to resolve three-dimensional structures of biofilms. Confocal Laser Scanning Microscopy (CLSM) has been used to visualize fully hydrated biofilm with cell-free channels extending from the surface to the biofilm (Moller et al., 1996). The use of computed axial tomography (CAT) scanning to determine the biofilm architecture of biofilter and biotrickling filters shown heterogeneous interfaces with air/water channels ranging from a few mm^2 to 380 mm^2 (Deshusses and Cox 1998). The development of biofilm structure formed by *Phragmitis communis* was analysed by CLSM. It revealed a network of channels partially occupied by exopolymer structures throughout the biofilm (Calderia et al.). The understanding of structural organization of established biofilm communities may be important for biofilter material and process, and improvement of its function.

Mathematical model

When actual biofilter units are applied in industry, realistic mathematical models are needed to predict biofilter performance. The most widely used model was developed by Ottengraf and van der Oever (1983) because it is easy to obtain the analytical expression from the solution of the model. Van lith et al. (1990) and Dharmavaran (1991) reports design criteria based on this model for pilot-scale biofilter units. Zarook et al. (1991) improved the work of Ottengraf and developed a steady-state biofiltration model for single VOC. They also analyzed and compared those models, for the validation of laboratory-scale experimental data and design of actual biofilters (Zarook et al. 1997) When using single VOC biofiltration model to describe VOC mixture removal, competitive inhibition kinetics should be considered.

Objectives

Multiple studies using different methods have shown the bioremediation of soil, air and wastewater contaminated with toluene, a major constituent of petroleum products (Krishna et al 1999, Vergara-Fernandez et al 2006, Cox and Deshusses 2002). The effects of co-metabolism and substrate inhibition among mixtures (VOCs) in water-gas-phase biofiltration processes are important because most industrial emissions contain a variety of compounds. The presence of nitrile compounds among VOC mixtures creates a challenge to biofilter performance since biodegradation of these xenobiotic compounds requires pathways normally not associated with heterotrophic bacteria. Consequently, most nitrile compounds of environmental concern exhibit recalcitrance and cannot serve as sole carbon and energy sources for heterotrophic bacteria under aerobic conditions. Also, AN degradation (in systems with only AN) is sensitive to AN toxicity and is carbon limited. Nevertheless, these nitrile compounds might be co-metabolized in the presence of a more easily biodegradable hydrocarbon serving as the primary carbon and energy

source. It was hypothesized that the inclusion of a degradable VOC (toluene) would better stabilize and enhance AN degradation.

In the preliminary experiments, *R. rhodochrous* culture showed a significantly greater density (1 log) when growing on nutrient medium supplemented with toluene and AN than nutrient medium alone. Separate experiment clearly showed that the cultures could utilize toluene (C-source) and AN (N-source). However, AN-biotransformation is very sensitive to AN concentration.

Klecka et al. (1996) used a GAC fluidized-bed reactor for the degradation of chlorobenzene in a influent stream at 125-145 mg l⁻¹, with more than 99% efficiency. Moustafa et al (2002) setup a laboratory-scale bioreactor (96.5 cm long, 10.2 cm i.d.) charged with 1.0 kg GAC and successfully treated formaldehyde anaerobically under both continuous and dynamic loading conditions. Formaldehyde removal rates of up to 99.99% were achieved under continuous loading while removal rates ranged from 97.4% to 99.9% under cyclic loading. Treatment of groundwater contaminated with toluene at 2.7 mg l⁻¹ in a GAC fluidized-bed bioreactor was achieved with 99.4% efficiency during steady-state operation, while during shock loading the GAC served to adsorb the compound for subsequent degradation (Shi et al. 1995)

It is hypothesized that effective treatment of AN in the waste water and gas could also be achieved by a biofilter designed based on a carbon-trickling-bed reactor. Since the dynamic change of the contaminant and community activity was not very clear yet, the aim of the study was to measure the parameters and conditions that result in the retention and maintenance of *R. rhodochrous* NHase cell activity, and the kinetics of the trickling bed bioreactor under both recycle batch conditions and single-pass system. For the purpose, a laboratory-scale trickling bed bioreactor was constructed and the biofiltration performance was evaluated and modeled.

Additionally the biofilm properties in the reactor were characterized.

In the study, a lab-scale model biofilter with *R. rhodochrous* strain 96622 cells immobilized on GAC was established. AN wastewater and gas was produced by mixing the AN from the syringe pump and air from the air pump to a desired concentration immediately after being introduced to the column and reaching the packed bed. The combination of toluene (co-treatment) may apply, as toluene may promote cometabolic transformation of AN. During the initial start-up period, the bioreactor was operated as a liquid-continuous batch reactor and the microorganisms were allowed to attach to the carbon surface. The performance of the biofilter for treating AN after shifting from liquid-continuous operation was evaluated and the response toward reaching a new steady state after changing the operating condition was measured. To evaluate steady-state biofiltration performance, the effects of inlet AN concentration and liquid flow rate or empty bed retention time (EBRT, bed volume/gas flow rate) on AN removal efficiency and elimination capacity was tested. It appears that the use of specialized microorganisms to degrade toxic industrial wastes combined with the procedure of adaptation of activated carbon system could be a methodology potentially applicable to industrial waste effluents.

MATERIALS AND METHODS

Microorganisms

Pure culture of *Rhodococcus rhodochrous* strain DAP 96622 was obtained from American Type Culture Collection (ATCC, Vienna, VA). DAP 96622 (ATCC 33278) was deposited as *Nocardia rhodochrous* with the depositor of LP Lechevalier. The culture was revived and initially maintained on yeast extract malt agar at 26 C according to the methods recommended by ATCC. Non-acclimated *R. rhodochrous* grows very slowly in contact with AN and toluene as carbon and nitrogen source as the enzymes are of inductive nature. DAP 96622 were first grown in Stanier's mineral medium (Stanier et al. 1966) with 5 g l⁻¹ glucose and 1g l⁻¹ ammonia sulfate and then acclimated to increased AN concentration up to 500 mg l⁻¹ and toluene concentration up to 1000mg l⁻¹. The acclimated culture at 500mg l⁻¹ AN and 1000 mg l⁻¹ toluene was used as the inoculum for degradation kinetic studies and the reactor start-up.

DAP 96622 was maintained either on yeast extract malt extract medium (YEMEA) (Dietz and Thayer 1980) or Stanier's medium with 5g l⁻¹ glucose and 1g l⁻¹ ammonia sulfate.

Preparation of Media

The required nutrients for the growth of DAP 96622 inoculated to batch flasks and reactor, were provided by a Stanier's mineral medium with the following composition per l of solution: EDTA 2.5 mg, ZnSO₄.7H₂O 10.95 mg, FeSO₄.7H₂O 5 mg, MnSO₄.H₂O 1.54 mg, CuSO₄.5H₂O 0.392 mg, Co (NO₃)₂.6H₂O 0.248 mg, Na₂B₄O₇.10H₂O 0.177 mg, MgSO₄ 289 mg, CaCl₂.2H₂O 66.7 mg, (NH₄)₂Mo₇O₂₄.4H₂O 0.185 mg, FeSO₄.7H₂O 1.98 mg, Nitrilotriacetic acid 200 mg(neutralizer with 146 mg KOH), 3984 mg Na₂HPO₄, 1828 mg NaH₂PO₄. Various

amounts of carbon or nitrogen sources for cell growth, such as glucose, ammonium sulfate, AN and toluene, as well as inducers for enzyme activity, could be aseptically added to Stanier's medium, directly from the stock solution to give desired final concentration.

Kinetic studies of free cells in flasks and immobilized cells in bioreactor

Rhodococcus DAP 96622 cells AN/toluene acclimated was investigated for their ability to degrade AN as sole carbon source. Each 125 ml Erlenmeyer flask containing 30ml Stanier's (with 0.3 mg cobalt and 0.225 g urea) was injected with AN to a desired final concentration of 100-1000 mg l⁻¹ and was inoculated with 5 ml cell suspension made from fresh culture pre-grown on Stanier's agar with AN and toluene. The initial OD of each flask was made around 0.6. Uninoculated flasks were incubated in an incubator shaker (26°C, 150 rpm). Flasks without inoculation were prepared and served as negative control to correct for AN removal due to abiotic loss. Liquid sample aliquots were periodically withdrawn to measure OD and AN concentrations.

Bioreactor setup and operation

1) Design and setup of trickling carbon bed biofilter

The trickling bed reactor was a Plexiglas column [19 cm x 5.5 cm] and had a total working volume of 190 ml (a bed volume of 130 ml and void volume of 60 ml, 6.2 cm bed height). It was filled with approximately 60 g of granular activated carbon (Calgon Filtersorb 300, Pittsburgh, PA) to support biofilm growth and retain organics. To supply nutrients to the cells, the liquid medium was continuously pumped to the top of the reactor and trickled down at a certain flow rate, using a peristaltic pump (model EW-07521-50, Masterflex L/S; Cole-Parmer, Vernon Hills, IL). Air generated by an air pump (DOA-V722-AA, Gast, Benton Harbor, MI) went to the buffer tank to aerate the buffer and also went to the influent tank to vaporize the

organics before they reached the bed. Aerated buffer was pumped to the influent tank and then to the top of the reactor with a peristaltic pump (model EW-07543-30, Masterflex L/S; Cole-Parmer, Vernon Hills, IL). Before the buffer enters the reactor, it carried AN (may also with toluene) pumped out by a syringe pump (Model 22, Harvard Apparatus, Holliston, MA). For the reactor start-up, air flow rates to the buffer tank and the reactor were 2 L/min and 0.15 L/min, respectively, controlled by mass flow meter (GFM 37, Aalborg, NY). Dissolved oxygen (DO) concentrations in the influent and effluent tanks were measured by DO probes (model 4300, Ingold; Mettler-Toledo, Wilmington, MA). DO probes were connected to paperless recorder (RD8900, Omega, Stamford, CT), which was monitoring the changes of DO concentration and temperature. The DO concentration was kept above 6 mg l⁻¹. GAC trap was connected to the top of the column to adsorbed escaped organics (Figure 3).

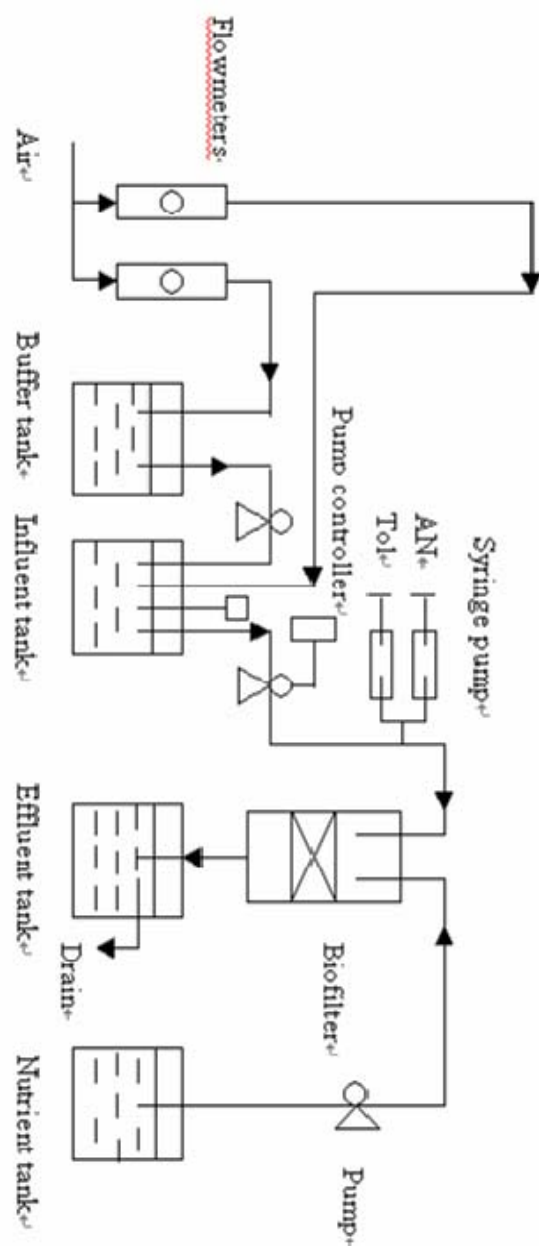


Figure 3. Schematic representation of the experimental set-up.

Table 2. Trickling bed parameters

Parameter	Units	Description
Bed height	cm	Height of media in the column
Bed volume	cm ³	Volume of media (GAC) in the column
Syringe pump flow	μl/min	Digital display on syringe pump
VOC addition rate	μl/min	Syringe pump flow(ratio of our syringe size and syringe size that pump flow is based on)
Media flow rate	ml/min	Pump rate of media
Influent and effluent flow	ml/min	Drip rate of liquid through trickling bed (media flow+recycle)
EBRT	min	Empty bed retention time=bed volume/influent flow rate
Inlet load	g m ⁻³ h ⁻¹	g VOC added to the bed per unit bed volume per hour

Table 3. Experimental setup and initial operating parameters of the biotrickling filter**Design**

Bed height and internal diameter	6.2x5.5 cm
Bed volume	120 ml
Filtering medium	Granular activated carbon F300
Pollutant	Toluene, Acrylonitrile
Microorganisms	<i>Rhodococcus rhodochrous</i> DAP 96622

Operation

Pollutant feed rate	0.01 ml/min(AN:Toluene=1:2)
Aeration rate for buffer	2 L/min
Aeration rate for column	0.15 L/min
Buffer flow rate	19.5 ml/min
Nutrient supply	Fortier (per l): 20 ml Hutner's, 1 g (NH ₄) ₂ SO ₄
Media flow rate	1 ml/min
Temperature	25 C

2) Reactor start-up and operation

A) Initial inoculation of trickling bed

60 g GAC was prewashed and pretreated at 25-27 C by soaking in DI water overnight containing 10,000 ppm toluene and 5,000 ppm acrylonitrile. A trickling bed inoculum was prepared by inoculating *Rhodococcus* DAP 96622 cells from acclimated culture plates to 500 ml Erlenmeyer flasks containing 200 ml R2A broth and incubating in a rotary shaker for 48 h at room temperature. Nutrients and chemical inducers were added to the flasks as described in the feeding schedule (Table 4). The cells were harvested in 50 ml Falcon conical tubes by centrifuging at 5000 rpm for 20 min (IEC HN-SII Centrifuge, International Equipment Company) and washed with sterile Stanier's broth without ammonium sulfate for three times. The remaining pellet weight was recorded. The pellet was suspended in 20 ml Stanier's broth without ammonium sulfate. The suspension was then introduced to the reactor and retained for several minutes to allow the cells to adhere to GAC. The liquid was then drained and poured back into the bed, soaking for 30 minutes. After that the valve on the bottom of the column was opened, and the mass flow began.

Table 4. The feeding schedule of nutrients and chemical inducers for preparation of a trickling bed inoculum culture

Time		Media (ml)	Urea (g)	CoCl ₂ (mg)	Cocktail* (ml)	Amidase inducer solution (Acrylamide/Acetamide)(ml)
0	Nitrile hydratase	5	1.5	2	1.3	
	Amidase	5	1.5	2		5
18 h	Nitrile hydratase	4			1.3	
	Amidase	4				1.3
21h	Nitrile hydratase				0.6	
	Amidase					0.6
25h	Nitrile hydratase	4			1.3	
	Amidase	4				
42h	Nitrile hydratase	2			1.3	
	Amidase	2				
46-48h	Harvest					

*Fortier cocktail was made by adding 3.82 ml acetonitrile, 3.72 ml acrylonitrile, 1.015 g succinonitrile and 0.02 N NaCN to 100ml DI water. The solution was filtered, wrapped with parafilm and stored in 4C.

*Amidase inducer solution was made by adding 2.212 g acetamide and 1.988 g acrylamide to 50 ml DI H₂O. The solution was filtered, wrapped with parafilm and stored in 4C.

B) Biofiltration study ---Batch-mode reactor

After inoculation, the reactor was operated as a liquid-continuous, batch reactor with recycled Stanier's medium to allow cell growth and attachment on the carbon surface. The composition of the recycled nutrient medium (500 ml) in the reservoir was: 10 ml Hutner's; 20 ml 1M PBS (pH: 7.0); 3.75 g Urea; 5 mg Cobalt and 470 ml DI H₂O. The flow rate might vary and the temperature was kept at 23~27 C. AN and toluene was periodically added to the recirculation bottle to allow continuous growth and biomass buildup. Samples were periodically withdrawn for measuring optical density, viable cell numbers and organic removal. After 1 month, carbon particles was taken from the upper section of the column and examined by

scanning electronic microscope. Microbial identification of the organisms attached to the surface of the carbon was also performed.

When the reactor reached steady state, kinetic studies were begun. AN and Tol (w:w=1:2) was injected to the recirculation bottle using microsyringe to a desirable concentration. Liquid samples were taken out of the recirculation bottle to monitor the AN concentration change. When substrate in the bottle was depleted, new substrate was injected to the bottle to start a new batch. Kinetic studies started from a low concentration of $\sim 50 \text{ mg l}^{-1}$ and the concentration was gradually increased to $\sim 1150 \text{ mg l}^{-1}$. The degradation rate (determined from the initial or maximum slope of the concentration curve) and specific growth rate (determined from the slope of semi logarithmic plot of OD vs. time) was compared with those of free cells grown on AN in the flasks.

C) Biofiltration study---Single-pass mode reactor

a) AN-toluene mixture (flow rate 1:8 from syringe pump)

When the biofilter showed a high removal efficiency of AN and Tol and reached the steady state, it was shifted from liquid-continuous mode to single-pass mode. AN and Tol waste water and gas was produced by mixing AN and Tol vapor from pure liquid AN in the syringe pump and aerated buffer to a desired concentration. Stanier's liquid medium was trickled down to the bed from the top of the reactor, at a rate of 1ml/min.

a1 Effect of inlet AN and Tol concentration (C_{in} , ppm) on the removal efficiency and elimination capacity

The removal efficiency (%) was tested at various inlet AN and Tol concentration under a constant EBRT of 6 min or liquid flow rate of 10 min. The elimination capacity (ppm/h) (the amount of AN and Tol removed/empty bed volume of medium) at different AN and Tol

concentration was also tested.

a2 Effect of volumetric liquid flow rate (Q , ml/min) on the removal efficiency and elimination capacity

The removal efficiency (%) and elimination capacity was tested at various liquid flow rates or EBRT under a constant AN and Tol concentration of 500 mg l^{-1} and 1000 mg l^{-1} , respectively.

a3 Effect of inlet load ($IL=C_{in}/EBRT$) on the removal efficiency and elimination capacity

The removal efficiency (%) was tested at various loading capacities under a constant AN and Tol concentration of 500 mg l^{-1} . The elimination capacity at different loading capacities was also tested.

a4 Effect of environment factors on the removal efficiency

AN biodegradation by pure culture of *Rhodococcus* was evaluated in 300ml closed shaken flasks at various pH (6.5-9.0) and temperatures (4-37 C). The flasks were loaded with 30ml Stanier's medium with 0.3 mg cobalt and 0.225 g urea. 1g/l AN was added and 0.3ml of the culture was inoculated. For pH optimization test, the desired pH values of Stanier's medium were set before inoculation. The flasks were incubated at room temperature for 48h. For temperature optimization, the flasks were incubated for 21h in incubators with different temperatures. AN removal and biomass production (OD and dry weight) was measured at the end of incubation. For dry weight, the wet biomass was placed on aluminum boats and put into 100 C incubator for 24h before being weighted again.

b) AN as single feed

The reactor performance in steady-state conditions when AN was the single feed was evaluated for two EBRT: 8min and 4min. AN flow rate from syringe pump was gradually increased from 0.2 to 1.0 $\mu\text{l}/\text{min}$.

Calculation

The experimental results were expressed in terms of the AN inlet load, IL (ppm/h); the elimination capacity, EC (ppm/h); the biofilter removal efficiency, RE (%). These process parameters were calculated according to equations below:

$$\text{Empty Bed Retention Time (EBRT)} = \text{Bed volume (Void)} / Q$$

$$\text{AN inlet load (IL)} = QC_{\text{in}}/V \text{ or } C_{\text{in}}/\text{EBRT}$$

$$\text{Removal efficiency (RE)} = (1 - C_{\text{out}}/C_{\text{in}}) * 100\%$$

$$\text{Elimination capacity (EC)} = Q (C_{\text{in}} - C_{\text{out}})/V$$

Where C_{in} was inlet concentration of the organics (ppm) and C_{out} was outlet concentration of the organics (mg l^{-1}). V was the volume of the filter bed (ml).

Biofilm cell activity

The biofilm activity was determined in samples removed from the upper, middle and lower sections of the reactor, respectively. 3 g GAC was taken out of the each section of the column rinsed with PBS for three times. The matrix was placed in flasks containing 20 ml of Stanier's minimum medium, incubated at 25 C and vigorously stirred to homogenize the suspension for 1 min. DO was measured using DO electrode. DO electrode was immersed in the suspension and the DO decay was recorded in the course of time, depending on the biofilm activity. Before adding the carbon source, the DO consumption rate caused by the biomass endogenous respiration, was determined. After that, a given volume of AN was added to the suspension in order to get a concentration of 50 mg l^{-1} . After a short period for the electrode

stabilization, the DO concentration was recorded again in the course of time. The increase in the DO consumption rate this time is due to the AN respiration and oxidation. Alcohol washed carbon without biofilm was used as the control. CO₂ was measured by Micro-Oxymax respirometer (Columbus Instrument, Columbus, OH)

Measurement of biofilm density and amount of biomass

Wet weight of the biomass was determined by measuring the volume of water necessary to fill the empty spaces between the support particles before and after the biomass attachment. Dry weight of the biomass was determined using filtering samples (15-25 ml) followed by 5ml of distilled water through pre-weighted dried cellulose acetate membrane filter. The filters were dried overnight at 105 C and cooled for 1h in a desiccator before being weighted again.

Adsorption and bioavailability test

50 ml Falcon tubes containing 0.2 g GAC with 30 ml Stanier's containing AN at 200-2000 mg/l. Tubes were placed in a rotary shaker at room temperature. After 24 h, samples were taken and centrifuged at 3000 rpm for 15 min and the amount of unbound AN in the supernatant was analyzed by gas chromatography. To determine the bioavailability of AN after adsorption to GAC, five flasks containing 10 g GAC and 600 ml of Stanier's containing different concentrations of AN (180-3600 mg l⁻¹, which equaled to 10.8-216mg AN g⁻¹ GAC) were incubated for 24 h at room temperature with gentle shaking, before adding an inoculum (10 ml cell suspension of *Rhodococcus* pre-grown on AN). The flasks were then incubated statically to allow biofilm development. Ammonia release, pH and AN concentration was measured periodically. Control without inoculum containing 1000 mg l⁻¹ AN was set up for calculating the loss of AN during the incubation.

To investigate adsorption, desorption and degradation of AN in the GAC bioreactor column, the column was first inoculated with AN batch-grown *Rhodococcus* DAP 96622, introduced by peristaltic pump. The reactor was operated as recirculation mode for 3 days to allow cell attachment. The decrease of OD was an indication of biomass loading. On the forth day, cell suspension in the reservoir was poured out and the column was washed 3 times using 500 ml 50 μ M PBS before fresh medium was filled into the reservoir. Over a 3-week period, gradually increased amount of AN was injected to the reservoir, with a EBRT of 15 min. In open mode operation, feeds of medium with different AN concentration or flow rate were passed through the column. The feeding periods occurred from day 24 to 26, day 46-48 and 66-68, with EBRT of 15 min, 8 min and 45 min, respectively. AN and ammonia amount in the reservoir was measured. At day 50 when two open mode and two batch mode had been done, reactor samples of GAC was taken from 2 or 3 randomly selected locations of upper, middle and lower section of the carbon column for confocal laser scanning microscopy.

Electron Microscopy

1) Scanning electron microscopy (SEM)

Distribution of microorganisms on the carbon surface was analyzed by microscopic examination of the biofilm. Carbon particles are taken from the upper section of the column. Samples were prepared referring to standard protocol (Bozzola and Russell 1999). The samples in 0.1M sodium cacodylate buffer (Electron Microscopy Science, Ft. Washington, PA) were fixed using 3% glutaraldehyde for 1 hour at room temperature. Then they were rinsed 15 minutes for three times in 0.1M sodium cacodylate buffer and post fixed in 1% osmium tetroxide in 0.1 M sodium cacodylate buffer for 1 hour at room temperature. After that, they were dehydrated in a grades series of ethanol dilutions (30%-100%) and infiltrated with

hexamethyldisilazane (Electron Microscopy Science, Ft. Washington, PA) and air dried. Finally, the samples were mounted on aluminum stubs and the sputter was coated with a gold/palladium alloy and examined using a Leo 1450 VP SEM.

2) Confocal laser scanning microscopy (CLSM)

GAC particles were taken from the reactor column and adsorption test flasks and stained with acridine orange, 0.005(w/v) in phosphate buffer (pH 7.2). Images of biofilms were generated by CLSM (Zeiss LSM510 Confocal Microscope, Carl Zeiss Inc. Thornwood, NY). The pinhole was set to 108 μm and excitation was obtained by using the 488-nm line. Sampling of the fluorochrome was achieved with a LP505 filter. Samples were examined in horizontal (x,y) and sagittal (x,z) planes as optically thin sections (1.0-1.1 μm). Images were optimized by adjusting the brightness and contrast settings. Stacks of images were analyzed and a number of variables characterizing the three-dimensional structures were calculated by COMSTAT, which was written as a script in MATLAB 5.3 (The Math Works Inc., Natick, MA).

Analytical Methods

1) Organic

AN and toluene were extracted from the medium using methylene chloride-methanol (85:15 (v/v)) based on EPA method 8031. Liquid sample extractions were analyzed using gas chromatography (HP5890, series II, Palo Alto, CA) equipped with a fused silica megabore column (75 m in length, 0.53 mm i.d., 3 μm film; DB-624, Agilent, J&W, Palo Alto, CA) and a flame ionization detector. Helium was used as the carrier gas at a flow rate of 18 ml/min. The temperature for column, injector and detector are 300 C, 300 C, 250 C, respectively. 0.5 μl sample from the extraction was injected with a liquid tight microsyringe (Agilent 5181-1273). The detection limits for AN and tol were 10 mg l^{-1} and 5 mg l^{-1} , respectively.

2) pH

pH of the liquid was measured directly using a ORION pH-meter, model 230A. For column GAC pH measurement, the trickling bed was opened and 2-3 g of column GAC was sampled into 40 ml vial. 5 ml of DI H₂O was then added and the vial was sonicated for 1 min. After 10 min for particulate to settle, pH was recorded after pH meter has stabilized.

3) Biomass

OD of the liquid sample taken from the recirculation bottle was measured spectrophotometrically (Spectrophotometer, Turner SP-830) at 600 nm. Total viable cell count and *Rhodococcus* DAP 96622 cell count was done in three types of media: R2A (BD, Sparks, MD) for heterotrophs, Stanier's with 5 g l⁻¹ glucose and 1 g l⁻¹ ammonium sulfate and Stanier's with 500 mg l⁻¹ AN and 1000 mg l⁻¹ toluene for specific carbon degraders. Samples periodically taken from the recirculation bottle were 10x diluted serially in 50mM sterile PBS (pH 7.0) and 100 µl dilution was placed in plates and spread evenly on the agar surface. All of the plates were turned over and incubated at 30C. R2A and Stanier's with glucose and ammonium plates were counted after 48 h, and Stanier's with AN and toluene plates were counted after 5 days.

4) Ammonia assay

Ammonia concentration was determined by the method of Scott and Fawcett (1960). Culture sample was centrifuged for 2 mins at 13,000 rpm (eppendorf centrifuge 5415D, Hamburg, Germany) and 1 ml supernatant was then transferred to a fresh microcentrifuge tube. Working amidase solution was prepared from a commercial solution (Sigma A-6691, 1000 units in 0.07 ml) by diluting it in phosphate buffer (vortexed for 30 secs) to a final concentration of 2.5 units amidase in 10 µl buffer. One unit of amidase was defined as the amount of enzyme that catalyzed the conversion of 1µM /min of AMD to 1 µM acrylic acid and 1 µM ammonia at 37 C,

pH 7. To each sample, 95 μ l of 8 M NaOH solution was added to neutralize acrylic acid and bring the pH back to 7. 10 μ l (2.5 U) of the working enzyme solution was added to each sample. Each vial was immediately vortex for 30 secs to ensure thorough mixing of the enzyme. The vials were then incubated at 37 C for 10 min to ensure conversion of all formed AMD to acrylic acid and ammonia. After incubation, 1ml sample was transferred to 15 ml clean glass tube and 2 ml sodium phenate (25 g phenol in 800 ml DI water, with 78 ml of 4 N NaOH), 3 ml 0.01% sodium nitroprusside (1 ml 1% stock solution in 99 ml DI H₂O) and 3 ml 0.02N sodium hypochlorite [2.44 ml Ultra Chlorox bleach (6.15% sodium hypochlorite) in 100 ml DI H₂O] were added and mixed. The reaction tubes were then incubated at 27 C in dark for 30 min. The absorbance at 630 nm was read by spectrophotometer and the ammonia concentration was determined against a standard curve of ammonium sulfate (0-5 mg l⁻¹). Figure 4 shows the standard curve of ammonia assay.

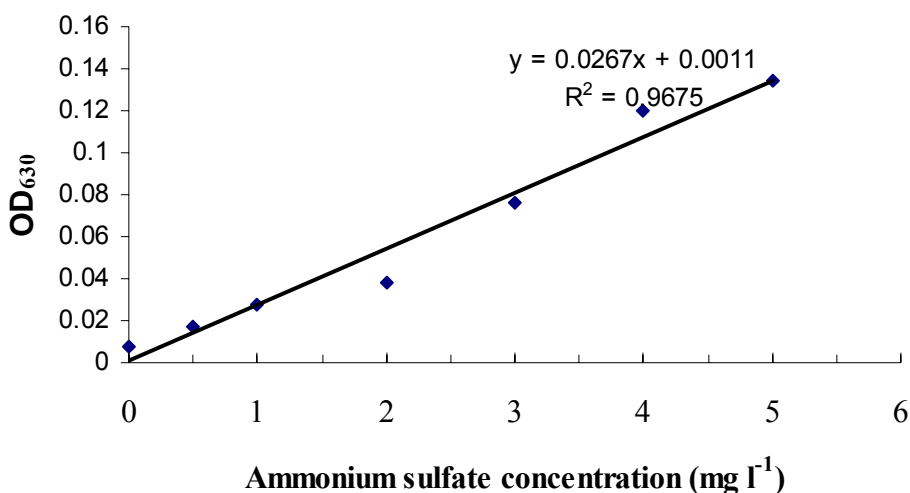


Figure 4. Ammonia assay: standard curve

RESULTS

Morphology and physiological characterization

Rhodococcus rhodochrous DAP 96622 exhibited colonies which were pale yellow to salmon-pink and with 1-3 mm diameter when grown on YEMEA solid medium. The colonies were dry, opaque, slightly raised and wrinkled when viewed by naked eyes. Time course studies showed a progressive change from distinct bacillary forms in nutrient broth to distinct cocci on solid media. Microscopic evaluations showed substrate mycelium formation on solid medium with no aerial mycelium or conidia produced. This distinguishes *Rhodococcus* from *Nocardia* and *Mycobacterium* among nocardioform actinomycetes. Table 5 presents certain specific strain characteristics of *Rhodococcus rhodochrous* DAP 96622.

Growth curve and effect of different substrates/substrate concentrations

Figure 5 shows the growth of *R. rhodococcus* DAP 96622 on 500 ppm AN, in the situation 1) with 1000 ppm toluene, Fortier cocktail (3.82 ml acetonitrile, 3.72 ml AN, 1.015 g succinonitrile and 0.02 N NaCN in 100 ml DI water) and amidase inducer solution (2.212 g acetamide and 1.988 g acrylamide in 50 ml DI H₂O); 2) without toluene but with cocktail and amidase inducer solution; 3) without cocktail and amidase inducer solution but with 1000 ppm toluene; 4) without either toluene, cocktail or amidase inducer solution. At the first 250 h, the cells in the situations 1 and 3 grow faster than those in situations 2 and 4. After that, growth of cells in the situation 2 speeded up at almost the same rate as that in the situation 1 until they reached the same level, while cells in situation 4 remained a low growth rate all the time. This suggests that regardless of toluene, the presence of cocktail and amidase inducer may be very important to the cell yield. AN by itself is a poor substrate. In the presence of other carbon sources (toluene and mixed cocktail), growth is improved. The lag phase was relatively shorter

when supplemented with 1000 ppm toluene, indicating that toluene could be a rate-limiting factor in the process.

R. rhodococcus DAP 96622 showed a significantly greater density (1 log) when grown on Stanier's mineral medium supplemented with toluene and AN than nutrient medium alone. Separate experiment clearly showed that the culture could utilize toluene (C-source) and AN (N-source). However, AN-biotodetoxification is very sensitive to AN concentration. Fig.6a shows growth of *R. rhodococcus* DAP 96622 on different concentrations of AN in the presence of 1000 ppm Tol. In some specific time points the cell density decreased with increasing the AN concentration, however, at the exponential phase, the cell growth rates were almost the same for AN concentration from 100 ppm to 1000 ppm and they all achieved a high cell density after 15 days. The slowest growth on 1000 ppm AN at the beginning was observed, which could be due to the substrate inhibition of excessive AN. From Fig. 6b, μ_{\max} and K_s were determined to be 0.021 h⁻¹ and 160 ppm, respectively.

Table 5. Characteristics of *Rhodococcus rhodochrous* DAP 96622.

<i>Rhodococcus rhodochrous</i> strain DAP 96622	
Differential Characteristic	Result
Catalase/Oxidase	(+)/(-)
Citrate Utilization	(+)
Triple sugar iron agar	no change
<u>Growth at</u>	
5 C	(-)
10C	(+)
25C	(+)
40C	(+)
45C	(-)
<u>Utilization of</u>	
Glucose	(+)
Lactose	(+)
Maltose	(+)
Arabinose	(-)
Sorbitol	(+)
Na-azide	(+)
Na-benzoate	(+)
Nitrate production	(-)
Gelatin hydrolysis	(-)
<u>Antibiotic resistance</u>	
Streptomycin	
Ampicillin	S
Gentamycin	S
Tobramycin	S
Penicillin G	S
Tetracycline	S
Carbenicillin	S
Kanamycin	S
Fluconazole	R
<u>Utilization of carbon and nitrogen</u>	
Acrylonitrile	(150ppm/300ppm) (+)/(+)
Acetonitrile	(150ppm/300ppm) (+)/(+)
Succinonitrile	(150ppm/300ppm) (+)/(+)
Fumaronitrile	(150ppm/300ppm) (+)/(+)
Acrylonitrile /Acetonitrile/Succinonitrile	(150/300ppm ea) (+)/(+)
Acrylonitrile /Acetonitrile/Fumaronitrile	(150/300ppm ea) (+)/(-)
Acetamide	(150ppm/300ppm) (+)/(+)

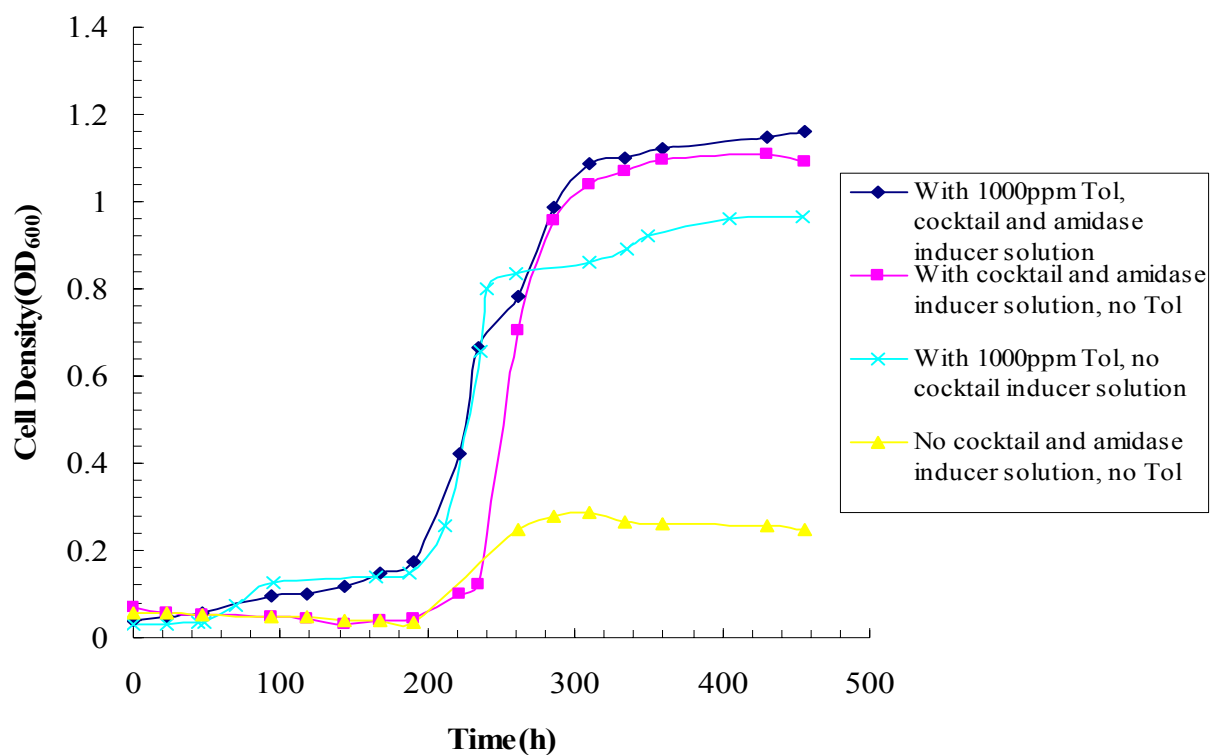


Figure 5. Growth of *Rhodococcus rhodochrous* DAP 96622 on 500 ppm AN.

Table 6. Average and maximum growth rate for different situations

Situations	Toluene (1000ppm)	Cocktail and amidase inducer solution	Average cell growth rate (h^{-1})	Maximum cell growth rate (h^{-1})	t_D max, hr
1	+	+	0.0032	0.019	36.5
2	-	+	0.0025	0.021	33
3	+	-	0.0038	0.028	25
4	-	-	0.00016	0.0029	239

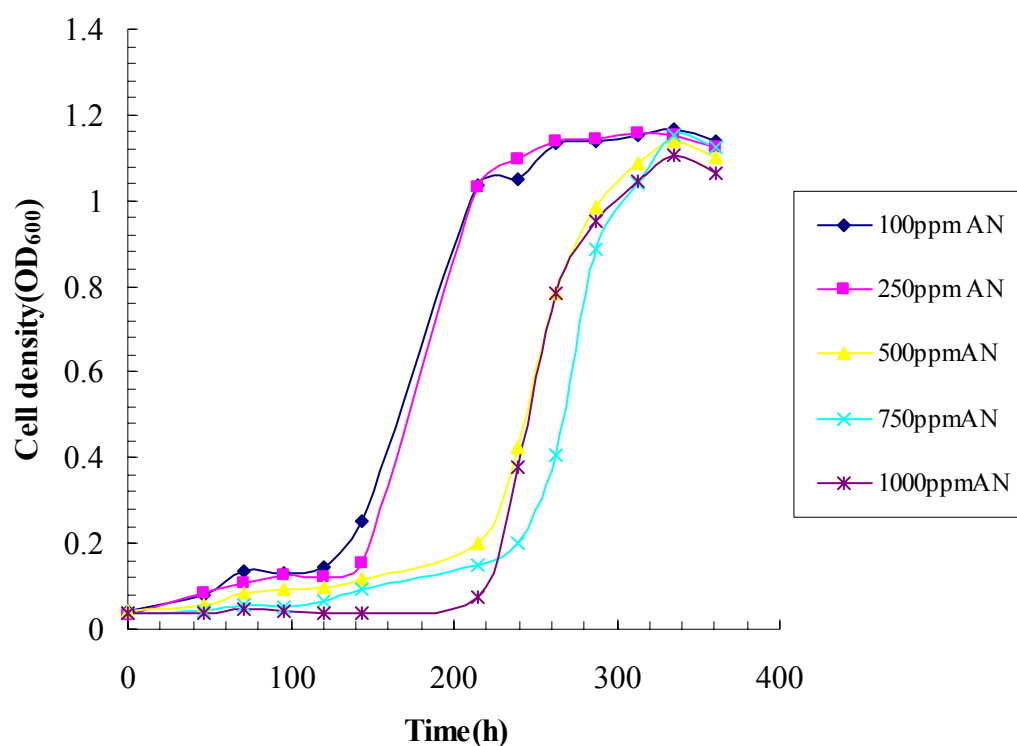


Figure 6a. Growth of *Rhodococcus rdohochrous* DAP 96622 on different concentrations of AN in flasks (with 1000 ppm toluene, urea, cobalt, cocktail and amidase inducer solution).

Table 7. Concentration of carbon, C/N ratio, average and maximum cell growth rate for different AN concentrations in flasks.

AN concentration (mg l ⁻¹)	Concentration of carbon present (mg l ⁻¹)	C/N ratio	Average cell growth rate (h ⁻¹), μ_g	Maximum cell growth rate (h ⁻¹), μ_{max}
100	978	38:1	0.0020	0.011
250	1080	17:1	0.0017	0.012
500	1250	10:1	0.0035	0.015
750	1420	7:1	0.0037	0.020
1000	1590	6:1	0.0035	0.017

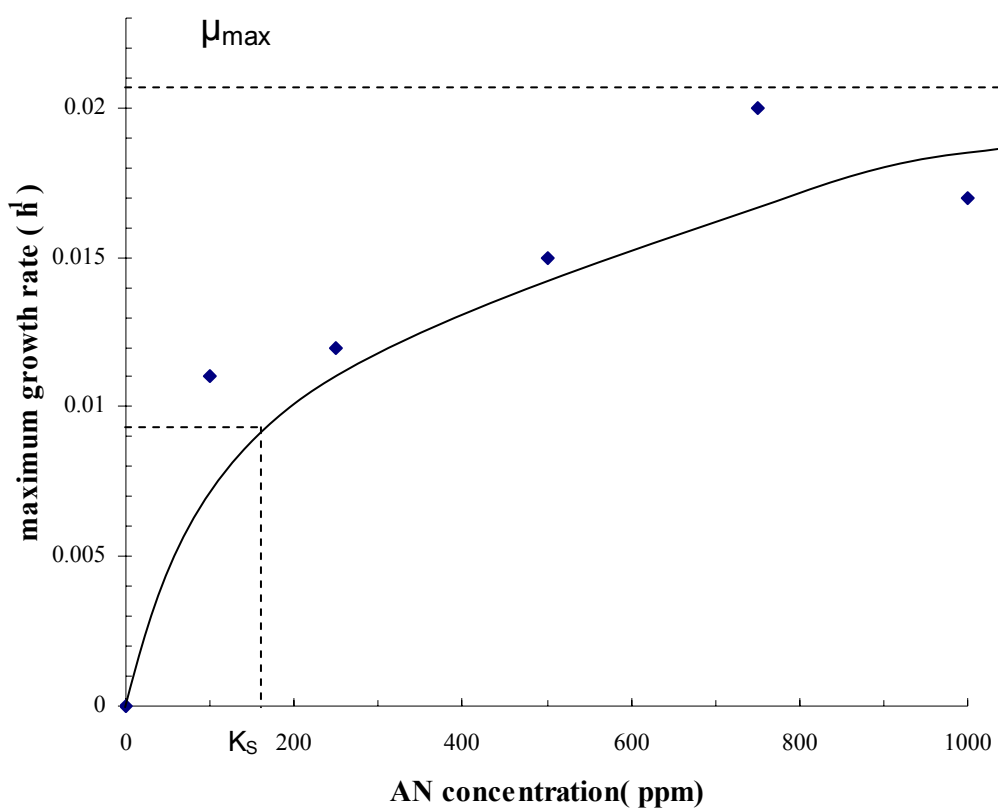


Figure 6b. AN concentration vs. maximum growth rate.

Kinetics studies of free cells in flasks and immobilized cell in the bioreactor

Batch studies were carried out under aerobic conditions using *R. rhodococcus* DAP 96622 acclimated with AN and Tol. The effect of substrate concentration on degradation rate and specific growth rate of free cells grown on AN in flasks are shown in Figure 7, both growth rate and biodegradation rate increased with increasing the AN concentration up to 500ppm and then decreased, showing kinetic inhibition. The apparent inhibition was more severe to growth rate than to degradation rate.

For immobilized cells in the batch-mode trickling bed bioreactor with toluene present (AN:Tol=1:2), the trends of response of cells to different AN initial concentrations was similar to that seen with free-cells kinetics, in that as the substrate concentration increased, the growth and degradation rate also increased until the substrate reached a particular concentration. The degradation rate started declining with increase in substrate concentration after that. However, there is a significant difference in the actual rates. The maximum growth and degradation rate was 0.019 h^{-1} and $115 \text{ mg l}^{-1} \text{ h}^{-1}$, respectively for immobilized cells, compared with 0.0035 h^{-1} and $0.75 \text{ mg l}^{-1} \text{ h}^{-1}$ for free cells (Figure 7 and 8). This demonstrates that the immobilized cells were able to degrade a higher substrate concentration more efficiently and yield a much higher amount of biomass, as compared to the free cells.

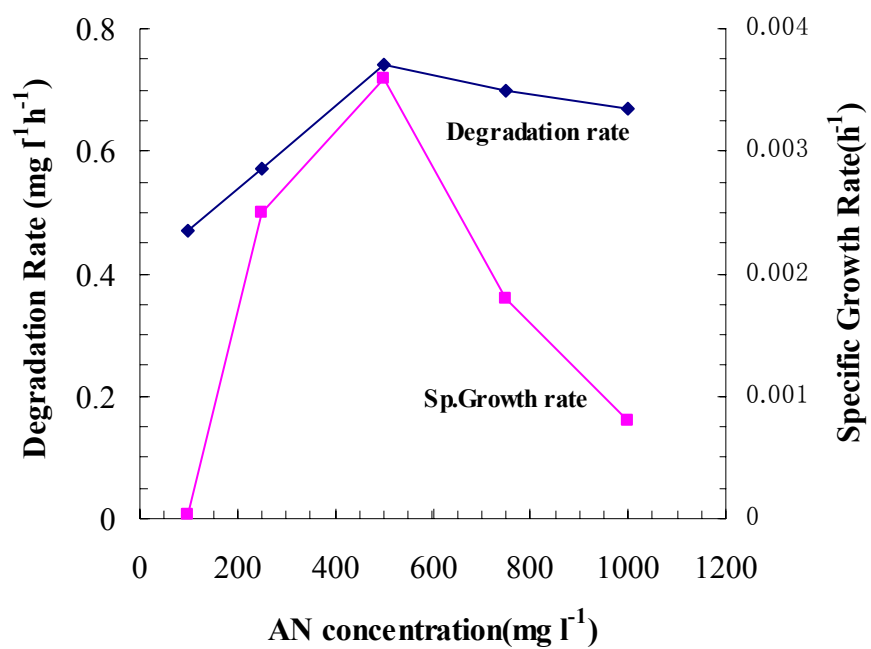


Figure 7. Effect of substrate concentration on degradation rate and specific growth rate for free cells grown on AN in flasks.

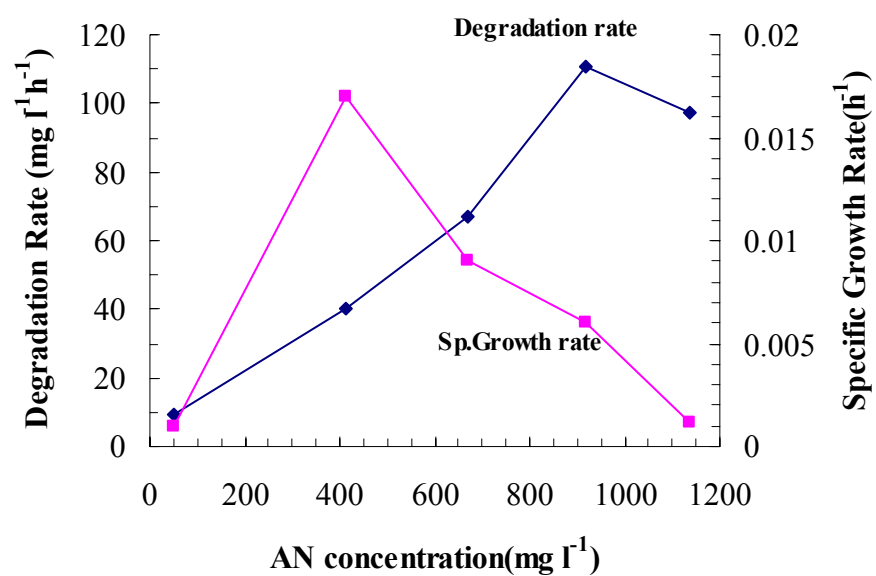


Figure 8. Effect of substrate concentration on growth rate and degradation rate of immobilized cells grown on AN in the feed-batch mode carbon-bed bioreactor (toluene is present).

Fed-batch-mode reactor

1) Start-up of fed-batch mode

20 ml *R. rhodococcus* DAP cell suspension (containing 50 mg wet weight cells) was inoculated and the reactor was operated in a continuously recycled mode, batch reactor with Stanier's medium containing an initial fed AN and Tol concentration of ~ 300 and ~ 1000 mg l⁻¹, respectively. Total liquid volume recycled was 500ml and the run last for 15 days. Liquid samples from the reservoir were periodically withdrawn to measure cell OD and determine AN and Tol concentrations. Within the start-up there was a lag phase of 6 days occurred before notable changes could be observed, for cells had to adapt or respond to the environment. After the initial adaptation phase the cell density began to increase exponentially reaching its maximum at day 12. Degradation occurred as cell grew and attached to GAC. Both AN and Tol were depleted after 5 and 9 days, respectively, while cell growth just began on day 6 (Figure 9). Cell growth didn't stop until 4 days after no organics were detected in the recirculation bottle. It could be assumed that the small portion of AN and Tol which could have been absorbed by the activated carbon may leach out very slowly and was later bioavailable and supported cell growth.

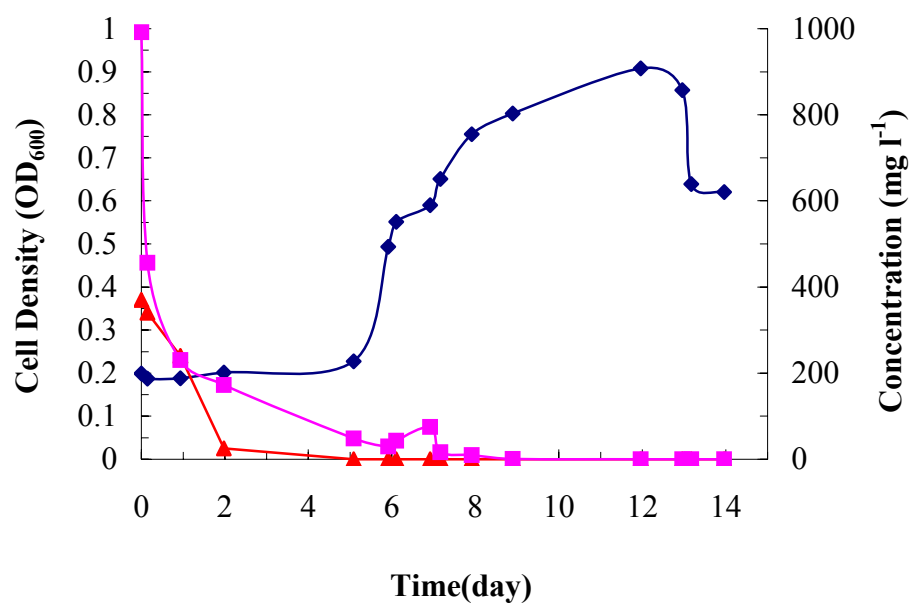


Figure 9. Cell density profile, and kinetics of AN and Tol degradation in batch-mode reactor. (♦) OD; (■): Tol concentration. (▲)AN concentration.

Plating were performed to characterize the process culture in the recycle medium. Over the course of the initial start-up, samples of the recycle reservoir were taken and plated on complex medium (R2A) and Stainier's medium Tol and AN as sole carbon source and AN as sole nitrogen source. Only culturable organisms can grow on selected media. This may constitute a small fraction of the total population in the biotrickling filter. The results in Table 8 indicate that Tol/AN degraders predominate and almost all culturable heterotrophs are AN and Tol degraders. At the beginning, *Rhodococcus* was the dominant species because it was the only inoculum. After 2 or 3 days, *Rhodococcus*' portion in total cells decreased for it had to compete with other species from the outside environment which were able to use either AN metabolites or Tol as carbon and nitrogen source (Figure 10& Table 8). After 166 h, *Rhodococcus*' number was recovered a little and actually *Rhodococcus* is only a small percentage of TOL/AN degraders. Three different types of colonies were visible on solid medium inoculated with a sample from the bioreactor including *Rhodococcus*, *Pseudomonas* and *Bacillus*. It could be assumed that toluene was depleted at that time and only *Rhodococcus* which could feed on AN was able to grow. Nitrile became the selective pressure at this situation.

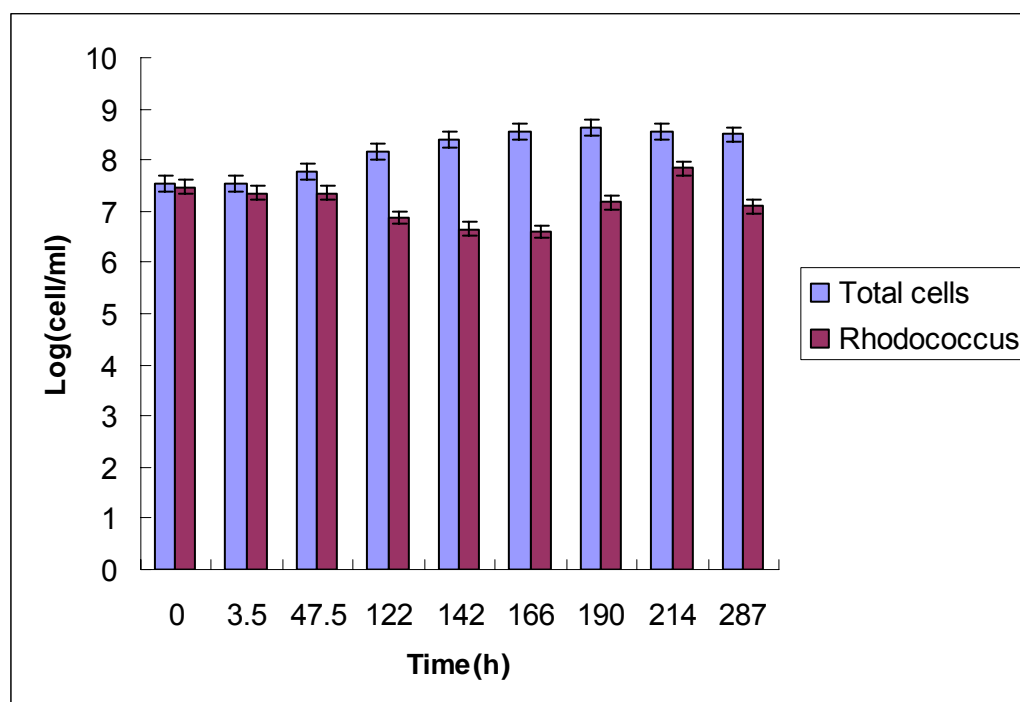


Figure 10. Viable cell counts vs. time on Stanier's agar with AN and toluene at the start-up of feed-batch mode bioreactor.

Table 8. Counts (log counts/ml) of microbial populations in the recycle liquid on different media at the start-up of feed-batch mode bioreactor.

Population (log CFU/ml) Time(h)	R2A			Stanier's+glucose +(NH ₄) ₂ SO ₄			Stanier's+AN+Tol		
	Total cells (heterotrophs)	<i>Rhodococcus</i>	% Rhodo- coccus	Total cells	<i>Rhodococcus</i>	% Rhodo- coccus	Total cells (AN, Tol degra ders)	<i>Rhodococcus</i>	% Rhodo- coccus
0	7.83	7.79	91	7.91	7.91	100	7.54	7.48	87
22.5	7.46	7.30	69	7.64	7.57	85	7.54	7.35	65
47.5	7.99	7.72	54	7.94	7.86	83	7.77	7.35	38
122	8.25	7.37	13	7.66	7.28	42	8.16	6.88	5.2
142	8.51	7.22	5	8.53	7.26	5	8.40	6.65	1.7
166	8.70	ND*	ND	8.19	6.48	2	8.57	6.60	1.1
190	8.80	7.18	2	8.62	7.93	20	8.64	7.18	3.5
213.5	8.65	ND	ND	8.17	ND	ND	8.56	7.85	19
287	8.42	ND	ND	8.33	7.48	14	8.50	7.10	4.0
311	8.98	ND	ND	8.53	ND	ND	7.78	ND	ND

*ND: Non-detectable

Scanning electron micrographs of cells on the carbon support after one-month's batch operation are shown in Fig 11a & b. The reactor showed a good ability in degrading AN and Tol in the liquid medium and a thin layer of biofilm containing evenly distributed cells attached to the carbon particles. Some cells formed large clumps and were present in the void space of the porous carbon matrix. Mostly rods but other morphological forms were visible. Also visible was a well developed "glycocalyx"-like matrix.

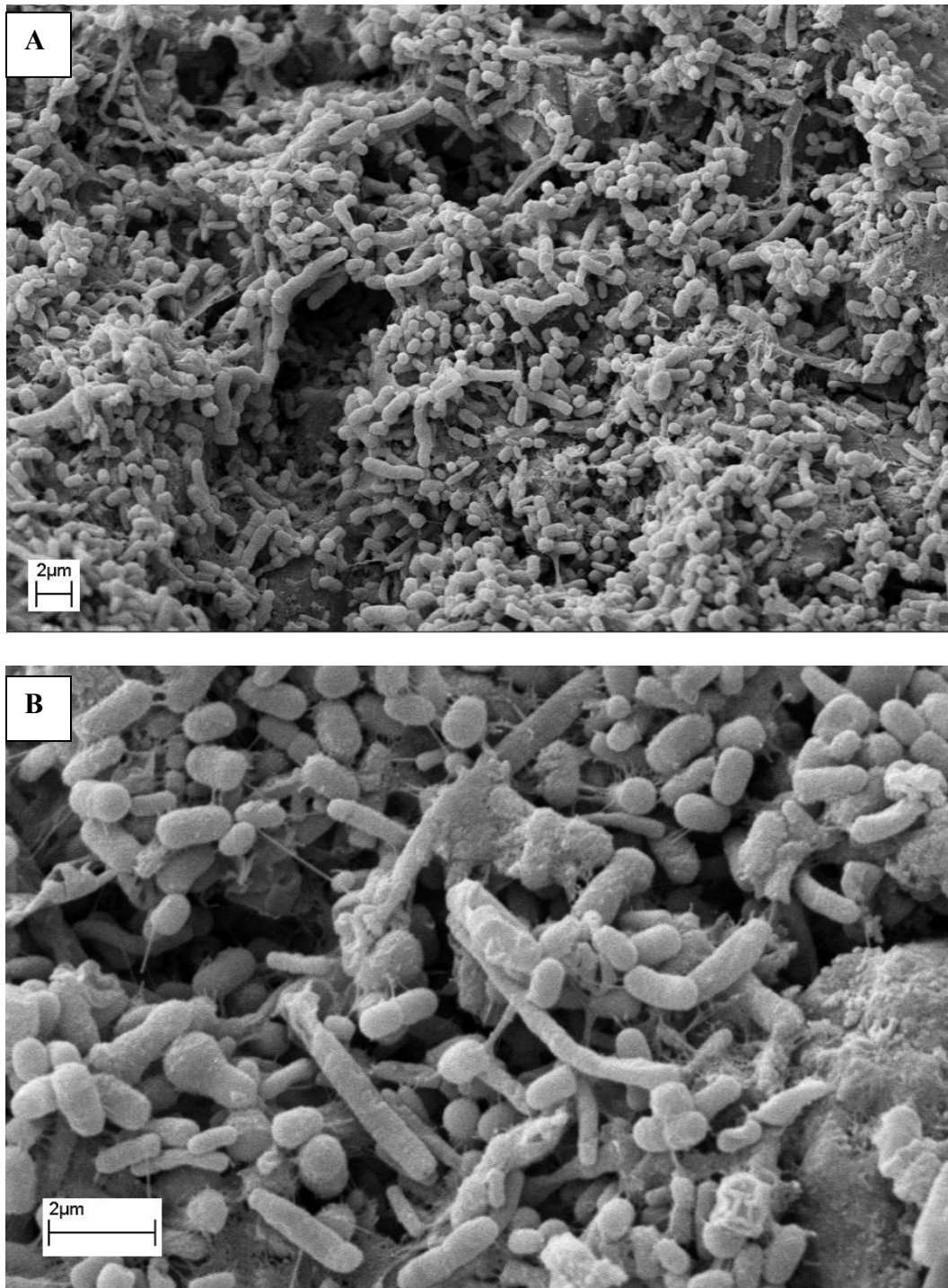


Figure 11. Scanning electronic microscopic image of the biofilm: A) 5,000x magnification and B) 15,000x magnification.

2) Effects of different AN and toluene flow rates on batch-mode reactor performance

Four different flow rates of AN and toluene in fed-batch mode reactor were tested. The conditions and the results are shown in Table 9 and in Figure 12-14. The mixtures of AN and Tol were supplied continuously to the top of the column for ~12 days. The liquid empty bed retention time (EBRT, bed volume/liquid flow rate) was set for 6 min and the bioreactor reached steady state after two or three days. Almost complete AN removal (>95%) was achieved at an organic load of 0.1 µl/min AN and 0.8 µl/min toluene (0.32g AN l⁻¹ day⁻¹ and 2g toluene l⁻¹ day⁻¹). The reactor efficiency was decreased to below 80% when the AN load was increased to 0.8 µl/min while toluene load was not changed (Figure13&14). Cell density profile with different flow rates of AN and toluene in feed- batch mode bioreactor shows consistence with the removal efficiency (Figure 12). Basically, AN removal rate decreased with increasing the loading capacity because of the insufficient contact between the organics and the biofiltration medium in the biofilter. For toluene, the removal efficiency could reach nearly 100% within 2 days.

Table 9 AN and Tol removal efficiency with different flow rates of AN and toluene in fed-batch-mode bioreactor.

Flow rate		AN removal (steady state) (%)	Tol removal (steady state) (%)
AN(µl/min)	Tol(µl/min)		
1	0	90-98	--
0.4	0.4	80-90	90-99
0.8	0.8	72-82	93-100
0.1	0.8	95-100	94-98

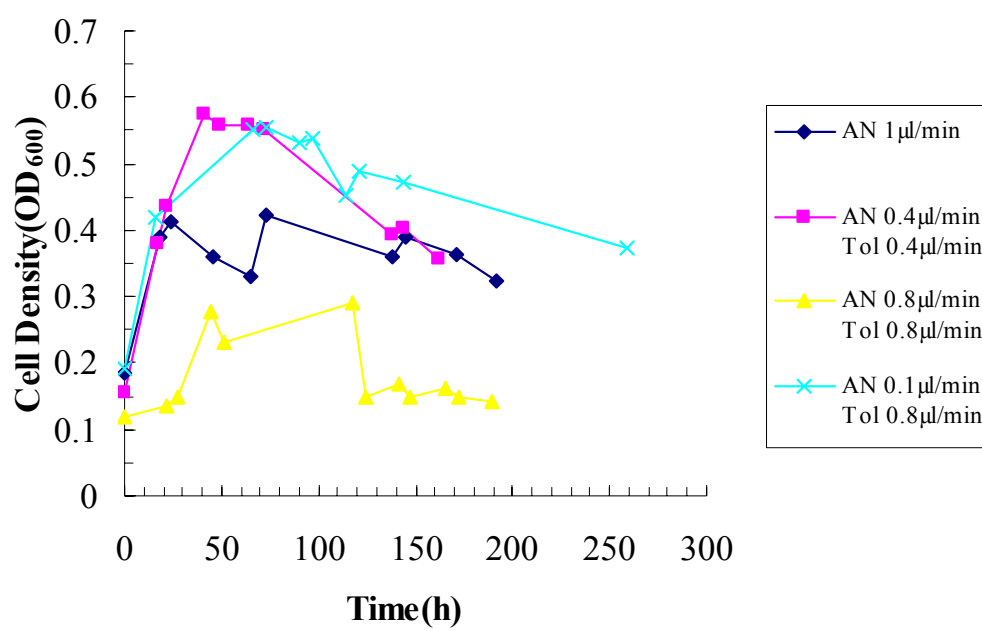


Figure 12. Cell density profile with different flow rates of AN and toluene in fed-batch mode bioreactor.

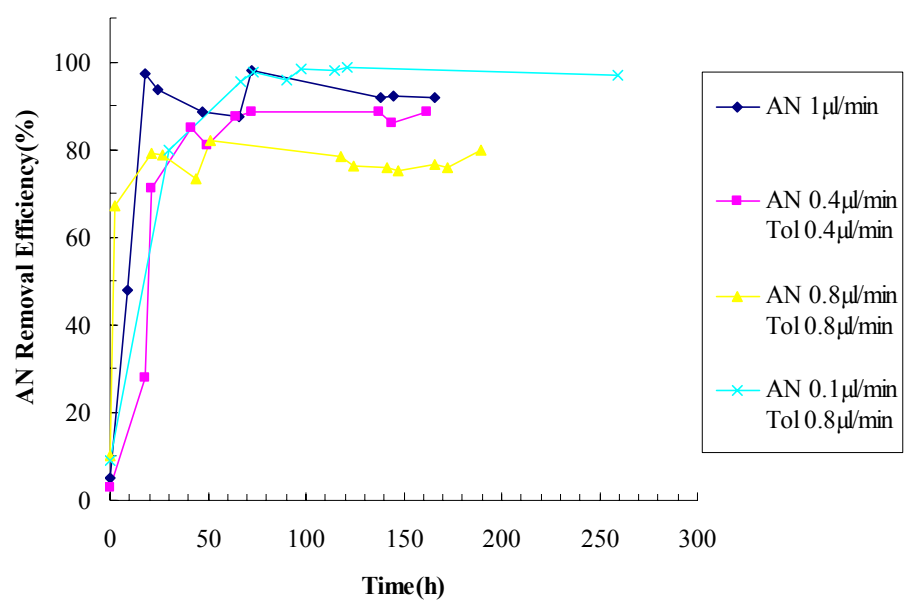


Figure 13. AN removal efficiency with different flow rates of AN and toluene in fed-batch-mode bioreactor.

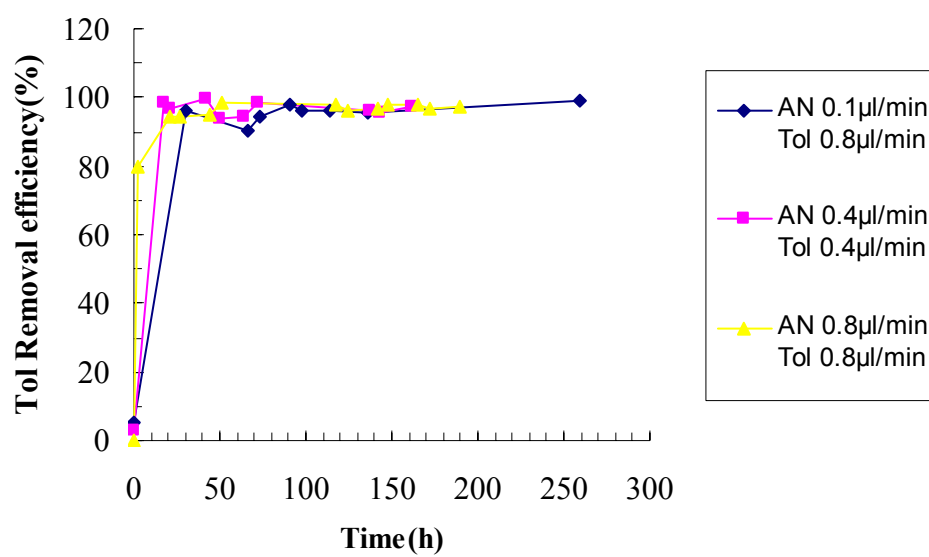


Figure 14. Tol removal efficiency with different flow rates of AN and toluene in feed-batch mode bioreactor.

Single-pass mode reactor

1) AN-Tol combined feed

A) Reactor start-up

The flow rates of AN and Tol from the syringe pump in continuous operation was 0.1 $\mu\text{l}/\text{min}$ and 0.8 $\mu\text{l}/\text{min}$, respectively. Figure 15a & b describes the performance of the biofilter for treating liquid- and gas-phase AN after shifting from the liquid-continuous operation to single-pass open mode. During the first 18 days, the liquid empty bed retention time (EBRT, bed volume/liquid flow rate) was set for 7.5 min. During the period, the removal efficiency fluctuated and then increased from 28.1 to 58.6%. EBRT was then kept at 4 min for the following period of 12 days. Generally, the removal efficiency went up with the increase of inlet load. The removal efficiency increased to 92% and the biofilter reached steady state.

Figure 16 depicts the evolution of the AN and Tol removal efficiencies based on combined feed across the trickling bed. After operating the reactor for 30 days, removal efficiency of AN reached ~90% while that of toluene decreased to ~30%. For toluene, the removal efficiency decreased over time and as EBRT decreased from 7.5 min and 4 min. The biofilter response depended on the physicochemical property of feed VOCs and aromatic compound like toluene may require relatively longer EBRT. Using high EBRT at high inlet concentration (flow rate: AN:Tol=1:8) may also caused problems related to oxygen limitation within the biofilm.

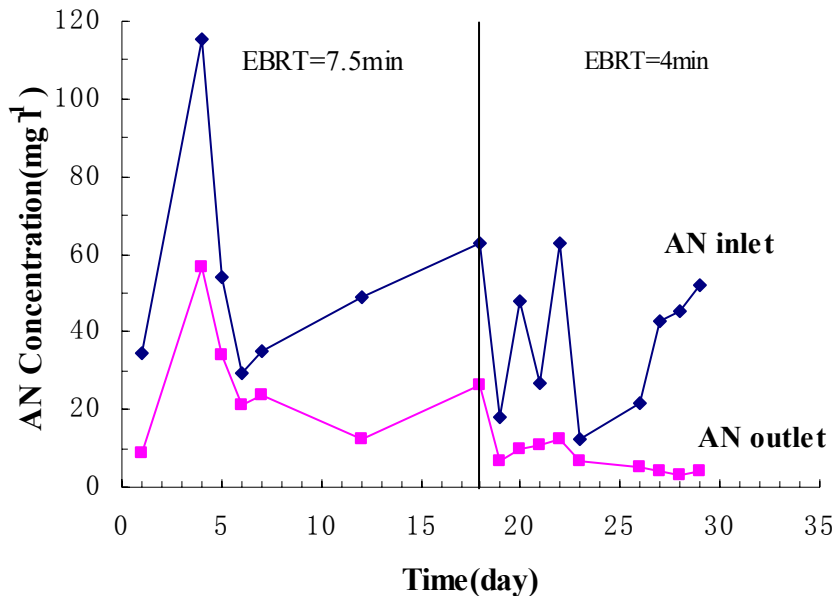


Figure 15a. Start-up performance of the biofilter: AN inlet and outlet concentration vs. time

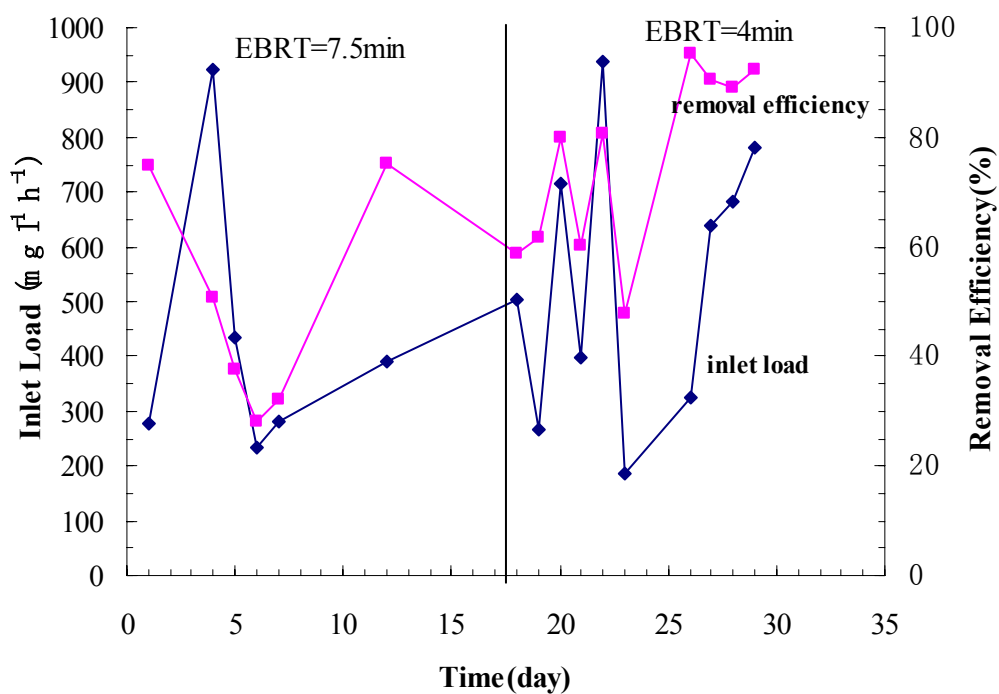


Figure 15b. Start-up performance of the biofilter: AN inlet load and removal efficiency vs. time

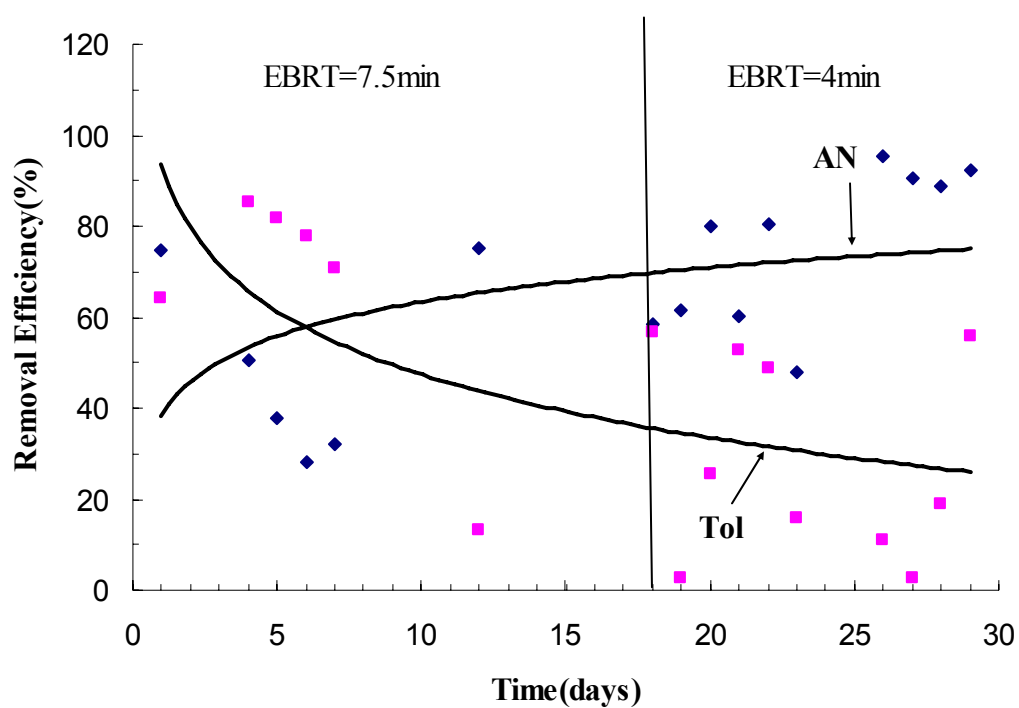


Figure 16. AN and Tol removal efficiencies during the start-up period.

B) Reactor performance at steady-state ----effects of inlet load on removal efficiency

The reactor inlet load, which is equal to the inlet concentration divided by EBRT, is an important process parameter. Figure 17 & 18 show the effect of inlet load on removal efficiency while maintaining a constant EBRT of 4 min or 8 min. At AN inlet load of $100\text{--}200\text{ mg l}^{-1}\text{ h}^{-1}$, the removal efficiency was able to achieve more than 90% at EBRT= 4min. Compared with AN, Tol removal efficiency was more sensitive to EBRT and to oxygen, since the transformation of AN to AMD is hydrolysis but Tol degradation is oxygen-dependent oxidation. Removal efficiency of more than 80% could be maintained at toluene loads around $400\text{ mg l}^{-1}\text{ h}^{-1}$ at EBRT=8min, while only 50% removal efficiency could be achieved when the same toluene load applied at EBRT= 4min(Figure 18). For both AN and Tol at high inlet load, the level of microorganism activity or the toxicity of the organics became the limiting factor for AN and Tol elimination.

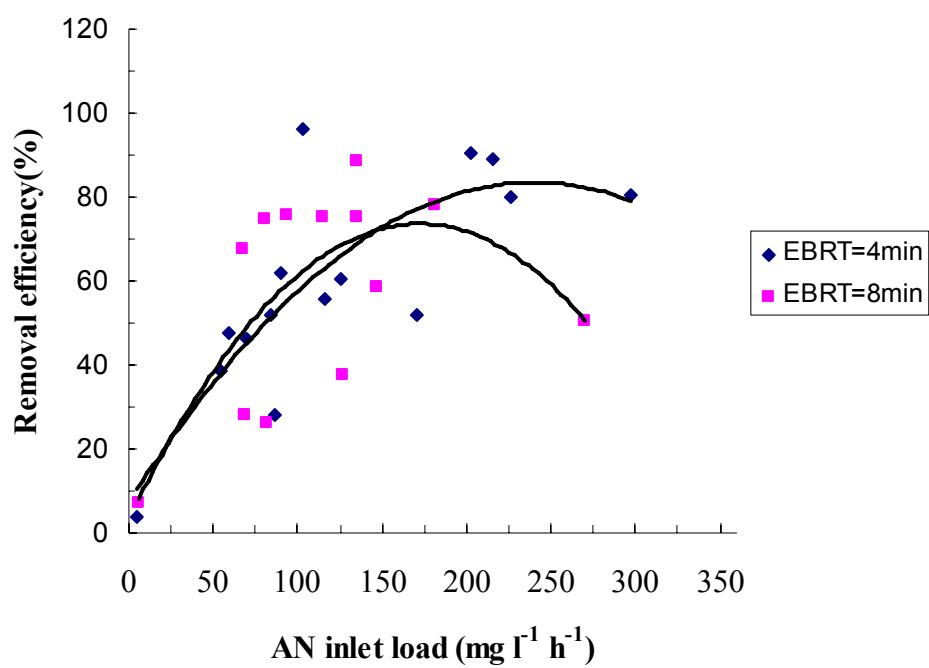


Figure 17. Effect of inlet load of AN and EBRT on removal efficiency (flow rate AN 0.1 μ l/min toluene 0.8 μ l/min)

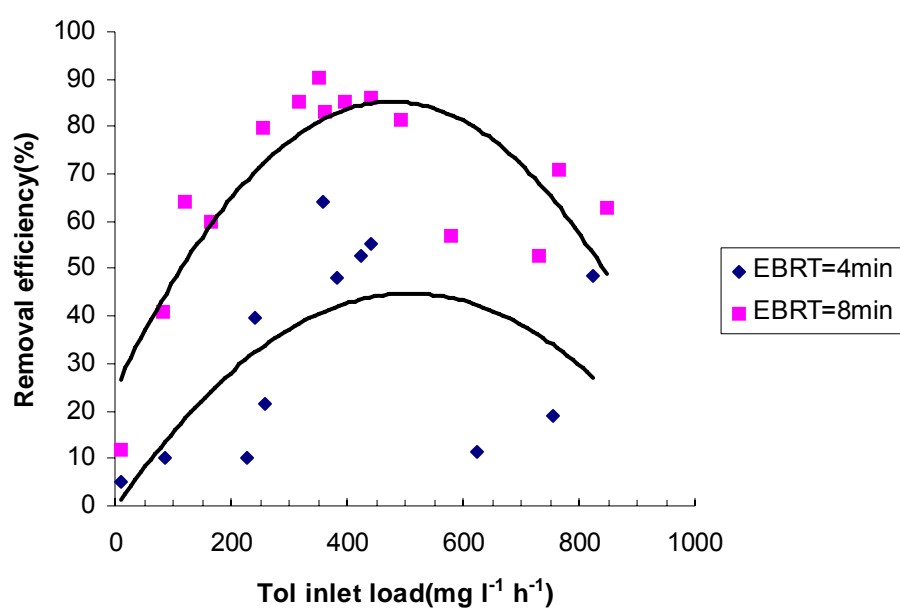


Figure 18. Effect of inlet load of Tol and EBRT on removal efficiency(flow rate AN 0.1ul/min toluene 0.8ul/min)

C) Reactor performance at steady-state ----effects of EBRT on removal efficiency

AN and toluene were introduced from the syringe pump to the top of the biofilter at flow rate of 0.05 $\mu\text{l}/\text{min}$ AN and 0.4 $\mu\text{l}/\text{min}$ Tol, 0.1 $\mu\text{l}/\text{min}$ AN and 0.8 $\mu\text{l}/\text{min}$ Tol, 0.2 $\mu\text{l}/\text{min}$ AN and 1.6 $\mu\text{l}/\text{min}$ Tol, respectively. The data shown in Fig. 19 are average values from measurements collected after the biofilter reached pseudo-steady state at each specific condition. When AN flow rate was 0.1 $\mu\text{l}/\text{min}$ and toluene flow rate was 0.8 $\mu\text{l}/\text{min}$, an EBRT of 8 min was found to be optimal with AN removal efficiency of 85%. Although for the same flow rate of AN and toluene, at EBRT=4 min, the removal efficiency achieved was only half of that for EBRT= 8min, actually, for a fixed bed volume, the same amount of AN was removed. When EBRT=8 min, for flow rate of 0.05 $\mu\text{l}/\text{min}$ AN with 0.4 $\mu\text{l}/\text{min}$ Tol and 0.2 $\mu\text{l}/\text{min}$ AN with 1.6 $\mu\text{l}/\text{min}$ Tol, removal efficiency can be obtained a relatively high value of more than 70%. The observed low value of removal efficiency at high EBRT (15 min) may be attributed to the flooding caused by the high liquid flow rate and the clogging caused by the overgrowth of the biomass.

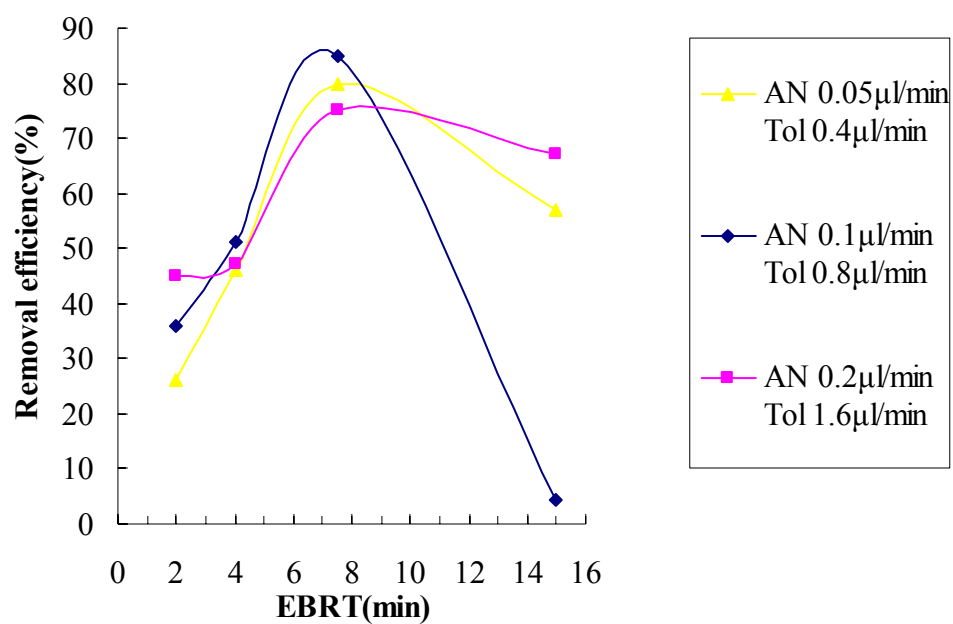


Figure 19. Effects of EBRT on AN removal efficiency at different AN and Tol flow rates.

D) Reactor performance at steady-state ----effects of inlet load on elimination capacity

Figure 20&21 shows AN and Tol elimination capacity vs. inlet load at a liquid flow rate of 7.5ml/min (EBRT=8min) and 15ml/min (EBRT=4min). The increasing inlet load enhanced the transfer of AN to the biofilm and the elimination capacity for AN increased in the degradation capacity of microorganisms. The maximum elimination capacity of AN was 142ppm/h for the liquid flow rate of 7.5ml/min and the removal efficiency varied from 28-89%. In both figures, a trend was observed that the elimination capacity of AN increased with the increase of the inlet load, which was diffusion (mass transfer)-limited. However, as inlet load was more increasing, it reached inhibition levels of AN degradation. The curves deviated from the 100% removal curve till the elimination capacity did not increase, which was reaction-limited. The relative position of points corresponding to Tol elimination at EBRT=8min and EBRT=4min verified that EBRT=8 min was more favorable for Tol degradation----although in both situations, the maximum elimination capacity was achieved was $\sim 550 \text{ mg l}^{-1} \text{ h}^{-1}$, the inlet load at EBRT=8min was relatively lower than that at EBRT=4min.

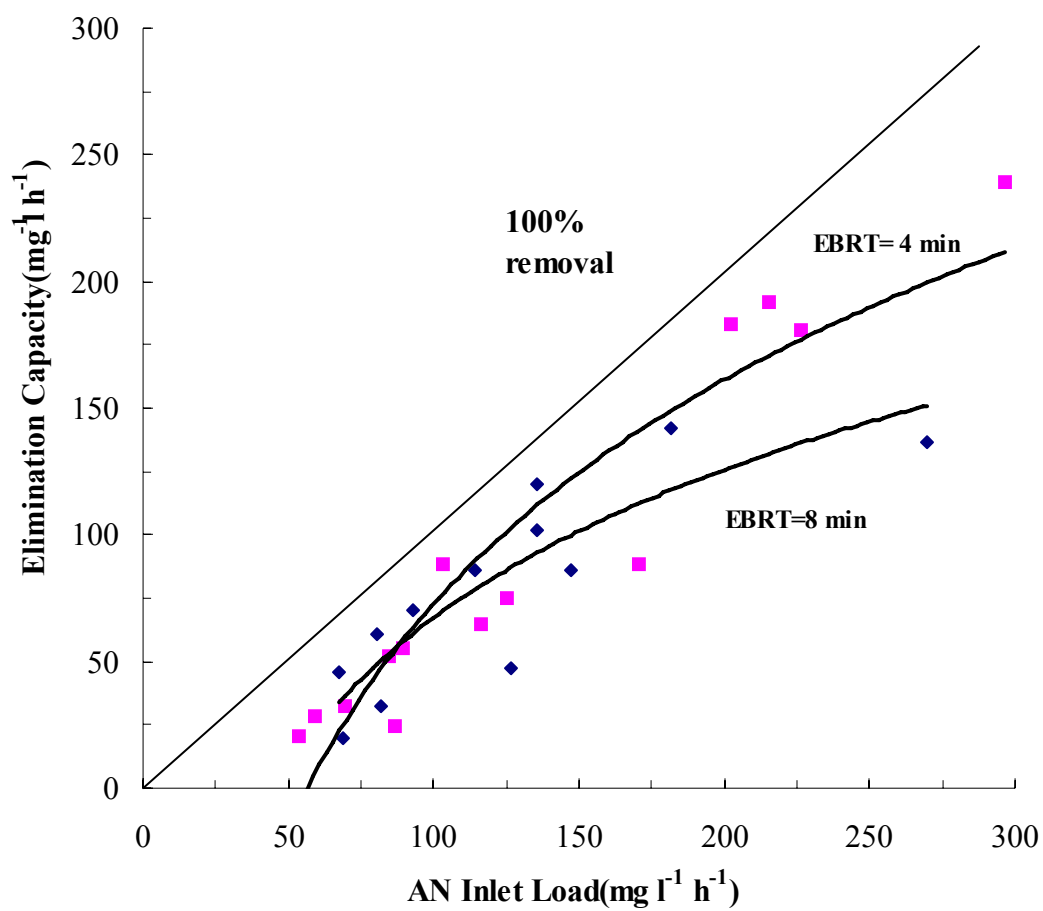


Figure 20. AN elimination capacity vs. inlet load at EBRT==4 min and 8 min.

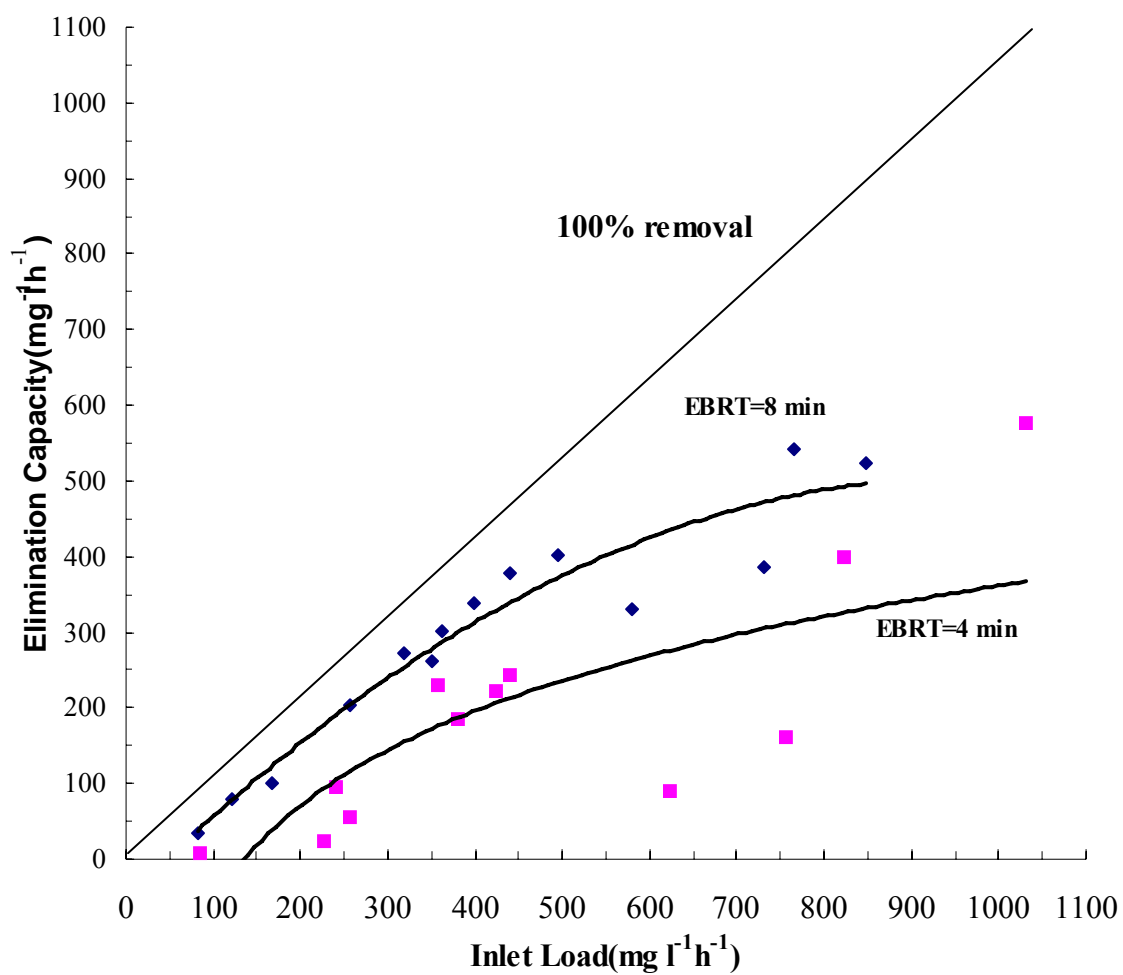


Figure 21. Tol elimination capacity vs. inlet load at EBRT=4 min and 8min.

AN as single feed

Figure 22 and 23 shows the elimination capacity (EC) and removal efficiency (RE) as affected by the inlet AN concentration at EBRT=8min and 4min when AN was the sole feed in open, single pass-mode reactor. Except for low AN inlet concentrations at EBRT=4min, the EC and RE generally increased with increasing the AN inlet concentration. When AN was the sole carbon and nitrogen source, decreasing the liquid flow rates would increase the substrate available for microorganisms, which may later result in the deterioration of biofiltration performance. However, high flow rates could cause severe flooding and limited mass transfer between gas-liquid phase and the biofilm (not shown in the figure), which resulted in low AN RE and EC.

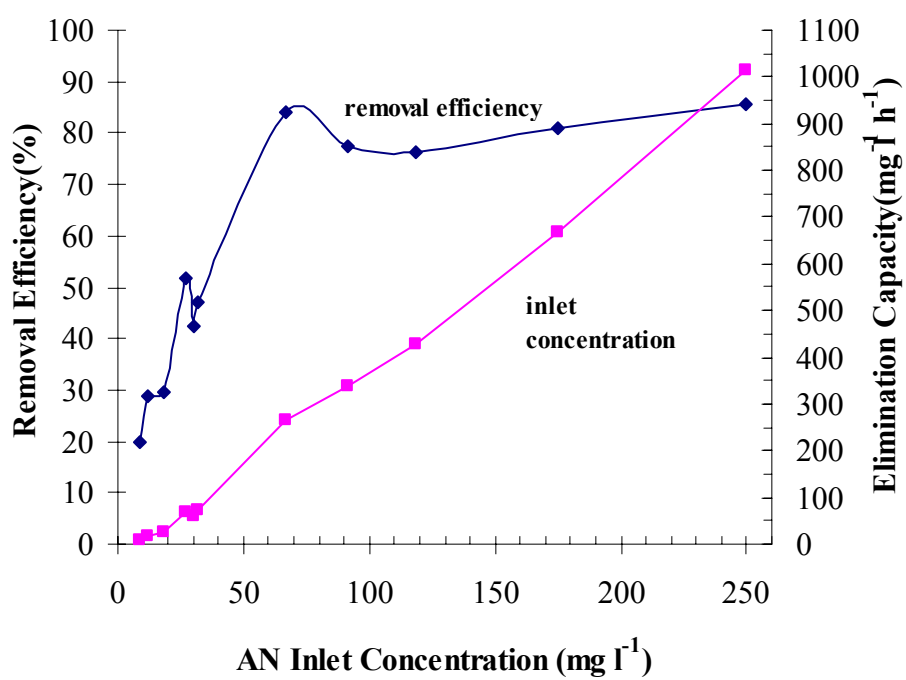


Figure 22. AN removal efficiency and elimination capacity vs. AN inlet concentration at EBRT=8min.

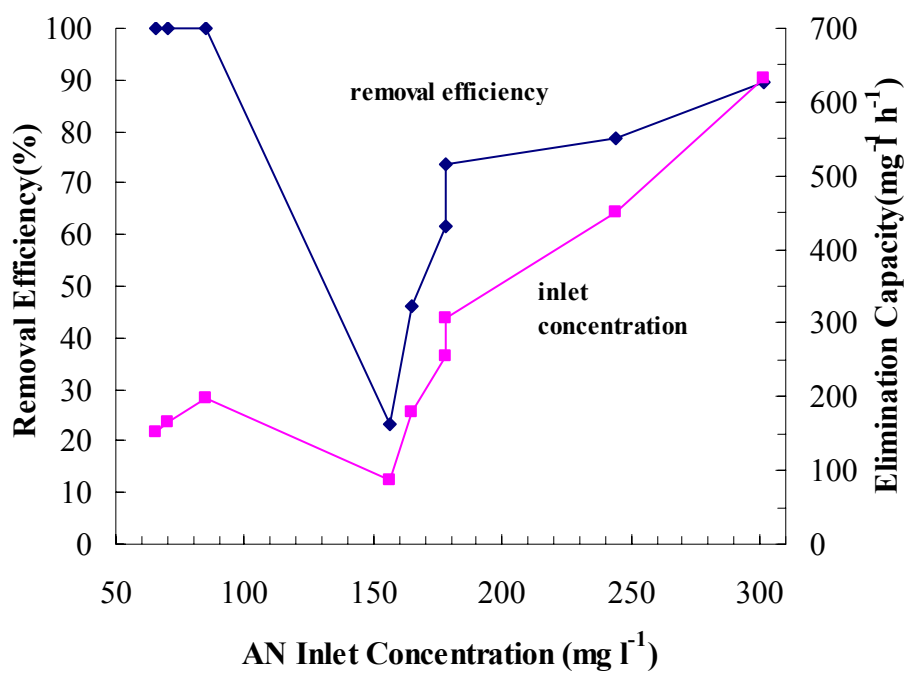


Figure 23. AN removal efficiency and elimination capacity vs. AN inlet concentration at EBRT=4min.

Adsorption and bioavailability test

1) Adsorption test in flasks with GAC and different concentrations of AN

The fact that low AN concentration was detected in the effluent at the beginning of the open mode suggested adsorption of AN to the GAC column. All the AN supplied was not immediately bioavailable. Therefore, the bioavailability of AN adsorbed to GAC was studied in batch system. Concentration of AN (10.8-216 mg/g GAC, corresponding to 180-3600ppm AN in the medium) was added to flasks containing 10g GAC suspended in 600ml Stanier's medium. Flasks were incubated in the rotary shaker for 24h before being inoculated with *R. rhodochrous* DAP 96622, which was pre-grown on AN. Prior to inoculation, for initial AN concentration of 180ppm and 360ppm, there was no AN detected in the solution, as determined by GC. For higher concentration, more than 85% of AN still remained unbound. This indicated that for uninoculated activated carbon, the adsorption capacity of AN is limited. CLSM was used to visualize the development of biofilms on the GAC in the flasks. The release of NH_3 was monitored for calculation of the amount of AN that was degraded by the organisms (Figure 24). Liquid samples were also taken and AN concentration in the samples was measured periodically (Figure 25). An uninoculated flask with 1000ppm AN was used as a control showed almost no NH_3 release. After 22 days, for all the flasks including the control, there was no AN remaining in the liquid medium. Except for the lowest concentration of AN supplied (180ppm), a residual fraction of AN (up to 71%) remained absorbed to the GAC and therefore was biologically unavailable. The slight drop of pH at the beginning (Figure 26) was caused by the nitrification of ammonium nitrogen ($\text{NH}_4^+\text{-N}$) to nitrate nitrogen ($\text{NO}_3\text{-N}$) when AN or its intermediate metabolites was assimilated. The media neutralized the proton and the increase of pH occurred after a couple of days.

Figure 27 shows a confocal laser scanning microscopic (CLSM) image of biofilm attached to GAC after 30 days of batch growth (one initial feed at the beginning). The image is a middle slice, which is halfway between the biofilm surface and the substratum. The square image was (x,y) plane and the top and side images were the (x, z) and (y, z) planes, respectively. Organisms were present in dense cell clusters (microcolonies) and as individual cells distributed throughout a biofilm. A sagittal section visualized channels and voids extending from the surface to deep region, which might facilitate the oxygen and nutrient transport into biofilms.

Figure 28 shows optical sectioning of a biofilm stained with acridine orange. Horizontal sections were taken at different depths from the biofilm surface to as deep as 120 μm . There was a higher cell density in the middle section of the biofilm. In a diffusion-limited biofilm, AN-degrading cells were proposed to survive and proliferate at the biofilm surface where substrate concentration was the highest. However, the location of AN degraders in this biofilter suggested that for a porous biofilm attached to a loose material like GAC, AN could penetrate the biofilm as deep as 100 μm , allowing cells colonizing deep inside the biofilm to degrade AN.

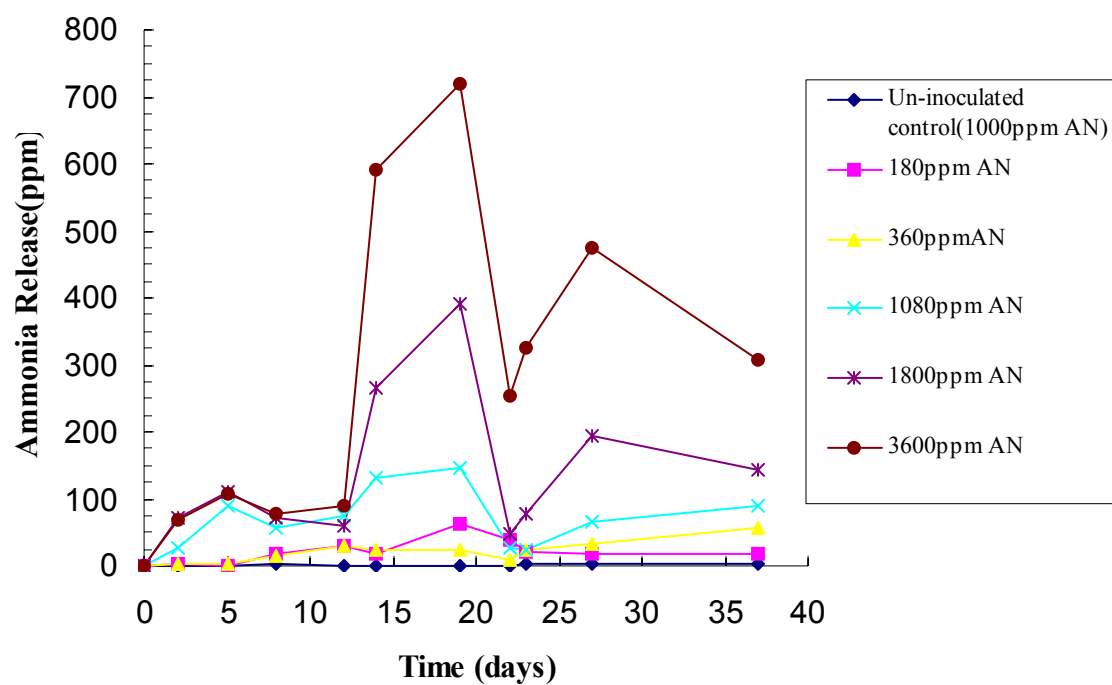


Figure 24. Bioavailability of adsorbed AN for biofilm development.

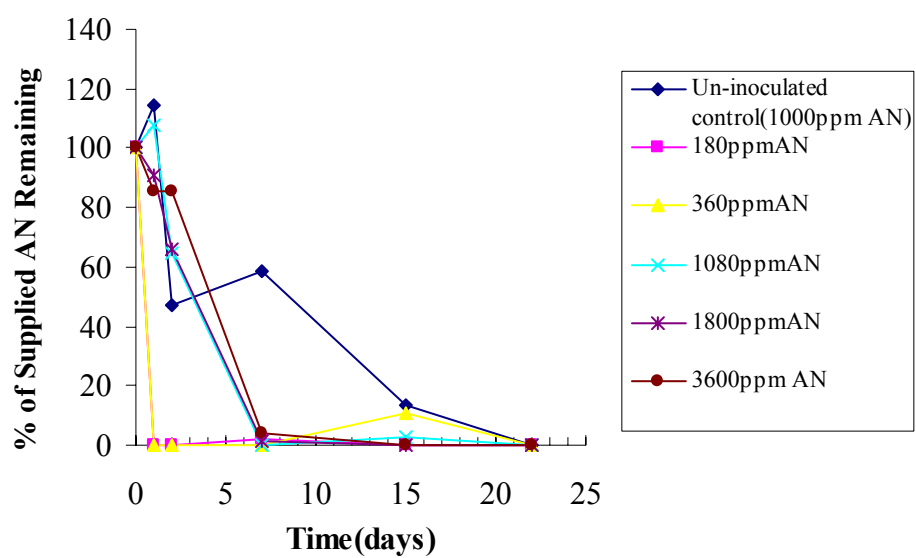


Figure 25. Degradation of AN in flasks with GAC.

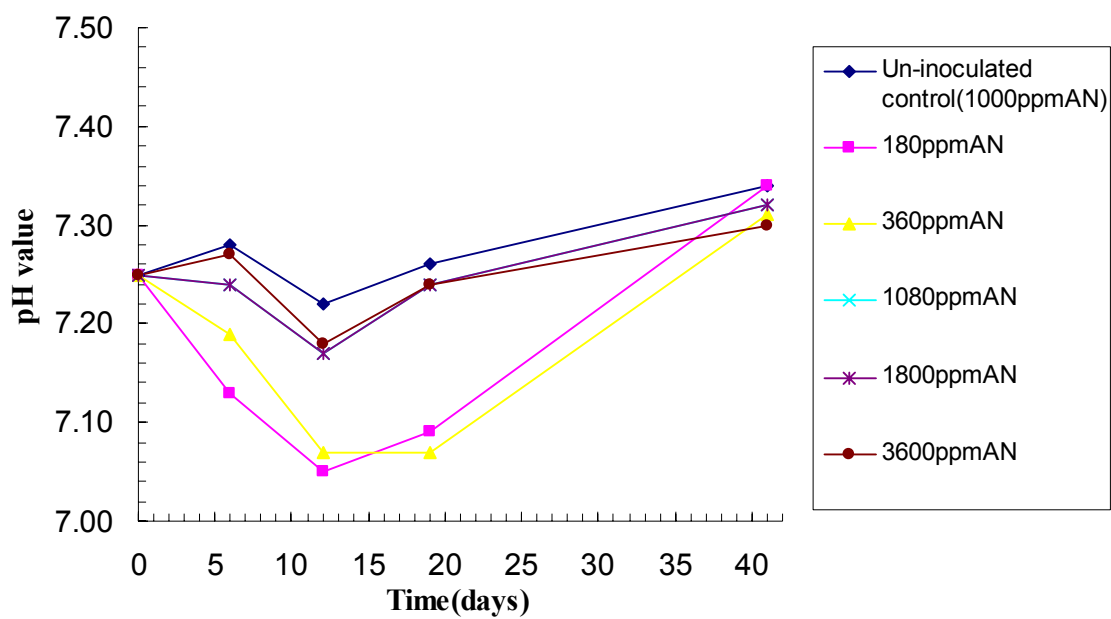


Figure 26. pH evolution in the medium.

Table 10. Bioavailability of AN 22 days after adsorption to GAC.

AN supplied mg g ⁻¹ GAC	AN remaining adsorbed to mg g ⁻¹ GAC	AN degraded based on NH ₃ release (mg g ⁻¹ GAC)	AN degraded (%)
10.8	0	10.8	100
21.6	11.4	10.2	47
64.8	28.8	36	56
108	69.2	38.8	29
216	142.1	73.9	34

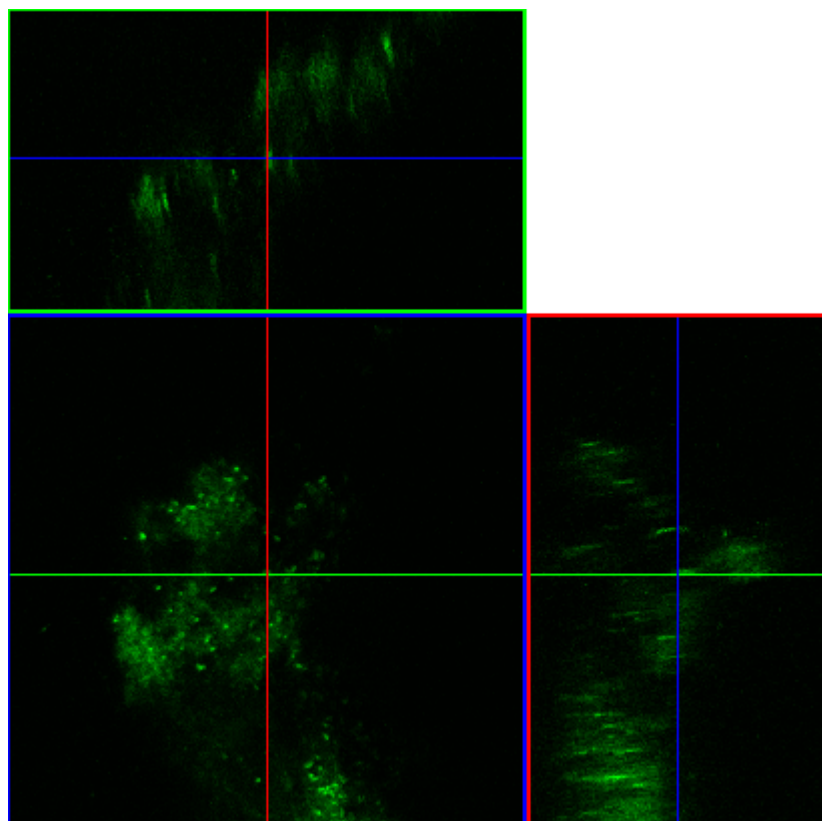


Figure 27. CLSM image of biofilm attached to GAC particle in flasks with *Rhodococcus rhodochrous* and 1080ppm AN after 30 days. Magnification: 400x. Red line: axis X; Green line: axis Y; Blue line: axis Z.

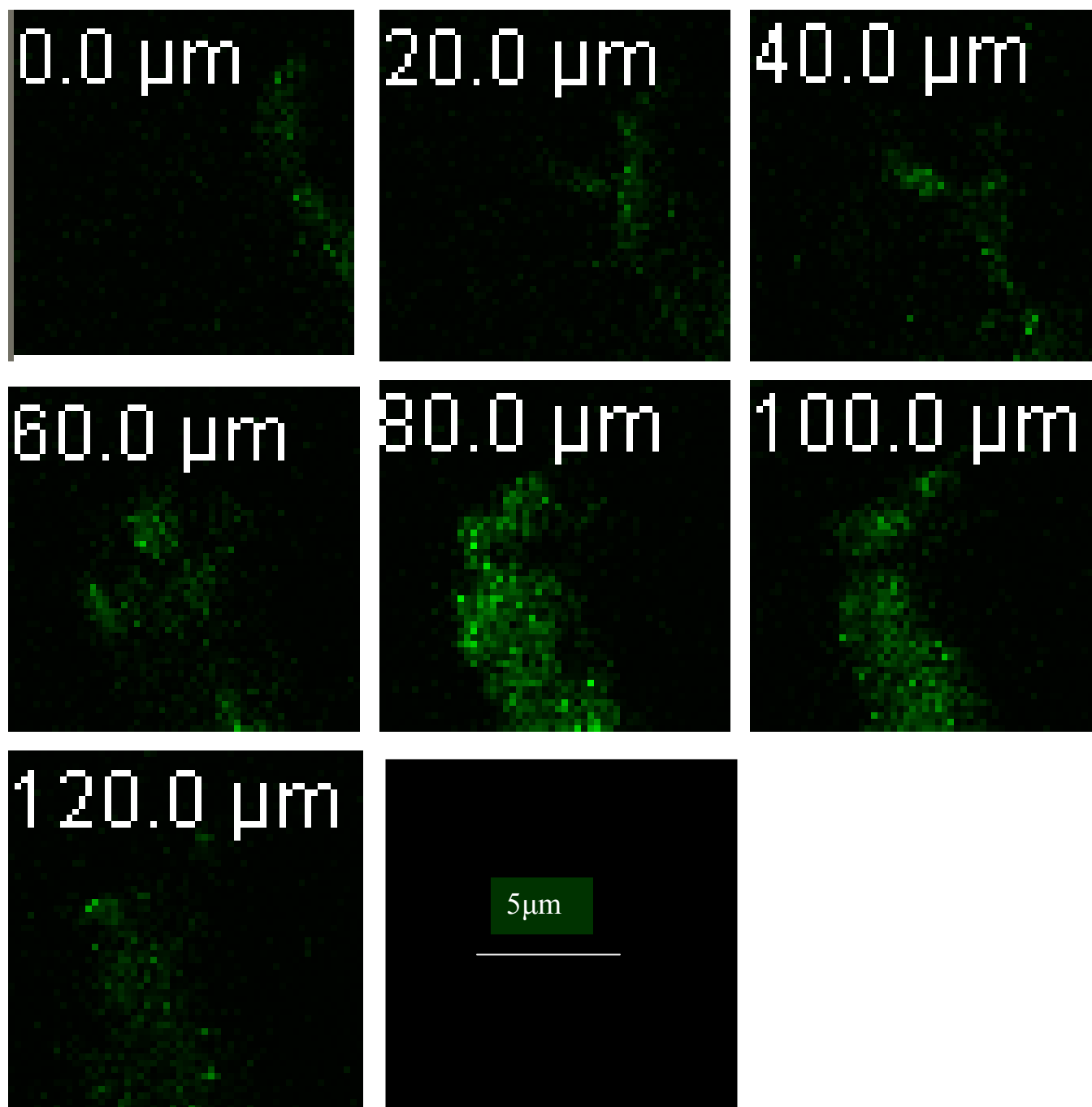


Figure 28. Optical sectioning of the AN-degrading biofilm taken from flasks with GAC, visualizing the special distribution of *R. rhodococcus*. Optical thin sections at different depths of the biofilm are shown. 0 μ m indicates the surface of the biofilm, whereas 20, 40, 60, 80, 100 and 120 μ m indicate the distance from the surface. Optical sections were sampled with 1.0 μ m increment. This visualizes channels extending from the surface into the biofilm, further indicating the heterogeneity of the biofilm structure.

2) Adsorption test in the reactor----batch-open switch mode

Three feeding periods occurred from day 24-26, 46-48 and 66-68, with different flow rates or AN inlet concentrations. AN supplied in open mode could either be adsorbed to the GAC or immediately available for degradation. For those AN adsorbed, its availability was investigated on the following batch mode. At the first feed period with a relative longer EBRT, no AN was detected in column effluent. NH_3 amount in the effluent indicate only 7.2% of AN was degraded and the rest was adsorbed to GAC particles. After the system returned to closed mode, only 150 mg AN was removed during the following 20 days. At the second feed period (day 46-48) when AN inlet concentration was 500mg l^{-1} and retention time was 8.5min during open mode, about 35% of AN was removed. The column was then returned to closed mode and a further of 2000mg AN was degraded in 18 days. At day 66 to 68, a third feed of AN was passed through the column at a very slow rate of 1.3ml/min, 8% of AN was degraded (Table 11, Figure 29). During three feed periods, AN amounts supplied were equal to 36, 315 and 53mg g^{-1} GAC, respectively. Based on the batch data in Table 10, for the first and third feed periods, 47-56% of AN should have been degraded, which were far more than actual number obtained in the experiment. The biological unavailability of AN might due to the saturation of carbon, clog of biofilter caused by the increased biomass and moving phase which made AN harder to be utilized.

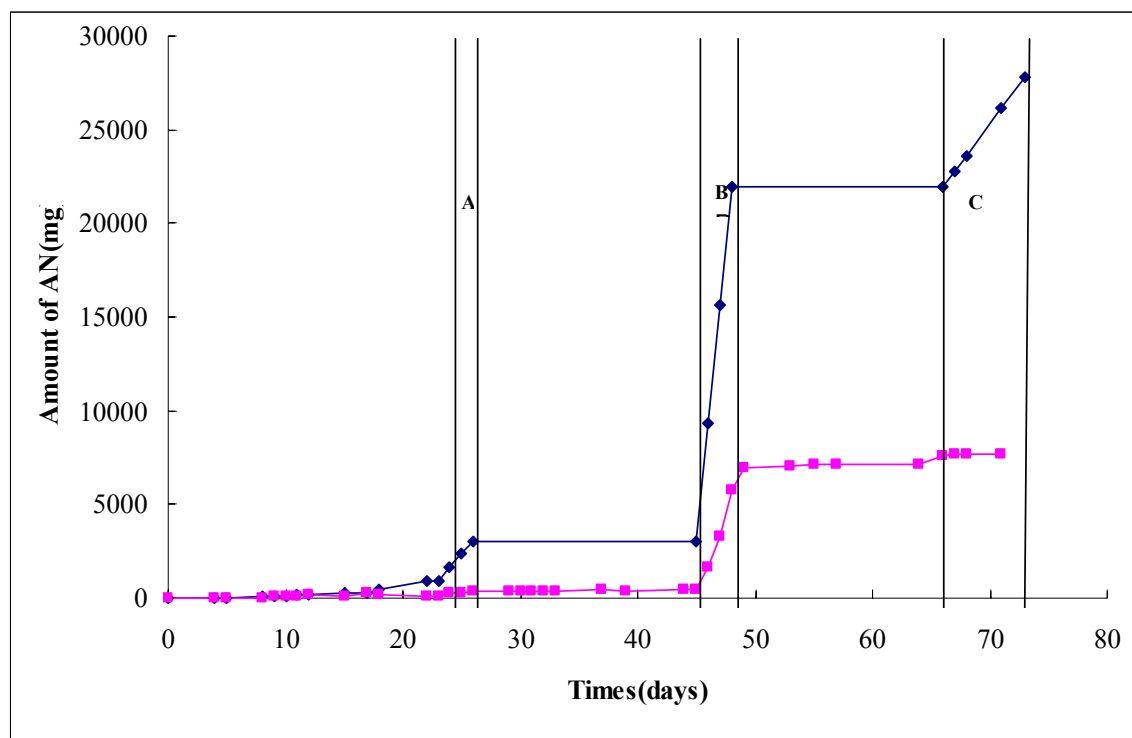


Figure 29. Adsorption and degradation test in batch-open switch mode reactor. (◆) cumulative supply of AN; (■): cumulative degradation of AN. Feed periods: (A)Day 24-26; (B)Day 46-48; (C)Day 66-73.

Table 11. Degradation of AN in GAC reactor during open mode operation, % of AN degraded is based on NH_3 (Ammonia) release in column effluent.

Feed period (days)	Total AN supplied (mg)	AN inlet concentration (ppm)	Flow rate (ml/min)	EBRT (min)	AN degraded during feed period (%)
24-26	2160 (0.625 μ l/min)	100	4	15	7.2
46-48	18900 (4.375 μ l/min)	500	7	8.5	34.8
66-73	3154(0.73 μ l/min)	500	1.3	45	7.9

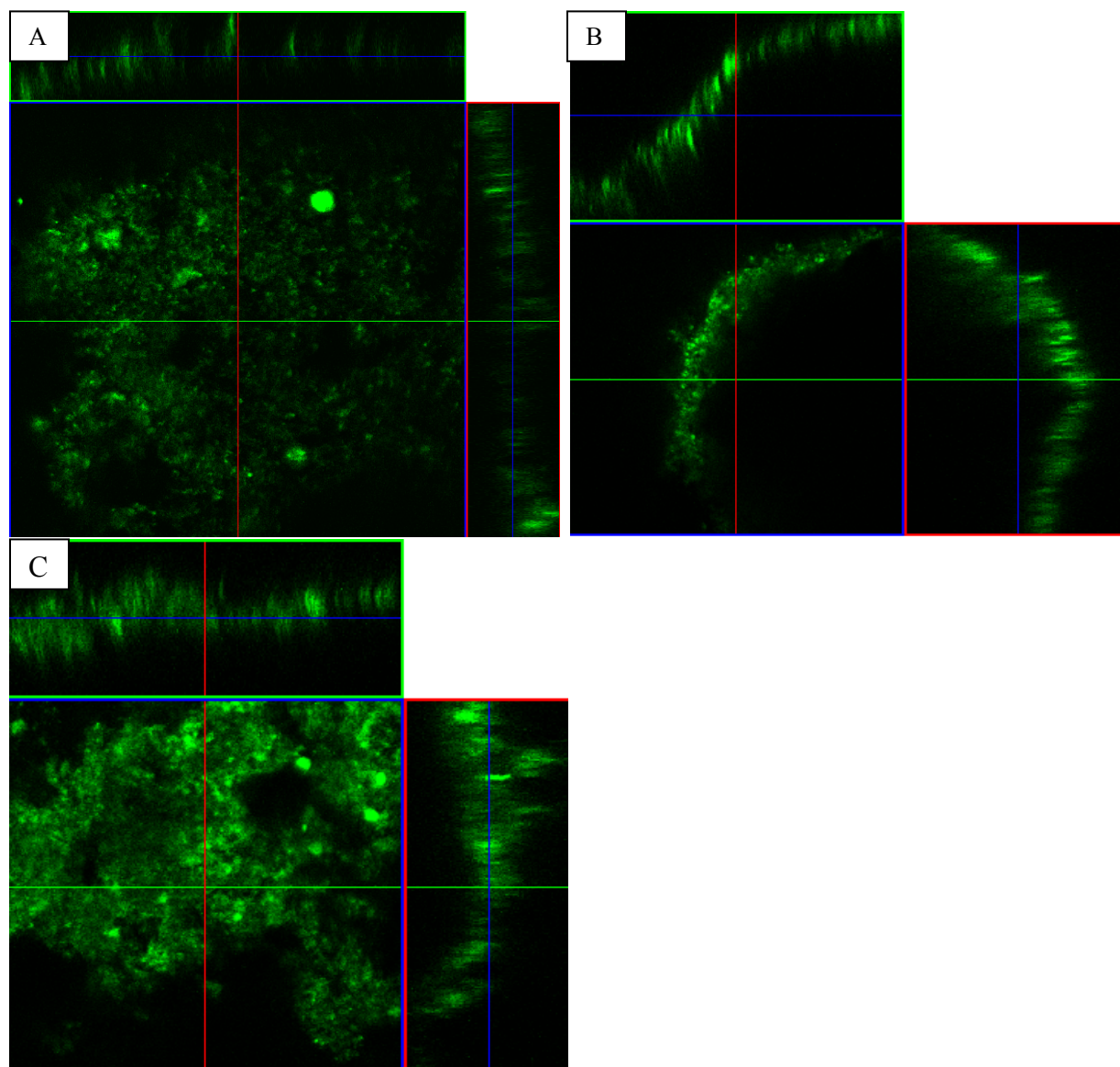


Figure 30. CLSM image of biofilm attached to GAC particles, taken from upper (A), middle (B) and lower (C) part of the reactor. Magnification, 400X. Red line: axis X; Green line: axis Y; Blue line: axis Z.

3) Biofilm activity

Biofilm activity expressed as the oxygen consumption, was measured at the different sections of the trickling bed reactor. Figure 31 shows the curves recorded by the recorder. The measurement was done in duplicate (Table 12). A lower activity was observed at the upper section, increasing along the column.

Samples were taken from different sections of carbon column and the three dimensional structure of the biofilm stained with acridine orange was visualized by Confocal Scanning Laser Microscopy. Figure 30 shows CLSM image of biofilm-attached on GAC at upper, middle and lower sections of the reactor. It revealed a very robust and heterogeneous biofilm, with microcolonies interspersed with voids and channels. Precise measurement of biofilm characteristics by a computer program, COMSTAT, agreed with the assumption that the biomass and thickness of the biofilm increased along the carbon column depth (Table 13).

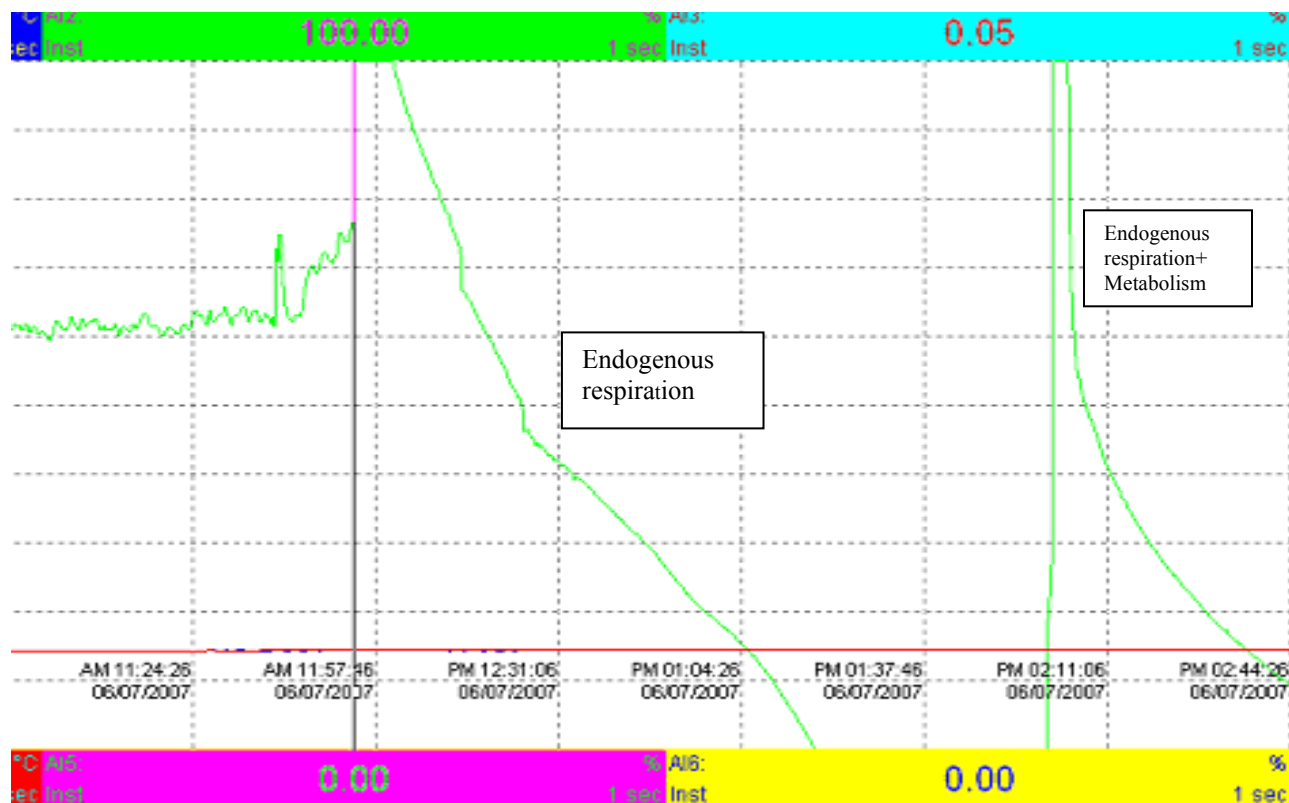


Figure 31. Biofilm cell activity expresses as the oxygen consumption rate (upper section)

Table 12. Biofilm cell activity of different sections of the column, expressed as the oxygen consumption rate referred to the homogenate volume

	Upper section		Middle section		Lower section	
O ₂ consumption rate(mg l ⁻¹ h ⁻¹ g ⁻¹ GAC) (endogenous respiration)	1.12	1.31	0.55	0.13	1.34	2.58
O ₂ consumption rate(mg l ⁻¹ h ⁻¹ g ⁻¹ GAC) (endogenous respiration+metabolism)	1.95	2.19	2.78	4.09	9.14	8.70
O ₂ consumption rate(mg l ⁻¹ h ⁻¹ g ⁻¹ GAC) (metabolism)	0.83	0.88	2.23	3.96	7.80	6.12

Table 13. Total biomass, average/maximum thickness, roughness, substratum coverage and surface to volume ratio of biofilms on GAC taken from upper, middle and lower part of the reactor. Values are means from two image stacks. The standard deviation is calculated as the square root of the mean of the variances of each of the two groups.

	upper section	middle section	lower section
Total biomass ($\mu\text{m}^3/\mu\text{m}^2$)	0.55 \pm 0.05	3.20 \pm 3.06	12.38 \pm 0.16
Average thickness (μm)	2.12 \pm 0.99	19.01 \pm 11.08	43.24 \pm 4.60
Maximum thickness(μm)	55.50 \pm 19.09	98.00 \pm 0.00	86.00 \pm 2.83
Roughness coefficient	1.85 \pm 0.00	1.38 \pm 0.43	0.45 \pm 0.03
Substratum coverage (%)	0.008 \pm 0.006	0.017 \pm 0.0095	0.03 \pm 0.03
Surface to biovolume ratio ($\mu\text{m}^2/\mu\text{m}^3$)	26.16 \pm 0.24	32.23 \pm 13.28	19.52 \pm 4.16

Discussion

The wastewater of the chemical manufacture of AN and AMD contains a complex mixture of organic nitriles, amides and acids. The effluent cannot be released into the environment due to its toxicity, high biological oxygen demand (BOD) and chemical oxygen demand (COD) values. Since the structure of characteristics of NHase produced by *Rhodococcus* and its catalytic mechanism has been well established and the microbial metabolism of nitriles has been investigated in detail in past three decades, the study has mainly focused on developing an economic and effective method to degrade AN and toluene, for the following industrial scale-up of the bioreactor.

There are two principle types of biodegradation studies for xenobiotics: the degradation of single compounds by pure and mixed cultures and degradation of xenobiotic mixtures, often industrial wastes, by mixed culture, of which individual types of bacteria or isolate are able to degrade each of the major components. The study combined the two strategies, by inoculating a well studied degrader microorganisms *Rhodococcus rhodochrous* DAP 96622 to a non-sterile carbon column. The following growth of mixed population has the ability to tolerate higher concentration of the toxic constituents and co-metabolism has the advantage of initiating growth of the organisms and inducing of catabolic enzymes. By switching the system between batch and open mode, optimizing the operating conditions, the biofilter is expected to give a stable population which could degrade AN and Tol, mineralizing them to carbon dioxide and biomass.

Granules and particle-supported biofilm reactor has good biomass retention and possibly higher biomass concentration. The reactor also had a higher specific surface area for biomass transfer. The transport of the substrate generally depends on the biofilm porosity, substrate concentration in the bulk liquid, mass transfer at the biofilm-liquid intersurface and reaction rate.

R. rhodochrous DAP 96622 are gram-positive non-motile short rods, showing optimal growth temperature of 26 C, being able to utilize multiple hydrocarbons, and sensitive to most bacterial antibiotics. *R. rhodochrous* DAP 96622 are capable of detoxifying the hazardous nitrile and amide components present in wastewater (Table 5). When subjected to multiple induction (with cobalt, urea, and a mix of nitriles and amides) and/or toluene as a co-substrate, the cell yield increases to a significant level (Figure 5). Although the strain shows high tolerance to cyanides, AN degradation is sensitive to AN concentration. A long lag phase was observed when the organisms were exposed to high concentration of AN, even if the culture had been induced and supplemented with other carbon sources.

A laboratory-scale activated carbon bioreactor process was tested for biodegradation of AN and Tol. The inoculation broth used in the process was obtained by 96 h cultivation of the *R. Rhodococcus* 96622 on Stanier's agar with AN and Tol before being suspended in PBS. Its enzyme activity was tested and found to be as high as above 50 U/mg dry cell weight and its cell concentration was 0.1 g wet cell per ml broth.

The whole biofiltration process can be divided into two stages; the fed-batch stage, and the steady state. In the fed-batch stage, the liquid (medium+buffer) recirculation rate was 8 ml/min. The AN and Tol feed rate was set to a specific value. The fed-batch process stopped when biomass was build-up and AN and Tol removal efficiency reached 90%. Then the steady-state began and the system started single-pass mode. Parameters (inlet load, EBRT, AN/Tol concentration, etc) were changed and the biofilter performance was monitored. At a steady-state, it could be assumed that activated carbons were saturated and the adsorption of the organics could be ignored.

The start-up operation was carried out in a closed circuit (100% recycle ratio), using a batch culture of *R. rhodochrous* DAP 96622 which has acclimated to AN/Tol before inoculation. As seen in Figure 9, cells used both AN and Tol for growth; AN/Tol degradation occurred as cells grew in the reservoir. Cells continued to grow for 3 days after neither AN nor Tol was detectable in the reservoir. Plate counting for the number of culturable cells was following. The increase in total viable cells indicates that AN and/or Tol was degraded and assimilated. Within two days, the portion of other microorganisms in total cells began to increase (Figure 10 & Table 6). Only *R. rhodochrous* can metabolize AN to AMD. However, many organisms are able to convert AMD to acrylic acid and ammonia, as well as utilize mono-cyclic aromatic hydrocarbons like toluene. It is speculated that under non-sterile condition other contaminants may enhance the degradation, helping speed-up the mineralization of the organics. After running the reactor for one month, a thin biofilm covering the particles were observed (Figure 11).

Comparisons of the performance of free and immobilized cells for the conversion of AN at starting concentrations up to 1150 mg l^{-1} indicated that, the immobilized cells in the bioreactor had 10- to 100- fold higher degradation rates than those of the free cells in flasks. The higher AN degradation rates for the bioreactor were attributed to the higher cell density, improved (adapted) culture and presence of toluene as a co-substrate. Immobilized cells in the bioreactor could tolerate a higher toxic concentration of AN: at AN concentration of 1150 mg l^{-1} , they continued to degrade AN efficiently, at a degradation rate as high as $95 \text{ mg l}^{-1} \text{ h}^{-1}$. However, real comparison of the data from free cells in flasks with the data from immobilized cells in packed bed is difficult because of the very different growth conditions during the two experiments (shaker incubated vs. flow recycled, suspended growth vs. attached, the pure culture vs. the complexity of bioreactor microflora). Cowan (1998) studied nitrile utilization at elevated

substrate concentrations and product inhibition by free and immobilized *Bacillus* strain RAPc8 cells with various acrylic acid concentration before the addition of AN. At production concentrations above 8 g L⁻¹ there was a significant inhibition of activity and at 20 g L⁻¹ there was complete inhibition of nitrile hydratase activity. Nagasawa et al. (1990) also reported that hydratase activity of *Rhodococcus rhodochrous* J1 decreased with increasing nitrile concentration up to 70 g/L. According to Haldane-Andrew's substrate inhibition equation:

$$\mu_g = \mu_{\max} S / (K_S + S + S^2/K_i)$$

(μ_g : specific growth rate; μ_{\max} : maximum specific growth rate; S: substrate concentration; K_S : substrate affinity constant; K_i : substrate inhibition constant)

Single substrate-limited microbial growth can be extended to the inhibition of microbial growth by high levels of substrates. Since in flasks AN showed inhibition to cell growth, the equation should be used in modeling kinetics with high substrate concentrations. The specific degradation rate should also follow a similar kinetic model. For immobilized cells, when the cell density in the bioreactor is relatively constant with respect to time, the substrate concentration rate can also be modeled by a similar equation.

At the beginning of single-pass open mode, the biofilter was run at a constant EBRT of 8 min. Even if liquid AN was pumped to the reactor at a constant rate, AN concentration detected at the influent varied between 30~118 mg l⁻¹. Complicated processes were taking place simultaneously after AN entered the filter bed; it could be volatilized to the headspace or GAC trap, or adsorbed by the carbon, or metabolized by the consortium, or flow out of the column

untreated. The reactor dynamic was examined by changing liquid flow rate and inlet load, then monitoring the reactor transient response. Compared with previous batch mode, removal efficiency was lower but still could be maintained between 30-80%. After 18 days when the EBRT decreased to 4 min, removal efficiency increased to 90% at day 26. During the same period AN concentration in the liquid medium remained at a level below the detection limit (5ppm). The biofilter had a slow response and retain stable performance when shifted from batch mode (Figure 15).

The biofilter inoculated with DAP 96622 was run to remove AN and Tol at different controlled parameters. Each time when the inlet load was increased within a certain range, removal efficiency was remarkably increased as well and after that, the removal efficiency tended to reach a stable state, indicating that gradually increasing AN and Tol load to a certain level may result in a relatively high and stable removal efficiency. The wastewater entered the biofilter with a higher load of contaminant, favoring the transfer of the contaminant mass to the biofilm. As the inlet load increased, to more than $200 \text{ mg l}^{-1} \text{ h}^{-1}$ for AN and $500 \text{ mg l}^{-1} \text{ h}^{-1}$ for Tol, a reduction in the efficiency of contaminant destruction was observed due to insufficient mass transfer within the biofilter, and decrease in the contact time between the influent and the microbial flora, although the absolute amount of contaminant removed was still high. However, the effectiveness of the treatment system at different inlet loads was high. When EBRT=8 min, AN and Tol inlet loads were between $50\text{-}200 \text{ mg l}^{-1} \text{ h}^{-1}$ and $200\text{-}500 \text{ mg l}^{-1} \text{ h}^{-1}$, respectively, the removal efficiency could be maintained at 75-85% for AN and 80%-90% for Tol (Figure 17 & 18). This indicates that when the inlet load was within a proper range, the system of biofiltration used was not affected by variations in inlet load. Oxygen limitation at high concentrations and shorter EBRT may cause the reduction in pollutant removal. At the critical

inlet load, biofilter performance may be improved by employing a longer EBRT if the inlet load or inlet concentration is high. The elimination capacities of AN to maintain 90% removal efficiency were $125 \text{ mg l}^{-1} \text{ h}^{-1}$ and $80 \text{ mg l}^{-1} \text{ h}^{-1}$, under EBRT= 8min and 4 min, respectively (Figure 20 &21).

When AN was sole carbon and nitrogen source to microorganisms in the biofilter, it appears that elimination capacity was an increasing function of the inlet concentration. For AN concentrations at the range of $250\text{-}300 \text{ mg l}^{-1}$, about 90% of AN was eliminated (Fig 22&23). The results also illustrate the reverse relationship between EC and EBRT, indicating limitations of diffusion rate of AN into the biomass. For biofiltration system, since AN hydrolysis does not involve oxygen, oxygen concentration is not limiting the conversion rate of AN to AMD. Elimination capacity can be described by the following equation:

$$EC = (V_{\max} \times C_{\text{in}}) / (K_m + C_{\text{in}})$$

(V_{\max} : the maximum degradation rate; K_m : half-saturation constant)

The degradation rate can be first-order ($C_{\text{in}} \ll K_m$) or zero-order ($C_{\text{in}} \gg K_m$). Fig. 22 shows that the data of inlet concentration vs. elimination capacity can be fitted satisfactorily by linear regression when AN was the single feed at EBRT=8min, indicating that the bioreaction follows first-order kinetics and one cannot clearly distinguish between reaction and diffusion limited regimes. Based on the kinetics recently developed by Jin et al. (2006)

$$V_{\max}/V = 1 + K_m/C$$

Where $C = (C_{in} - C_{out}) / \ln(C_{in} / C_{out})$

There is a relationship between substrate consumption rate and the mean log of inlet/outlet concentrations. V can be expressed as a function of the mean log of the concentrations C , $V = f(C)$. When C_{in} is plotted against C , one can get a good-fit linear regression with a regression coefficient $R^2 = 0.99$.

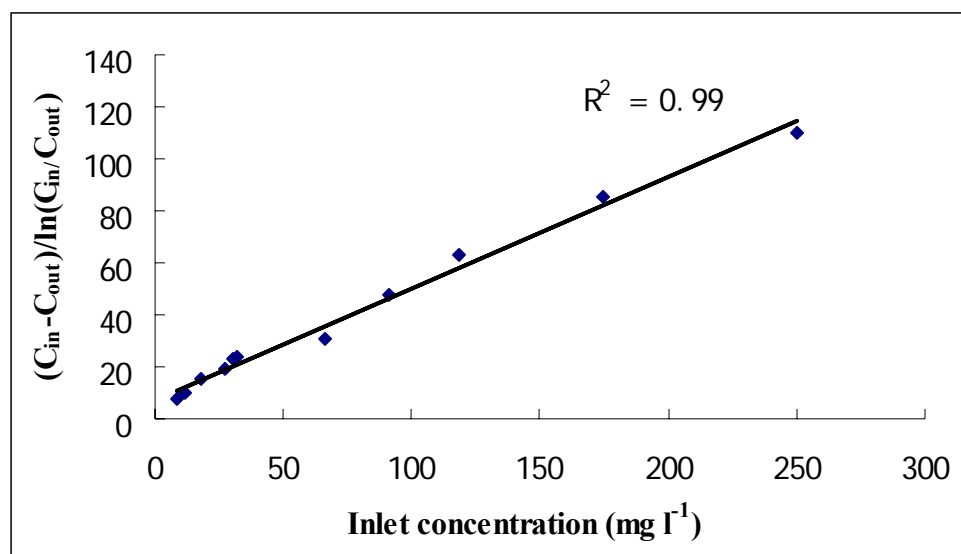


Figure 31. AN inlet concentration VS. $(C_{in} - C_{out}) / \ln(C_{in} / C_{out})$ when AN was single feed at EBRT=8min.

The microbial flora appears to survive a fairly long period during which the filter bed is not loaded. The microbial activity was hardly lost if the packed bed did not receive any nutrient supply but keep moisturized for two or three weeks. The population dynamic should be responsible for keeping the activity during discontinuous operations and it requires a very short starting time after long periods of not operating the filter bed.

For a GAC biofilm column reactor, adsorption of target compounds, desorption and biotreatment occur simultaneously. When AN concentration was 500ppm and flow through GAC

column at a rate of 1 gal/min at room temperature of 25 C , the adsorption of AN to GAC is 5.87g/100g carbon. In this study, for both batch flask and reactor, AN was adsorbed to GAC, being slowing bioavailable and was hydrolyzed and metabolized by the biofilm, as indicated by the NH_3 release (Table 7&8, Figure 24&29). The advantage of adsorption and desorption is to allow affectively metabolize the compound by holding it for a period of time. However, the desorption of the adsorbed compound may slow biodegradation process. During the feed period, low AN degradation efficiency suggest adsorption of AN, which was subsequently available for AN degradation in closed mode. The adsorption-desorption method gives the bioremediation more stability and system efficiency.

The assimilation of ammonium nitrogen ($\text{NH}_4\text{-N}$), as well as the production of acrylic acid, results in a decrease of the pH of the medium. The following accumulation of NH_3 increases pH value to around 8.0. In this study, the slight pH drop (≤ 0.3) or increase (< 1.0) did not exhibit any apparent adverse impact on reactor's performance. The increase of pH later on suggested that from the assimilation of the carbon and nitrogen source, the medium may neutralize the H^+ . Otherwise if the pH keeps going down, acidification of the filter bed and reduction on removal efficiency will occur.

There is generally well accepted that if a bioreactor was run in the down-flow mode, a thin layer of cells presents at the upper section, which has a relatively easier access to the substrates, whereas an anaerobic, inactive layer settles in deeper parts of the packed bed or near the outlet of the biofilter. However, in this study, comparison of oxygen profiles in the different sections of the reactor indicated that inactive cells had accumulated at the top of the packed bed while active cells located close to the deep bottom (Figure 31&Table13). It could be assumed that the inactive biofilm at the upper section protects the active microorganisms from the toxic

effects of high concentrations of AN/Tol. High concentrations of Tol were reported to increase the non-toluene-associated respiration rate, and the number of stressed and non-respiring cells (Villaverde and Fernandez, 1997). Although the endogenous respiration is commonly ignored when VOC degradations are modeled (Oh and Bartha, 1994; Shareefdeen and Baltzis 1993; Diks and Ottengraf 1991), the endogenous metabolism can influence the rate of decomposition of xenobiotics by microbial biofilms.

Biofilm was once viewed as uniform structures where microorganisms were randomly distributed in the matrix. Advanced non-destructive analysis using CLSM have pictured biofilm in a more detailed way, where cell aggregated within the biofilm and on exopolysaccharide matrices. It also allows the quantification of biofilm constituents. In an AN-degrading biofilm microorganisms were present at all depth, either in dense cell clusters or as individuals. The formation of EPS increased with time and the amount of biomass, which binds bacteria together and enhance the adhesion. A sagittal plane or stacks of slicers reveal a network of channels either as long void spaces or filled with cells embedded on the EPS. Porosity of the carbon particle, as well as EPS production may be an important factor in the maintenance of optimum reactor operation. Microorganisms not only colonize on the carbon surface but also the crevices, which make the heterogeneity of the biofilm structure. The penetration depth of oxygen and VOCs is shallow (typically 100-150 μ m). In aerobic biofilm reactors, 50% of the oxygen consumed by the biofilm was supplied by the channels (Debeer et al. 1994). The change of channel structures over the operation time of the reactor and their relationship with EPS may be critical in modeling biofilm growth and reaction kinetics.

Structures variation of steady-state biofilms between different sections of the reactor and different depth of a biofilm was high (Figure 27, 28&30). The variation could be ascribed to the

uneven distribution of the microcolonies. Big colonies colonize somewhere on the carbon bed, exhausting the nutrient and leaving the rest of the column a single layer of cells. In multi-species biofilm, the growth rate gradient will make the biofilm a layered structure. The organisms which have the highest growth rate will be found at the outside of the biofilm, while the slower growing ones will be inside, protected from external shear force and the following-up detachment and washed-out. In steady state, the physical structure of the biofilm was determined by the balance between biofilm growth and detachment. Biofilm characteristics of each section can be quantified using CLSM (Table 10). The CLSM is capable of capturing images of stained cells at various depths of biofilm (Figure 28). In the study, total biomass, average/maximum thickness, roughness, substratum coverage and surface to volume ratio were selected to characterize the biofilm because they are fairly easy to interpret biologically and physically. Total biomass presents the overall volume of the biofilm. Average thickness provides a special size of the biofilm. Roughness coefficient is an indicator of biofilm heterogeneity. Substratum coverage reflects how efficiently the strain colonizes the substratum. The surface-volume ratio reflects the fraction of the biofilm which is exposed to the nutrient flow and thus indicates how the biofilm adapts to the environment. In the present bioreactor study, the consortia had a stronger tendency to form micro-colonies in the deeper part of the column, which was indicated by the total biomass average thickness and substratum coverage. Large amount of biomass accumulated in the lower zone may cause channeling problem, leading to a reduced overall removal efficiency. This phenomenon may be due to the supply of the nutrient and buffer solution displacing part of the biomass from the top to the bottom, especially during backwashing in a high flow rate and the following liquid drainage. The roughness coefficient for upper section was higher, because of the formation of elongated cell clusters and long filaments. The surface-volume ratio was

relatively higher for upper and middle sections, because they have better access to the limited supply of nutrients. Previous studies showed that steady-state biofilm thickness decreased with the decreasing nutrient concentration along the column depth (Kennes and Veiga 2001, Mendoza et al 2004), however, the study indicates that for a porous attachment material like GAC, substrate diffusion is most likely not a limiting factor for AN degradation. CLSM analysis also revealed a channeling structure partially filled with EPS.

Volumetric pollutant elimination requires continuous supply of mineral nutrients. For toluene-degrading biotrickling filter, while degrading on average $20\text{-}40 \text{ g m}^{-3} \text{ reactor day}^{-1}$, the wet biomass accumulated at $3.1\text{-}9.8 \text{ kg m}^{-3} \text{ reactor day}^{-1}$ (Cox et al.1998). If there is no control on biomass accumulation, the amount of immobilized biomass will increase to fill the pore space and the biofilter gets clogged. In this study, after 3-5 months of operation, when the biofilter was running continuously at $\text{EBRT} \leq 8 \text{ min}$ for 3 days, the packed bed got flooded, which ended up in a reduced efficiency because of the reduction of the biofilm-specific surface area. Although GAC is an inorganic packing material which has an advantage of having a uniform structure which reduces compaction and allow better liquid and gas flow distribution, there is still not enough area to sustain growth and activity of the microbial community, which results in high pressure drop in the packed bed. If there are filamentous fungi, the clogging problem will be more severe. Biomass control strategies could be either reduction of the biomass accumulation rate by addition of growth-inhibiting chemicals or periodical removal of excess biomass by backwashing if the packing material can be fluidized. However, the bed expansion may affect the biofiltration process of the scaled-up industrial trickling filter. In addition, active biomass may be pushed into pumps. Sometimes particles need to be filtered out, the biofilm removed and the clear particle returned to the reactor. An alternative is to combine organic and inorganic packing

materials in biofilter beds, which can provide both nutrient for microbial growth, and large surface area for resisting compaction.

The results presented in this study showed that AN and Tol can be efficiently degraded in the GAC bioreactor under high inlet load/substrate concentration; generally immobilized cells are less sensitive and more tolerable to the toxic organics than free cells. The load treated would be similar to industrial levels (Table 1), and compared with conventional biofilters, the reactor is superior in its removal efficiency, elimination capacity, and long-term stability. Although the GAC reactor failed occasionally due to excessive buildup of attached biomass during the phase of continuous loading, it still maintained excellent overall removal efficiencies. The study is also a contribution for understanding the operation of biofilm reactors established on GAC and further pilot/full scale applications. The adsorption-desorption of compounds by GAC could affect the removal efficiency and the structure organization of the biofilm may be important for microorganisms to exert their functions.

Future directions would be understanding of secondary processes which is not directly associated with the pollutant elimination, and the control of the biomass for the stability of the reactor. In addition, the kinetics for biodegradation of mixtures of pollutions should be developed and more studies involving *situ* analysis should be conducted for determining the change of environmental conditions on the degradation efficiency and biomass yield. The operation and optimization of lab and pilot-scale biotrickling filters could enhance the transfer and application of biotechnology tools from the lab to the real world.

REFERENCES

- Alfani, F., M. Cantarella, A. Spera and P. Viparelli (2001). Operational stability of *Brevibacterium imperialis* CBS 489-74 nitrile hydratase. *J. Mol. Catal. B.* 11: 687-697.
- Arcangeli J.P. and E. Arvin (1992). Toluene biodegradation and biofilm growth in an aerobic fixed-film reactor. *Appl. Microbiol. Biotechnol.* 37: 510-517.
- Asano, Y., M. Tashibana, Y. Tani and H. Yamada (1982). Aliphatic nitrile hydratase from *Arthrobacter* sp. J1: purification and characterization. *Agric. Biol. Chem.* 46: 1183-1189.
- Agency for Toxic Substances and Disease Registry (ATSDR) (1999). Managing Hazardous Materials Incidents. Volume III – Medical Management Guidelines for Acute Chemical Exposures: [Acrylonitrile](#). Atlanta, GA: U.S. Department of Health and Human Services, Public Health Service.
- Bauer, R., B. Hirrlinger, N. Layh, A. Stolz and H.J. Knackmuss (1994). Enantioselective hydrolysis of racemic 2-phenylpropionitrile and other (R,S) 2-arylpropionitriles by a new bacterial isolate, *Agrobacterium tumefaciens* train d3. *Appl. Microbiol. Biotechnol.* 42: 1-7.
- Calderia, M., S.C. Heald, M.F. Carvalho, I. Vasconcelos, A.T. Bull and P.M.L. Castro (1999). 4-Chlorophenol degradation by a bacterial consortium: development of a granular activated carbon biofilm reactor. *Appl. Microbiol. Biotechnol.* 52:722-729.
- Collins, J.J., L.C. Page, J.C. Caprossi, H.M. Utidjian and J. Saipher (1989). Mortality patterns among employees exposed to acrylonitrile. *J. Occup. Med.* 31: 368-371.
- Cowan, D.A., R.A. Cramp, R.A. Pereira and Q. Almatawah (1998). Biochemistry and biotechnology of nitrile-metabolizing enzymes. *Extremophiles* 2: 207-216.
- Cox, H.J.J., T.T. Nguyen and M.A. Dessusses (1998). Elimination of toluene vapors in biotrickling filters: performance and carbon balances. In *Proceedings of the 91st Annual Meeting and Exhibition of the Air & Waste Management Association*. 1-15.
- Cox, H.H.J. and M.A. Deshusses (2002). Effect of starvation on the performance and re-acclimation of biotrickling filters for air pollution control. *Environ. Sci. Technol.* 36: 3069–3073.
- Cox, H.H.J. and M.A. Deshusses (2002). Cotreatment of H₂S and toluene in a biotrickling filter. *Chemical Engineering Journal* 87: 101-110.
- De Meester, C., F. Poncelet, M. Ropberfroid and M. Mercier (1978). Mutagenicity of acrylonitrile. *Toxicology* 11: 19-27.

Dessusses, M.A., H.J.J.Cox and D.W. Miller (1998). The use of CAT scanning to characterize bioreactors for waster air treatment. In proceedings of the 91st Annual Meeting and Exhibition of the Air & Water Management Association: 1998 June 14-18; San Diego, CA., Pittsburgh, PA: Air and Waste Management Association; 1998: 1-12.

Deshusses, M.A. and H.H.J.Cox (1998). Biological waste air treatment in biotrickling filters. Curr. Opin. Biotechnol. 9:256-262.

Dharmavaram, S. (1991). Biofiltration, a lean emissions abatement technology. Proceedings of the 84th Annual Meeting & Exhibition of the Air & Waste Management Association, Vancouver, British Columbia June: 16-21.

Dietz, A. and D.W. Thayer, Eds (1980). Actinomycete taxonomy (procedures for studying aerobic actinomycetes with emphasis on the Streptomyces). Society for Industrial Microbiology special publication number 6: 28.

Digeronimo, M.J. and A.D.Antoine (1976). Metabolism of Acetonitrile by *Nocardia rhodochrous* LL100-21. Appl. Environ. Microbiol. 31(6): 900-906.

Diks, R. and S. Ottengraf (1991). Verification studies of a simplified model for the removal of dichloromethane from waste gases using a biological trickling filter (Part II), Bioprocess Eng. 6: 131-134.

Diks, R. and S. Ottengraf (1991a) Verification studies of a simplified model for the removal of dichloromethane from waste gases using a biological trickling filter. Part I. Bioprocess Eng. 6: 93-99.

Edwards, J.F. and R.B.Simpson (1988). *Norcadiform actinomycete (Rhodococcus trubopertinctus)*-induced abortion in a mare. Vet. Pathol.25: 529-30.

Elliott, G., H.K. Lawson and C.P. Mackenzie (1986). *Rhodococcus equi* infection in cats. Vet. Rec. 118: 693-94.

Endo, I., M. Okada and M. Yohda (1999). An enzyme controlled by light: the molecular mechanism of photo reactivity in nitrile hydratase. Trends Biotechnol. 17: 244-248.

Environment Canada (EC). (2000). *Priority Substances List Assessment Report: Acrylonitrile*. Canadian Environmental Protection Act, 1999. Environment Canada. Ottawa, ON.

Estevez, E. M. Veiga and C. Kennes (2005). Biofiltration of waste gases with the fungi *Exophiala oligasperma* and *Paecilomyces variotii*. Appl. Microbiol Biotechnol. 67: 563-568.

Fawcett, J.K. and J.E. Scott (1960). A rapid and precise method for the determination of urea. J. Clin. Path. 13: 156-159.

Finnerty, W.R. (1992). The biology and genetics of the genus *Rhodococcus*. Annu. Rev. Microbiol. 46: 193-218.

Ganguly, S. (2005). Dissertation: Enhanced stabilization of nitrile hydratase from *Rhodococcus* sp. DAP 96253 and *Rhodococcus rhodochrous* DAP 96622. Georgia State University Dec, 2005.

Gates, B., C. Katzer, R. James and G.C.A. Schuit (1979). Chemistry of Catalytic Processes. McGraw-Hill Book Company. New York.

Goodfellow, M. (1989). *Nocardiform actinomycetes*, genus *Rhodococcus*. In: Bergey's Manual of Systematic Bacteriology 2362-2371. Holt, J.G., Ed., Williams and Wilkins, Baltimore, MD.

Grabam, D., R. Pereira, D. Barfield and D. Cowan (2000). Nitrile biotransformations using free and immobilized cells of a thermophilic *Bacillus* spp. Enzyme and Microbial Technology 26: 368-373.

Harper, D.B. (1977). Microbial metabolism of aromatic nitriles. Biochem. J. 165: 309-319.

Harper, D.B. (1985). Characterization of a nitrilase from *Nocardia* sp. (*Rhodococcus* Group. N.C.I.B. 11215, using hydroxybenzoxitrile as sole carbon source. Int. J. Bioche. 17: 677-683.

International Agency for Research on Cancer (IARC) (1987). IARC Monographs on the Evaluation of Carcinogenic Risks to Humans. Suppl. 7:79-80.

IARC (1985). IARC Monographs on the Evaluation of the Carcinogenic Risk of Chemicals to Humans, Some Chemicals Used in Plastics and Elastomers, Vol. 39. IARC. Lyon, France. pp. 41-66.

Jin, Y., C.M. Veiga and C. Kennes (2006). Performance optimization of the fungal biodegradation of α -pinene in gas-phase biofilter. Process Biochemistry 41: 1722-1728.

Jorio, H., L. Bibeau, G. Vieland and M. Heitz (2000). Effects of gas flow rate and inlet concentration on xylene vapors biofiltration performance, Chem. Eng. J. 76: 209-221.

Juteau, P., R. Laroque, D.Rho and A. Leduy (1999). Analysis of the abundance of different types of bacteria capable of toluene degradation in a compost biofilter. Appl. Microbiol. Biotechnol. 52: 863-868.

Kiared, K., B. Fundenberger, R.Brzezinski, G. Viel and M.Heitz (1997). Biofiltration of air polluted with toluene under steady-state conditions: Experimental observations, Ind. Eng. Chem. Res. 36: 4719-4725.

Kim, D., Z. Cai and G.A. Sorial. (2004). Evaluation of trickle-bed air biofilter performance for removal of paint booth VOCs under stressed operating conditions, in: 97th Annual Conference and Exhibition of the Air and Waste Management Association, Indianapolis, Indiana, Paper 36.

Kim, D., Z. Cai, and G.A. Sorial (2005). Evaluation of trickle bed air biofilter performance under periodic stressed operating conditions as a function of styrene loading, J. Air Waste Manage. Assoc. 55: 200–209.

Kennes, C. and M.C. Veige (2001). Bioreactor of waste gas treatment. Kluwer, Dordrecht.

Klecka G.M., S. G. McDaniel, P.S. Wilson, C. L. Carpenter, J. E. Clarck, A. Thomas, J.C. Spain (1996). Field-evaluation of a granular activated carbon fluid-bed bioreactor for treatment of chlorobenzene in groundwater. Environ. Pro. 15:93-107.

Kobayshi, M., H.Izui and T. Nagasawa (1993). Nitrilase in biosynthesis of plant hormone indole-acetic acid from indole-3-acetonitrile: cloning of the *Alcaligenes* gene and site directed mutagenesis of cysteine residues. Proc. Natl. Acad. Sci. 90: 247-251.

Kobayashi, M. and S. Shimizu (1998). Metalloenzyme nitrile hydratase: Structure, regulation, and application to biotechnology. Nature Biotechnology 16: 733-736.

Kornaros, M. and G. Lyberotos (2006). Biological treatment of wastewaters from a dye manufacturing company using a trickling filter. J. Harzardous Materials Languardt, P. W. "Acrylonitrile". Ullmann's Encyclopedia of Industrial Chemistry, Fifth Edition: Vol. A1.

Krishna, R., R.S. Reddy and J. A. Adams (1999). Air flow optimization and surfactant enhancement to remediate toluene-contaminated saturated soils using air sparging. Environmental Management and Health 10: 52-63.

Manolov, T., H. Kristina and G. Benoit (2005). Continuous acetonitrile degradation in a packed-bed bioreactor. Environmental Biotechnology 66: 567-574.

Martin, F.J. and R.C. Loehr (1996). Effect of periods of non-use on biofilter performance. J. Air Waste Manage. Assoc. 46: 539–546.

Martinkova, L., J. Hruzova, F. Machek, L. Seichert, J. Panos and P. Juzlova (1992). Isolation of acetonitrile-utilizing bacteria. Folia Microbiologica. 37: 372-376.

Mendoza, J.A., O.J. Prado, M.C.Veiga and C. Kennes (2004). Hydrodynamic behaviour and comparison of technologies for the removal of excess biomass in gas-phase biofilters. Water Res. 38: 404-413.

Moe, W.M. and R.L. Irvine (2000). Performance of periodically operated-gas phase biofilters during transient loading conditions. Water Sci. Technol. 41: 441–444.

Moller, S., A.R.Pedersen,L.K. Poulsen, E.Arvin and S. Molin (1996). Activity and three-dimensional distribution of toluene-degrading *Pseudomonas putida* in a multispecies biofilm assessed by quantitative in situ hybridization and scanning confocal laser microscopy. Appl. Environ. Microbiol. 62: 4632-4640.

Moustafa, A.M., M.T. Suidan, J. Kim and S.W. Maloney (2002). Pertubated loading of a formaldehyde waste in an anaerobic granular activated carbon fluidized bed reactor. *Water Res.* 36: 3775-3785.

Murai, N., F. Skoog, M.E. Doyle and R.S.Hanson (1980). Relationship between cytokinin production, presence of plasmids and fasciation caused by strains of *Corynebacterium fascians*. *Proc. Natl. Acad. Sci. USA* 77: 619-23.

Nagasawa, T., C.D. Mathew, J. Mauger and H.Yamada (1988). Nitrile hydratase catalysed production of niconamide from 3-cyanopyridine in *Rhodococcus rhodochrous* J1. *Appl. Environ. Microbiol.* 54: 1766-1769.

Nagasawa, T. and H. Yamada (1990). Application of nitrile converting enzymes for the production of useful compounds. *Pure Appl. Chem.* 62:1441-1444.

Namkoong, W., J.S. Park and J.S. Vander-Gheynst (2004). Effect of gas velocity and influent concentration on biofiltration of gasoline off-gas from soil vapor extraction. *Chemosphere* 57: 721-730.

Nawaz, M.S., J.D. Richardson, K.D. Chapatwala and J.H. Wolfram. (1989). Degradation of acetonitriles by *Pseudomonas aeruginosa*. 43rd Purdue Ind. Waste Conf. Proc. 251-256.

Nawaz, M.S., W. Franklin and C.E. Cerniglia. (1993). Degradation of acrylamide by immobilized cells of *Pseudomonas sp.* and *Xanthomonas maltophilia*. *Can. J. Microbiol.* 39: 207-212.

Oh, Y-S and R.Bartha (1994). Design and performance of a trickling air biofilter for chlorobenzene and o-dichlorobenzene vapors. *Appl. Environ. Microbiol.* 60: 2717-2722.

Okada, M., K. Fuji, T.Noguchi, M.Tsujimura, S. Nagashima, J. Honda, T.Nagamune, H. Sasabe, Y.Inoue and I. Endo (1997). Activity regulation of photoreactive nitrile hydratase by nitric oxide. *J.Am. Chem. Soc.* 119: 3785-3791.

Ottengraf, S.P.P. and A.H.C. van den Oever. (1983). Kinetics of organic compound removal from waste gases with a biological filter. *Biotechnol. Bioeng.* 25: 3089-3102.

Parkin, G.F. and R.E. Speece (1983). Attached versus suspended growth reactors: response to toxic substances. *Water Sci. Technol.* 15:261-289.

Pedersn, A.R., S. Molier, S.Molin and E.Arvin (1997). Activity of toluene-degrading *Pseudomonas putida* in the early growth phase of a biofilm for waste gas treatment. *Biotechnol. Bioeng.* 54: 131-141.

Pierce, G.E. (1999). Methods for the detoxification of nitrile and/or amide compounds. US Patent 5, 863, 750. Filed 12.18.1996, Issued January 26,1999.

Pierce, G.E. (1999). Methods for the detoxification of nitrile and/or amide compounds. US Patent 6,060,265. Filed 6.25.1998, Issued May 9, 2000.

Pierce, G. E. (2000). Methods for the detoxification of nitrile and/or amide compounds. US Patent 6, 132,985. Issued October 17, 2000.

Popescu, V. C., E. Munck, B.G. Fox, Y. Sanakis, J.G. Cummings, I.M.Turner and M.J. Nelson (2001). Mossbauer and EPR studies of the photoactivation of nitrile hydratase. *Biochemistry* 40: 7984-7991.

Ramakrishna, C., D. Karand and J. Desai (1989). Biotreatment of acrylonitrile plant effluent by powered activated carbon-activated sludge process. *J. Ferment. and Bioeng.* 67(6): 430-432.

Sa, C.S.A.and R.A.R. Bonaventura (2001). Biodegradation of phenol by *Pseudomonas putida* DSM 548 in a trickling bed reactor. *Biochemical Engineering Journal* 9: 211-219.

Shareefdeen, Z and B.C.Baltzis (1993). Biofiltration of methanol vapor. *Biotechnol Bioeng.* 41: 512-524.

Shi J., X.D.Zhao, R.F.Hickey and T.C.Voice (1995) Role of adsorption in granular activated carbon-fluidized bed reactors. *Water Environ Res.* 67:302-309.

Sorial, G.A., F.L. Smith, M.T. Suidan, P. Biswas and R.C. Brenner (1997). Performance of peat biofilter: impact of the empty bed residence time, temperature and toluene loading. *J. Hazard. Mater.* 53:19–33.

Stanier, R.Y., N.J. Palleroni and M. Doudoroff (1966). The aerobic pseudomonads: a taxonomic study. *J. Gen. Microbio.* 43: 159-271.

U.S. EPA (1985). U.S. Environmental Protection Agency. Health and Environmental Effects Profile for Acrylonitrile. Environmental Criteria and Assessment Office, U.S, EPA, Cincinnati, OH.

U.S. EPA (1992). The Clean Air Act Amendments of 1990: A guide for small business.

U.S.EPA(1994a). U.S. Environmental Protection Agency. Integrated Risk Information System(IRIS) Database. Reference concentration (RfC) for acrylonitrile. Available online at <http://www.epa.gov/iris/subst/0206.htm>.

U.S. EPA(1994b). U.S. Environmental Protection Agency. Integrated Risk Information System (IRIS) Online. Coversheet for Acrylamide. Office of Health and Environmental Assessment, U.S. EPA, Cincinnati, OH.

U.S. EPA (2003). National Emission Standards for Hazardous Air Pollutants: Miscellaneous Organic Chemical Manufacturing. November 10, 2003 (Volume 68, Number 217)

Van Lith, C., S.L. David and R. Marsh (1990). Design criteria for biofilters. Trans. IChemE. 68: pt B, 127-132.

Vergara-Fernandez, A., L.L. Molina, N.A. Pulido and G. Aroca (2007). Effects of gas flow rate, inlet concentration and temperature on the biofiltration of toluene vapors. Journal of Environmental Management 84: 115-122.

Villaverde, S. and M.T. Fernandez (1997). Non-toluene-associated respiration in a *Pseudomonas putida* 54G biofilm grown on toluene in a flat-plate vapor-phase bioreactor. Appl. Microbiol. Biotechnol. 48: 357-362.

Watanabe, I., S. Yoshiaki and K. Enomoto (1987). Screening, isolation and taxonomical properties of microorganisms having acrylonitrile-hydrating activity. Agric. Biol. Chem. 51: 3193-3199.

Watanabe, I. (1987). Optimal conditions for cultivation of *Rhodococcus* sp. N-774 and for conversion of acrylonitrile to acrylamide by resting cells. Agric. Biol. Chem. 51: 3201-3206.

Weber F. J. and S. Hartman (1996). Prevention of clogging in a biological trickle-bed reactor removing toluene from contaminated air. Biotechnol. Bioeng. 50: 91-97.

Weissmehl, K. and H.J. Arpe (1997). Industrial Organic Chemistry. 3rd Revised Edition. VCH Publishers Inc., New York, NY 302-310.

Wilkinsin, Gary R. The Manufacture and Use of Selected Inorganic Cyanides. Kansas City: Midwest Research Institute (for the U.S.EPA), April 2, 1976.

Wilson, J. (1983) Cyanide in Human Disease: A Review of Clinical and Laboratory Evidence. *Toxicol. Sci.* 3: 397-399

Wyatt, J.M. and C.J. Knowles (1995a). The development of a novel strategy for the microbial treatment of acrylonitrile effluents. Biodegradation 6: 93-107.

Wyatt, J.M. and C.J. Knowles (1995b). Microbial degradation of acrylonitrile waste effluents: the degradation of effluents and condensates from the manufacture of acrylonitrile. Int. Biodeter. Biodegr. 35: 227-248.

Xu, D.X. Q. X. Zhu, L.K. Zheng, Q.N. Wang, H. M. Shen, L. X. Deng and C.N. Ong (2003) Exposure to acrylonitrile induced DNA strand breakage and sex chromosome aneuploidy in human spermatozoa. Mutation Research/Genetic Toxicology and Environmental Mutagenesis. 537: 93-100.

Yamada, H. and M. Kobayashi (1996). Nitrile hydratase and its application to industrial production of acrylamide. Biosci. Biotechnol. Biochem. 60: 1391-1400.

Yamaki, T., T. Oikawa, K. Ito, and T. Nakamura (1997). Cloning and sequencing of a nitrile hydratase gene from *Pseudonocardia thermophila* JCM3095. J. Ferment. Bioeng. 83: 474-477.

Yamamoto, K., Y. Ueno, K. Otsubo, Kawakami and K. Komatsu (1990). Production of S-(+)-Ibuprofen from a nitrile compound by *Acinetobacter* sp. strain AK226. Appl. Environ. Microbiol. 56: 3125-3129.

Zarook, S.M. and A.A. Shaikh. (1997). Analysis and comparison of biofilter models. Chemical Engineering Journal 55-61.

Zarook, S.M. A.A. Shaikh and Z. Ansar (1997). Development, experimental validation and dynamic analysis of a general transient biofilter model. Chem. Eng. Sci. 52 : 759–773.

Zhou, Q., Y.L Huang, D. H. Tseng, H. Shim and S.T. Yang (1998). A trickling fibrous-bed bioreactor for biofiltration of benzene in air. J. Chem. Technol. Biotechnol. 73: 359-368.

APPENDICE

Acrylonitrile/Toluene Extraction Protocol (Based on EPA method 8031)

1. Stocks standard solution (500ppm AN or 1000ppm Toluene)

To prepare the stock solution by volume: inject 62 μ l AN or 116 μ l toluene into a 100ml volumetric flask. Make up to volume with organic-free HPLC grade water.

2. Working standard solutions

Prepare a minimum of 5 working standard solution that cover the range of analyte concentrations expected in the samples. Working standards of 100ppm, 200ppm, 300ppm, 400ppm, 500ppm AN or 200ppm, 400ppm, 600ppm, 800ppm, 1000ppm Toluene may be prepared by injecting 1, 2, 3, 4, 5ml of the stock standard solution into 5 separate 30ml separatory funnels containing 5, 4, 3, 2, 1ml of organic-free reagent water, respectively.

Inject 5ml of methylene chloride and methanol mixture (85:15) into separatory funnel, shake vigorously, and let it stand 5 minutes, or until layers have separated.

3. Remove 2ml of bottom layer and place in a 2ml GC vial.

4. Keep all standard solutions below 4°C until used.

Sample extraction: Filter 5ml of the sample into a 30ml separatory funnel. Pipet 5ml of methylene chloride and methanol mixture into separatory funnel, shake vigorously, and let it stand 5 minutes, or until layers have separated.

Gas chromatography for AN and Tol

Injection volume: 1.0 μ l

Syringe size: 5.0 μ l

	Preinjection	postinjection
Sample	3.0 μ l	
Solvent A		2.0 μ l
B		0 μ l
Pumps	2.0 μ l	

Zone Temperatures

Injector 300C

Detector 300C

Oven program

Initial Temperature 50C

Initial Time 2.30min

Rate 10C/min

Final Temperature 120C

Final Time 2min

Oven parameters

Oven Equib.Time 3.00min

Oven Max. 250C

Valve A off Splitless

Valve B off Splitless

Peak width 0.427min

Data rate 0.625HZ

Time	Integration Events	Value
------	--------------------	-------

Initial	Slope Sensitivity	500
---------	-------------------	-----

Initial	Peak width	0.08
---------	------------	------

Initial	Area Reject	1500
---------	-------------	------

Initial	Height Reject	2000
---------	---------------	------

Initial	Shoulders	off
---------	-----------	-----

Boiling point (C)

Methnol bp760=64.7

Acrylonitrile bp760=77.3

Toluene bp760=110.6